ISSN 2078-7405

МІНІСТЕРСТВО ОСВІТИ ТА НАУКИ УКРАЇНИ

РІЗАННЯ ТА ІНСТРУМЕНТИ

В ТЕХНОЛОГІЧНИХ СИСТЕМАХ

96'2022

МІНІСТЕРСТВО ОСВІТИ ТА НАУКИ УКРАЇНИ

НАЦІОНАЛЬНИЙ ТЕХНІЧНИЙ УНІВЕРСИТЕТ
«ХАРКІВСЬКИЙ ПОЛІТЕХНІЧНИЙ ІНСТИТУТ»

Ministry of Education & Science of Ukraine
National Technical University
«Kharkiv Polytechnic Institute»

РІЗАННЯ ТА ІНСТРУМЕНТИ в технологічних системах

CUTTING & TOOLS IN TECHNOLOGICAL SYSTEM

Міжнародний науково-технічний збірник
International Scientific-Technical Collection

Заснований у 1966 р. М. Ф. Семко
Found by M. F. Semko in 1966

ВИПУСК № 96
Edition № 96

Харків НТУ «ХПІ» – 2022 – Kharkiv NTU «KhPI»

ББК 34.63
УДК 621.91

Державне видання
Свідоцтво Державного комітету телебачення і радіомовлення України
КВ № 7840 від 8 вересня 2003 року
Друкується за рішенням Вченої Ради НТУ "ХПІ",
протокол № 2 від 04 лютого 2022 р.

У збірнику представлені наукові статті, в яких розглядаються актуальні питання в області механічної обробки різних сучасних матеріалів із застосуванням високопродуктивних технологій, нових методик, вимірювальних приладів для контролю якості оброблених поверхонь і високоефективних різальних інструментів. Розглядаються аспекти оптимізації та математичного моделювання на різних етапах технологічного процесу.

Для інженерів і наукових співробітників, що працюють в області технології машинобудування, різання матеріалів, проектування різальних інструментів в технологічних системах.

Науковий збірник «Різання та інструменти в технологічних системах» включений в Перелік фахових видань України категорії «Б», наказ МОН України від 17.03.2020 р., №409

Р34 Резание и инструменты в технологических системах: Междунар. науч.- техн. сб. – Харьков: НТУ «ХПИ», 2022. – Вып. 96. – 147 с.

Адреса редакційної колегії: вул. Кирпичова, 2, Харків, 61002, Національний технічний університет «Харківський політехнічний інститут», кафедра «Інтегровані технології машинобудування» ім. М.Ф. Семка, тел. +38 (057) 706-41-43.

ББК 34.63

UDC 658.511 **doi: 10.20998/2078-7405.2022.96.01**

Á. Bányai, Miskolc, Hungary

OPTIMISATION OF PURCHASING STRATEGY OF TOOLS AND COMPONENTS BASED ON EXCHANGE CURVE THEORY

Abstract *The optimal inventory control of tools and components in manufacturing systems plays an important role in the success of sustainable operation from financial and ecologic point of view. This study discusses an inventory control method, which is based on the transformation of investment of inventory into annual order cost or vice versa. The study presents the mathematical model of the exchange curve model for tools and components in the case of economic order quantity inventory strategy. The described methodology makes it possible to optimise available purchasing strategies for tools and components. The approach was tested with a scenario analysis, where different parameters of the purchasing process including inventory related constraints were taken into consideration. The computational results validated the exchange curve based inventory control methodology and showed that the inventory strategy can be improved with cost transformation Practical implications of the proposed model and method regard the possibility of finding optimal inventory policies that can affect the operation costs of manufacturing systems.*
Keywords: *purchasing logistics, optimisation, inventory control, exchange curve*

1. INTRODUCTION

Today, in order to increase the efficiency of production systems and meet the dynamically changing demands of customers, manufacturing companies are doing their utmost to optimise not only their production systems, but also the related service processes, especially focusing on logistics. This means that the optimisation of procurement, distribution and recycling logistics activities is becoming increasingly important for sustainable production systems. In the field of production logistics, strategic issues can be defined in two cases: design of a new production logistics systems or improve an existing production logistics systems. Logistics strategies should support the following production logistics objectives: increasing capacity utilisation of production and logistics resources, reducing lead times, reducing production process inventories (work in process) without increasing supply risk, reducing the operation costs of the technological and logistical process, increasing flexibility a reliability, increasing the transparency of the technological process, reducing the environmental impact and integration of the production logistics process into the overall company logistics system [1].

This paper studies the optimisation potentials of purchasing policies of tools and components in a manufacturing system, while the economic order quantity is taken into consideration. As the literature review section will show, modern optimisation algorithms play an important role in the design and operation of logistics systems [2] and the majority of the articles in the field of purchasing policy optimisation are focusing on conventional manufacturing environment and

only a few of them describes the purchasing policy optimization in a cyber-physical system, where available real time status information based on digital twin technology makes it possible to define a dynamic purchasing strategy optimisation of tools and components. The article is organized as follows. Section 2 presents a systematic literature review, which summarizes the research background of purchasing policy optimization based on exchange curve. Section 3 describes the mathematical model of exchange curve-based purchasing policy optimisation including three different scenarios depending on the constraints. Section 4 demonstrates the scenario analysis, which validates the model. Conclusions, future research directions and managerial impacts are discussed in Section 5.

2. LITERATURE REVIEW

As previous studies show, the optimisation of the inventory level and the costs of inventory management has a great impact on the competitiveness of manufacturing processes. A wide range of objective functions and constraints can be taken into consideration regarding purchasing policy optimisation: purchasing and stock holding costs; financial, technological and logistics consequence of shortages; uncertainties of the manufacturing and service environment [3-5] or the warehousing system [6]. The technologies of the fourth industrial revolution and the transformation of conventional manufacturing and service systems into cyber-physical systems lead to a more complex supply chain structure, where the four supply chain levers have to be taken into consideration as an integrated, interconnected or hyperconnected system, where the key performance indicators of the supply chain subsystems (procurement, warehousing, fulfilment and transportation) have a great impact on each other [7]. Statistical survey shows, that the application of Industry 4.0 technologies leads to a cost savings of about 10% regarding administrative costs for each purchasing [8]. Industry 4.0 technologies are changing the role of purchasers, because the co-creation of specifications, automatized prequalification and negotiations lead to the improvement of procurement processes [9,10], especially from reduced uncertainties resulted by the application of digital twin technologies point of view. The big data oriented smart tool condition monitoring makes it possible to evaluate the present status of the tools and make prediction including lifetime expectancies, which can support the optimisation of tool procurement processes [11].

About 60% of the articles were published in the last five years. This result indicates the scientific potential of the research of purchasing policy optimisation in Industry 4.0 era. The articles that addressed the development of purchasing policy optimisation are focusing on different fields of procurement and buying aspects of supply chain solutions in the field of manufacturing, but only a few of them focuses on the potentials of Industry 4.0 technologies. As a consequence, the

main contribution of this article is the exchange curve-based mathematical model of purchasing policy optimisation and the description of computational results validating the described model.

3. TOOL AND COMPONENT MANAGEMENT IN CYBER-PHYSICAL MANUFACTURING

However, there are different ways to optimise conventional manufacturing systems, but Industry 4.0 technologies offer new opportunities and potentials to improve the optimisation, especially focusing on the real time data-based design and operation based on smart sensors and digital twin solutions. In cyber-physical manufacturing systems, it is possible to use the real time status information to optimize the manufacturing related operations including purchasing, distribution and in-process recycling and reuse. Figure 1 shows a possible solution of the optimisation of purchasing strategies of tools and components of a cyber-physical manufacturing system. The proposed model includes the following main phases:

1. Smart micro sensors can be mounted into intelligent tools, and these sensors can collect real time status information of the tool (temperature, deformation, tension, etc.).
2. The collected information can be uploaded indirectly to a database, or directly to a digital twin solution.
3. The digital twin solution can build real time models of the analysed tool, or tool-machine, or tool-machine-product system. This real time model can be uploaded into a discrete event simulation software, where the model represents the present status of the system.
4. Using discrete event simulation, it is possible to analyse the modelled system and make predictions.
5. The tool inventory is a basic information for the prediction, especially if this information focuses on both quality and quantity of available tools.
6. The enterprise resource planning includes a wide range of modules, from these the production planning and scheduling module is responsible for the design, operation, supervision and controlling of the manufacturing system.
7. The production planning and scheduling module determines the master production schedule, which is the most important input parameter for the purchasing policy.
8. Using the master production schedule, it is possible to define resource demands (machine tools, tools, components, human resources, logistics resources, packaging).

9. Based on the status information of inventory of tools and components and the prediction information, the future potential status of the system can be predicted, which is the basic information for the optimisation of the purchasing policy.

10. Based on the prediction regarding tools, it is possible to make predictions according the whole analysed systems including tools and components.

11. The master production schedule is an important input parameter of the purchasing policy optimisation.

12. The optimised purchasing policy has a great impact on the component inventory, because the resulted changes in annual order cost and annual investment in inventories of components lead to new parameters of the purchasing process, which influences in this way the component inventory.

13. The optimised purchasing policy has a great impact on the tool inventory, because the resulted changes in annual order cost and annual investment in inventories of tools lead to new parameters of the purchasing process, which influences in this way the tool inventory.

14. Predictions and lifetime expectancies of tool and products is an important input parameter for the exchange curve-based purchasing policy optimisation.

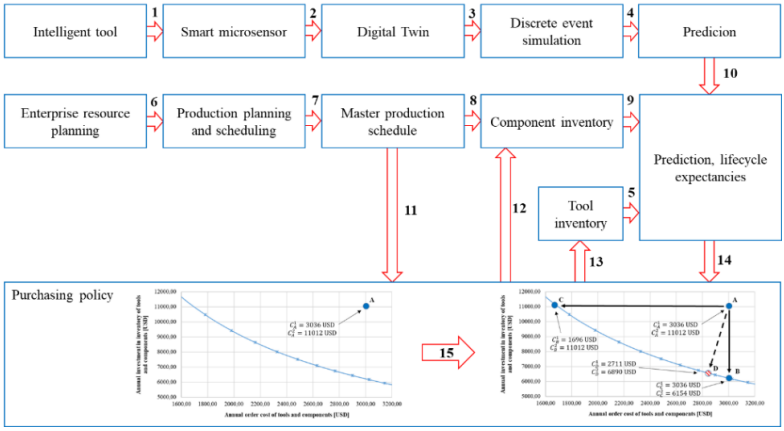

Figure 1 – Digital twin-based optimization of purchasing policy of tools and components

4. MATHEMATICAL MODEL

To optimise the operation of production systems, it is essential to design related logistics processes in a cost-effective way. Since one of the key elements of

efficiency in production systems is the availability of tools and parts, it is of great importance to define an optimal inventory strategy. Inventory management processes have great importance in company's logistics system and have a major impact on its economic operation. The aim of inventory management is to smooth out the fluctuations in quantity resulting from imbalances between input and output flows in the material system or from external environmental disturbances.

The purchasing policy of tools and components of manufacturing systems can be optimised in many ways, depending on the characteristics of goods. If the purchasing policy is based on economic order quantity methodology, then in the mathematical model of the exchange curve based inventory control the average inventory investment can be defined depending on the specific purchasing cost of tools and components:

$$C^1 = \sum_{l=1}^{p} \frac{q_l}{2} \cdot \alpha_l. \quad (1)$$

where α_l is the specific purchasing cost of tools and components and q_l is the economic order quantity, which can be calculated using the following equation:

$$q_l = \sqrt{\frac{2 \cdot AD_l \cdot \alpha_l}{\beta_l \cdot \gamma}}, \quad (2)$$

where AD_l is the annual demand of tools and components, α_l is the specific order cost of tools and components, β_l specific purchasing cost of tools and components, γ is the specific warehousing cost of tools and components.

Using the economic order quantity for all tools and components, the average inventory investment can be calculated:

$$C^1 = \frac{1}{2} \cdot \sum_{l=1}^{p} \beta_l \cdot \sqrt{\frac{2 \cdot AD_l \cdot \alpha_l}{\beta_l \cdot \gamma}} = \frac{1}{\sqrt{2 \cdot \gamma}} \cdot \sum_{l=1}^{p} \sqrt{AD_l \cdot \alpha_l \cdot \beta_l}. \quad (3)$$

The second part of the cost function is based on the annual order cost of tools and components, which can be calculated in the following way:

$$C^2 = \sum_{l=1}^{p} \frac{AD_l \cdot \alpha_l}{q_l}. \quad (4)$$

Using the economic order quantity for all tools and components, the annual order cost can be calculated in the following way:

$$C^2 = \sum_{l=1}^{p} AD_l \cdot \alpha_l \cdot \sqrt{\frac{\beta_l \cdot \gamma}{2 \cdot AD_l \cdot \alpha_l}} = \sqrt{\frac{\gamma}{2}} \cdot \sum_{l=1}^{p} \sqrt{AD_l \cdot \alpha_l \cdot \beta_l}. \quad (5)$$

Depending on the value of the average inventory investment and the annual order cost, it is possible to draw a curve between these costs. This $C^1 - C^2$ curve makes it possible to analyse and optimise the present inventory policy of tools and components depending on the position of the present inventory policy related to the $C^1 - C^2$ curve (see Figure 2).

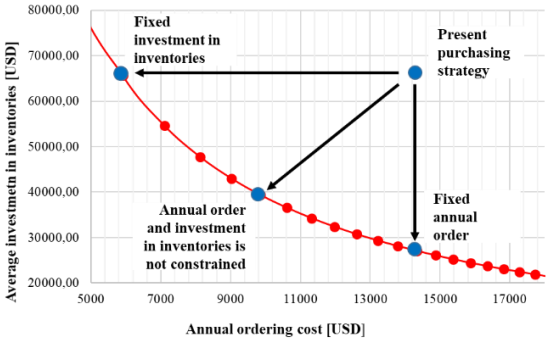

Figure 2 – Potential optimization directions of the purchasing policy depending on the position of the present situation related to the exchange curve

Depending on the constraints defined by the purchasing policy based on economic order quantity, we can define three different types of optimisation of purchasing policy:

- In the first case, the purchasing policy defines the number of annual orders regarding tools and components as a constant value (annual order constraint). Depending on the parameters of the purchasing policy, we can minimize the inventory costs, while it is not allowed to change the number of annual orders which lead to a constant annual order cost. In this case, the optimization of the purchasing policy means the transformation of investments in inventories of tools and components to annual order costs.
- In the second case, the purchasing policy defines the investment in inventories of tools and components as a constant value (investment in inventory constraint). Depending on the parameters of purchasing policy, we can minimize the annual order costs, while it is not allowed to change the investments in inventory of tools and components. In this case, the optimization of the purchasing policy means the transformation of annual order costs to investments in inventories of tools and components.
- In the third case, neither the annual orders nor the investment in inventories of tools and components are constrained by the purchasing policy based on economic order quantity model. In this case, we are talking about a mixed transformation, where we have to find the nearest point on the $C^1 - C^2$ curve, which means, the it is possible that both parts of the purchasing cost will be changed. In the case of this purchasing optimisation we can minimize the change in the parameters related to the present purchasing strategy.

This $C^1 - C^2$ plot is a rectangular hyperbola, which is named as an exchange curve:

$$C^1 \cdot C^2 = \frac{1}{2} \cdot \left\{ \sum_{l=1}^{p} \beta_l \cdot \sqrt{AD_l \cdot \alpha_l \cdot \beta_l} \right\}^2 \quad (6)$$

Within the frame of the next chapter some scenarios and numerical exampled demonstrate the usability and efficiency of the exchange curve-based purchasing policy optimisation in the case of tools and components in a manufacturing system.

5. NUMERICAL EXAMPLES

In the case of conventional manufacturing systems, where no real time status information is available it is almost impossible to perform a real time optimization a smoothing of purchasing policy. In cyber-physical systems, where the digital twin of the manufacturing system collects status information from the resources and processes of the manufacturing system through smart sensors, it is possible to make real time decisions and optimize the purchasing strategy regarding tools and components. In the case of intelligent tools, the inbuilt micro sensors can collect status information, and based on this information it is possible to predict the future status and life expectancy and the purchasing policy can be permanently changed.

In this scenario, the purchasing policy of tools and components in a cyber-physical manufacturing system is analysed. The input parameters of the purchasing optimization problem are given in Table 1, including the annual demand of tools and components depending on the master production plan based on ERP, the specific order cost and purchasing cost of tools and components (see Table 1). The company orders the required tools and components monthly (12 times yearly) and the annual order cost of this solution is 3036 USD, while the average inventory investment is 11012 USD.

Table 1 – Input parameters of the purchasing policy optimisation problem

ID	X1201	X1202	X1203	X1204	X1205	X1206	X1207
α_l [USD]	320	200	80	90	50	90	120
AD_l [pcs]	450	260	320	215	35	120	90
β_l [USD]	10	30	50	40	22	34	67

Depending on the specific warehousing cost of tools and components (γ), it is possible to compute both parts of the cost function regarding purchasing of tools and components. As Figure 3 demonstrates, regarding to the methodology of the economic order quantity, the specific warehousing cost has the opposite impact on the annual order cost and on the annual investment in inventory. The increased specific warehousing cost lead to increased annual order cost, while the increased specific warehousing cost lead to decreased annual investment in inventory of tools and components.

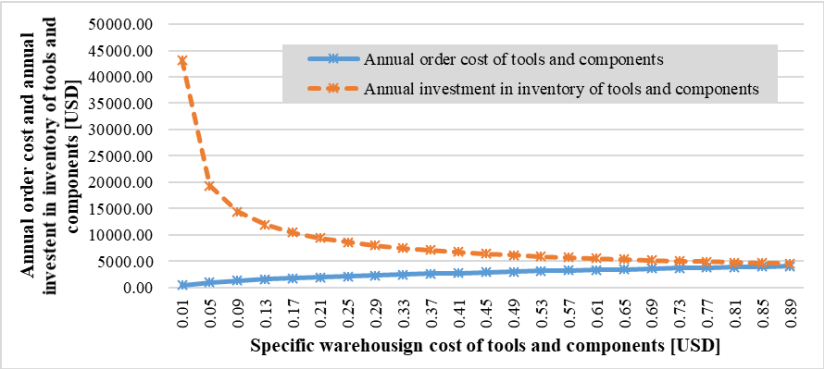

Figure 3 – Annual order cost and annual investment of inventory of tools and components depending on the specific warehousing cost

As Figure 4 demonstrates, in the case of this scenario there are three different ways to optimize the present purchasing strategy of tools and components (see point A in Figure 4). In the case of monthly order of tools and components, the annual order cost is 3036 USD and the annual investment in inventories is 11012 USD. The three potential optimisation directions are the followings:

- We can fix the annual order cost of tools and components and it is possible to find a potential solution on the $C^1 - C^2$ curve with a reduced investment in inventory of tools and components. This solution is represented by point B in Figure 4, where the annual order cost is 3036 USD and the annual investment in inventories is 6154 USD, which results a total annual purchasing cost reduction of 4858 USD.
- We can fix the investment in inventory of tools and components and it is possible to find a potential solution on the $C^1 - C^2$ curve with a reduced annual order cost of tools and components. This solution is represented by point C in Figure 4, where the annual order cost is 1696 USD and the annual investment in inventories is 11012 USD, which results a total annual purchasing cost reduction of 1340 USD.
- In the case of the third potential way, there are no constraints defined for the annual order and investment in inventory, therefore we can find a potential solution on the $C^1 - C^2$ curve to minimize the distance between point representing the present solution and point representing the new solution. A new procedure to find the minimum distance from the operating point representing the present purchasing strategy makes it possible to find this solution [12], which represents a potential solution with minor changes in the purchasing strategy. Using the suggested methodology, we can define this minimal distance point (see point D in Figure 4), where the annual order cost is 2711 USD and the annual investment in

inventories is 6890 USD, which results a total annual purchasing cost reduction of 4447 USD.

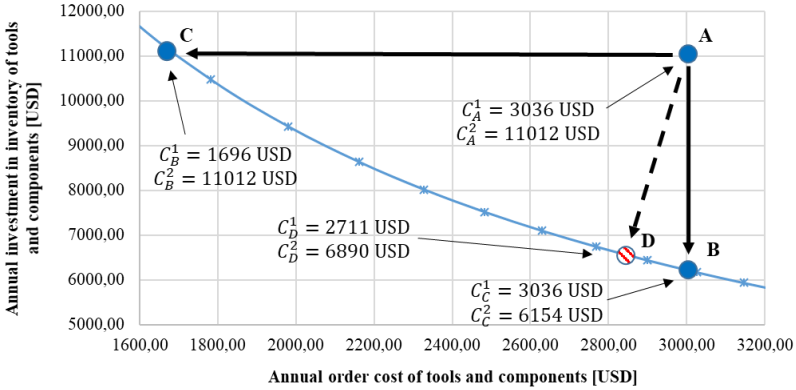

Figure 4 – Potential optimization directions of the purchasing policy

The above mentioned purchasing policy optimisation is a macro-level optimisation, because this methodology supports the detection of bottlenecks in purchasing strategy regarding annual order cost and annual investment in inventories of tools and components. After finding the bottleneck and changing the better strategy for the purchasing the next important task is to perform a micro-level purchasing policy optimisation, which can be based in this case on the economic order quality methodology, because after finding a better macro-level strategy on the $C^1 - C^2$ curve we can compute the new parameters for the new policy and we can determine the new parameters for the purchasing of tools and components while depending on the manufacturing and logistics environment different other components of the whole manufacturing system must be taken into consideration (triggers in Kanban systems, stock out management, age management and safety stock planning).

6. CONCLUSIONS

The efficiency of production systems is affected by the efficiency of both technological and logistic subsystems. An important factor of the optimisation of production systems is the optimisation of available resources, which is an important task of purchasing logistics, especially for tools and components. Within the frame of this article the author described an exchange curve-based purchasing strategy optimisation approach, which makes it possible to optimise the present purchasing policy depending on the value of annual order cost and annual investment in inventory of tools and components. The proposed model focuses on the potentials of Industry 4.0 technologies and describes a solution including

intelligent tools, smart micro sensors, digital twin technology and discrete event simulation. Purchasing policies are extensively discussed in a wide range of research works, but only a few of them focuses on the potentials of real time optimisation using Industry 4.0 technologies. To try to fill this gap, this work has introduced a purchasing policy optimization methodology based on exchange curve theory to analyse the structure of purchasing cost of tools and components and suggest more efficient policies for the analysed purchasing. The described methodology shows that the optimization of purchasing policy in cyber-physical systems has a great impact on the profit of the manufacturing system and digital twin solutions can support the optimization of purchasing policy, because real-time data collection can improve the efficiency of failure data forecast, prediction and status information collection. The most important managerial impact of this methodology is, that the application of the proposed model and method can support managerial decisions regarding buying, purchasing, procurement and warehousing. A further study of the proposed work would be the modelling and optimisation of the fourth optimisation direction, which objective function is the maximisation of the profit between the present purchasing policy and the new purchasing policy regarding the $C^1 - C^2$ rectangular hyperbola.

References: 1. *Baker, R. C., Urban, T. L.:* A Deterministic Inventory System with an Inventory-Level-Dependent Demand Rate, Journal of the Operational Research Society vol.39(8) (1988) pp. 823-831. https://doi.org/10.1057/jors.1988.142 **2.** *Akkad, M. Z., Bányai, T.:* Analytical review on the modern optimization algorithms in logistics, Advanced Logistic Systems - Theory and Practice vol. 14(1) (2021) pp. 25-31. https://doi.org/10.32971/als.2020.006 **3.** *Korponai, J., Bányainé Tóth, Á., Illés, B.:* Context of the inventory management expenses in the case of planned shortages, Engineering Management in Production and Services vol.9(1) (2017) pp. 26-35. https://doi.org/10.1515/emj-2017-0003 **4.** *Korponai, J., Bányainé Tóth, Á., Illés, B.:* The effect of the safety stock on the occurrence probability of the stock shortage, Management and Production Engineering Review vol. 8(1) (2017) pp. 69-77. https://doi.org/10.1515/mper-2017-0008 **5.** *Korponai, J., Bányainé Tóth, Á., Illés, B.:* Sensibility analysis of the planned availability period and of the impact of the cost factors on total costs, Advanced Logistic Systems: Theory and Practice vol.10(1) (2016) pp. 13-28. **6.** *Dobos, P., Cservenák, Á., Skapinyecz, R., Illés, B., Tamás, P.:* Development of an Industry 4.0-based analytical method for the value stream centered optimization of demand-driven warehousing systems, Sustainability vol.13(21) (2021) 11914. https://doi.org/10.3390/su132111914 **7.** *Tjahjono, B., Esplugues, C., Ares, E., Pelaez, G.:* What does Industry 4.0 mean to Supply Chain?, Procedia Manufacturing vol.13 (2017) pp. 1175-1182. https://doi.org/10.1016/j.promfg.2017.09.191. **8.** *Nicoletti, B.:* Industry 4.0 and Procurement 4.0. In: Procurement 4.0 and the Fourth Industrial Revolution. Palgrave Macmillan, Cham 2020. https://doi.org/10.1007/978-3-030-35979-9_2 **9.** *Gottge, S., Menzel, T. and Forslund, H.:* Industry 4.0 technologies in the purchasing process, Industrial Management & Data Systems vol.120(4) (2020) pp. 730-748. https://doi.org/10.1108/IMDS-05-2019-0304 **10.** *Jahani, N., Sepehri, A., Vandchali, H. R., Tirkolaee, E.B.:* Application of Industry 4.0 in the Procurement Processes of Supply Chains: A Systematic Literature Review, Sustainability vol.13(14) (2021) 7520. https://doi.org/10.3390/su13147520 **11.** *Zhu, K., Li, G., Zhang, Y.:* Big Data Oriented Smart Tool Condition Monitoring System, IEEE Transactions on Industrial Informatics vol.16(6) (2020) pp. 4007-4016. https://doi.org/10.1109/TII.2019.2957107 **12.** *Silver, E. A., Bischak, D. P., da Silveira, G. J. C.:* An efficient method for calculating the minimum distance from an operating point to a specific (hyberbolic) efficient frontier, IMA Journal of Management Mathematics vol.20(3) (2009) pp. 251-261. https://doi.org/10.1093/imaman/dpn023

Агота Баньяї, Мішкольц, Угорщина

ОПТИМІЗАЦІЯ СТРАТЕГІЇ ЗАКУПІВЕЛЬ ІНСТРУМЕНТІВ І КОМПЛЕКТУЮЧИХ НА ОСНОВІ ТЕОРІЇ ОБМІННИХ КРИВИХ

Анотація. *На ефективність виробничих систем впливає ефективність як технологічної, і логістичної підсистем. Важливим фактором оптимізації виробничих систем є оптимізація наявних ресурсів, що є важливим завданням закупівельної логістики, особливо інструментів та комплектуючих. У рамках цієї статті автор описав підхід до оптимізації стратегії закупівель на основі кривої обміну, що дозволяє оптимізувати існуючу політику закупівель залежно від величини річної вартості замовлення та щорічних інвестицій у запаси інструментів та комплектуючих. Пропонована модель фокусується на можливостях технологій Індустрії 4.0 та описує рішення, що включає інтелектуальні інструменти, інтелектуальні мікродатчики, технологію цифрових двійників та моделювання дискретних подій. Політика закупівель широко обговорюється у великій кількості досліджень, але лише деякі з них присвячені можливостям оптимізації в реальному часі з використанням технологій Індустрії 4.0. Щоб спробувати заповнити цю прогалину, у цій роботі була представлена методологія оптимізації політики закупівель, що базується на теорії кривої обміну, для аналізу структури закупівельної вартості інструментів та компонентів та пропозиції більш ефективних політик для аналізованих закупівель.Описана методологія показує, що оптимізація політики закупівель у кіберфізичних системах дуже впливає на прибуток виробничої системи, а рішення цифрових двійників можуть сприяти оптимізації політики закупівель, оскільки збір даних в режимі реального часу може підвищити ефективність прогнозування даних щодо відмови, прогнозування та збір інформації про реальне. стані. Найбільш важливим управлінським ефектом цієї методології є те, що застосування запропонованої моделі та методу може підтримувати управлінські рішення щодо закупівель, постачання та складування. Подальшим дослідженням запропонованої роботи буде моделювання та оптимізація четвертого напряму оптимізації, цільовою функцією якого є максимізація прибутку між існуючою політикою закупівель та новою політикою закупівель щодо прямокутної гіперболи C^1-C^2.*

Ключові слова: *закупівельна логістика; оптимізація; контроль запасів; крива обміну.*

UDC 621.7 **doi: 10.20998/2078-7405.2022.96.02**

Ya. Garashchenko, Kharkiv, Ukraine

EVALUATION OF PERFORMANCE EFFICIENCY OF PACKING A GROUP OF PRODUCTS IN THE WORKPLACE OF ADDITIVE MACHINE USING A GENETIC ALGORITHM

Abstract. *Research results of possibilities of packing a group of 3D-models of products in a layered build space using a genetic algorithm are presented. It is proposed to determine the efficiency of the optimization problem of rational arrangement of 3D-models group in the workspace of additive machines depending on the number of loaded products. Condition for efficient use of the layered build workspace is the minimum number of layers per product and the largest relative filling. Such criteria are important, for example, for SLS/SLM technologies.*

Examples of evaluation based on the analysis of derived voxel 3D model of the workspace with located products are considered. Industrial products with different geometrical complexity were selected as test 3D models. This approach allowed to perform a comparative analysis of the results depending on the design features of products.

The practical realization was performed in the subsystem of packing 3D-models in a workspace, which is part of the technological preparation system for the manufacture of complex products by additive methods. This system was developed at the Department of "Integrated Technologies of Mechanical Engineering" named after M. Semko of NTU "KhPI".

Keywords: *technology planning; additive manufacturing; triangulated model; voxel model, packing.*

Introduction. One of the main optimization tasks of technological preparation of additive processes (Additive Manufacturing) is to determine the rational location of the product in the working area of layered building [1]. The ability to solve this optimization problem significantly depends on the geometric complexity of the products and requirements for effective use of additive machines [2]. When applied to methods such as SLS and SLA, one of the important factors in the effectiveness of layering processes is the degree of filling the workspace with products. The provisional estimate of the product in technological preparation for adaptation to the task of rational location is of interest to ensure the level of efficiency of additive processes of layered building [3].

Literature analysis. Rational placement of products 3D models refers to the problems of packaging, which are characterized by significant complexity of solution [4, 5]. Product placement problems are solved both for single-build and multi-build of one or more machines (single- or multi-machine) [6].

In the known works various approaches and algorithms on a rational arrangement of products group in a workspace of additive technologies machine are used. The genetic algorithm is one of the most common for solving such a problem [7-9].

Choice of rational location of the product in the working space of additive machine, as a rule, is performed by solving the optimization problem based on one or many criteria [6]:

- build height [10];
- surface roughness, support volume [11];
- layering time [12];
- total cost [13];
- profit [14];
- nesting rate [15];
- number of products parts obtained during their decomposition [3].

The main problem is that existing works have not created a methodological basis for a comparative analysis of the effectiveness of algorithms for placing a group of 3D models, taking into account geometric features of products. Initial research of genetic algorithm possibilities for the placement of products with different designs was carried out in [16]. But the problem remains to ensure sufficiently high efficiency of using the workspace of machine in the manufacture of small groups of products in one load.

The purpose of the article is to validate the possibility of effectively performing the optimization problem of rational arrangement of 3D models of products group with complex geometry in the workspace of additive machines using a genetic algorithm.

Research methodology. A study of the possibilities of the solving optimization problem of packing 3D models of products group was carried out in the system "Technological preparation of materialization of complex products by additive technologies", developed at the Department of Integrated Mechanical Engineering Technologies of NTU "KhPI". This system makes it possible to assess the technological effectiveness of solving technological preparation problems based on the statistical analysis of studied features of polygonal, voxel, and layered 3D models of products [16].

Optimization problem of product placement was performed using voxel product models [3]. Voxel model consists of an ordered set of voxels, which are volume elements with a given location in space (coordinates $x_{V(i)}$, $y_{V(i)}$, $z_{V(i)}$). Therefore, the voxel model is a set of elementary volumes $V = \{v[0], v[1], \ldots v[nv]\} = \{v[i]\}$. Voxel models offer a quite simple way to process data for given task.

The developed subsystem provides for the following modes of placing products 3D models in the workspace of AM machine [16]: manual mode; random search (Monte Carlo method); using a genetic algorithm.

Placement of products 3D models in the workspace was carried out with a step-by-step check of the free space and fixation of orientation using a genetic algorithm [6, 16, 17].

In fig. 1 are the test 3D models placed in the workspace of Vanguard Si2 SLS machine (made by 3D Systems).

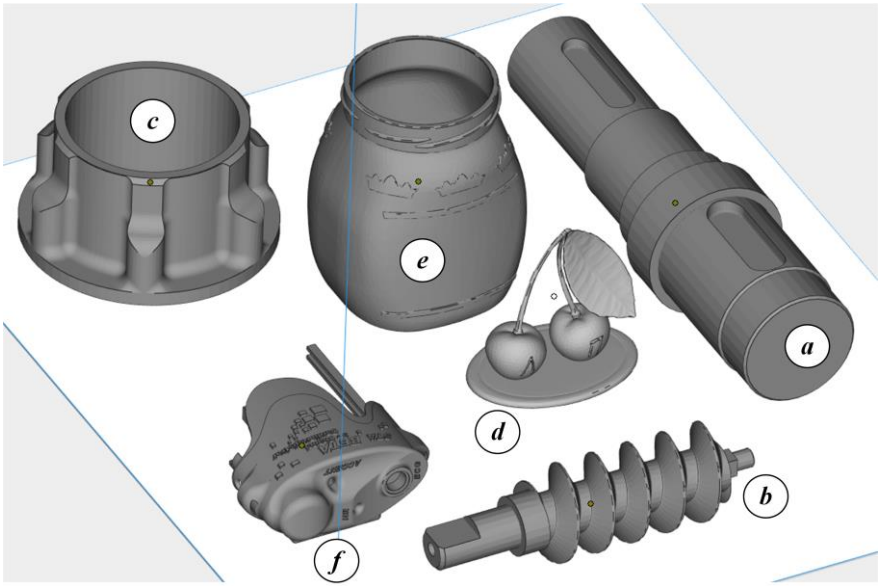

a – shaft, *b* – auger, *c* – case, *d* – souvenir, *e* – container, *f* – lid.
Figure 1 - Test 3D models

Research of the possibilities of developed algorithm for packing products 3D-models (Fig. 1) was carried out by means of comparative analysis by a number of layers N_L, coefficient of the relative use of the layered build workspace K_V. Additionally, a relative number of filled and unfilled subspaces was considered to evaluate the efficiency of the algorithm for uniform use of the workspace of the additive machine.

Results of the research. The study of developed algorithm capabilities described in [16] was carried out on the example of placing a group of products in an amount of 5-20 pieces. Envelope sizes were set using the example of Vanguard Si2 SLS machine. The estimated flow was considered by the number of building layers, and the efficiency of the machine was considered by relative used workspace of layered building. Slicing strategy with a constant building step h_i = 0.1 mm, and with a variable step was carried out with the following characteristics: maximum permissible value of deflection from the correct shape Δ_{Smax} = 0,1 mm (for a description of slicing method is in [18]). Parameters of genetic algorithm:

probability of crossing p_c = 80%, mutation probability p_m = 2%, population size N_p = 20 pcs., generations limiting number (generations) N_g = 50.

Results of analysis of options for placing 3D-models' groups of products in the workspace of the additive machine (Vanguard Si2 SLS) are shown in table. 1.

Table 1 - Researched features obtained in the analysis of options for 3D-models packing in the workspace

Test 3D-model (overall dimensions)	Number of models	Number of building layers		Build height, H_B	Coefficient of space utilization, K_V
		constant step	variable step		
Shaft (60x216x60 mm^3)	5	600	424	61.0	0.244
	10	1816	1481	182.6	0.163
	15	2958	2086	251.5	0.178
	20	3219	2813	322.9	0.184
Auger (40x144x40 mm^3)	5	582	503	61.2	0.042
	10	1020	901	104.9	0.049
	15	1387	1255	141.7	0.055
	20	1317	1226	134.68	0.077
Case (210x210x125 mm^3)	5	1297	679	132.2	0.034
	10	2342	1279	236.7	0.038
	15	3917	2156	393.0	0.034
	20	4092	2452	413.1	0.043
Souvenir (73x51.3x70.1 mm^3)	5	1072	911	110.1	0.008
	10	774	633	80.2	0.021
	15	1473	1309	151.1	0.017
	20	1475	1341	150.5	0.023
Container (102x93.6x125.5 mm^3)	5	1005	469	104.0	0.014
	10	2054	954	208.9	0.014
	15	4245	2380	428.1	0.010
	20	3460	2353	347.5	0.016
Lid (83.9x101.3x43.2 mm^3)	5	806	738	84.3	0.016
	10	1357	1285	139.5	0.019
	15	1883	1817	192.1	0.021
	20	2055	2001	209.3	0.025

Analysis of research characteristics, given in table. 1 shows a clear advantage of the approach to load more products into the machine workspace. The exception is the shaft and container 3D models. For a shaft 3D model, it is not possible to increase the efficiency of manufacturing. This is due to rather large overall

dimensions in relation to the working space dimensions. This circumstance does not allow efficient use of the machine`s workspace. The explanation for the container can be the fact that the model belongs to thin-walled products. In this case, regardless of the number of models placement, it is impossible to achieve a noticeable increase of K_V coefficient. We can also suppose that K_V coefficient is slightly dependent on the choice of a packing algorithm. Models with more complex geometry - auger, souvenir, lid show an essential increase of K_V with an increase in the number of loaded products. Container and case show an essential reduction in the number of layers for adaptive slicing strategy relative to constant step (common slicing). This circumstance can be explained by greater initial efficiency from the task performance of rational orientation of part according to the optimization criterion of minimum of the area with greatest deviations from correct surface shape.

Comparative analysis of the obtained results (table. 1) was carried out according to graphs shown in Fig. 2.

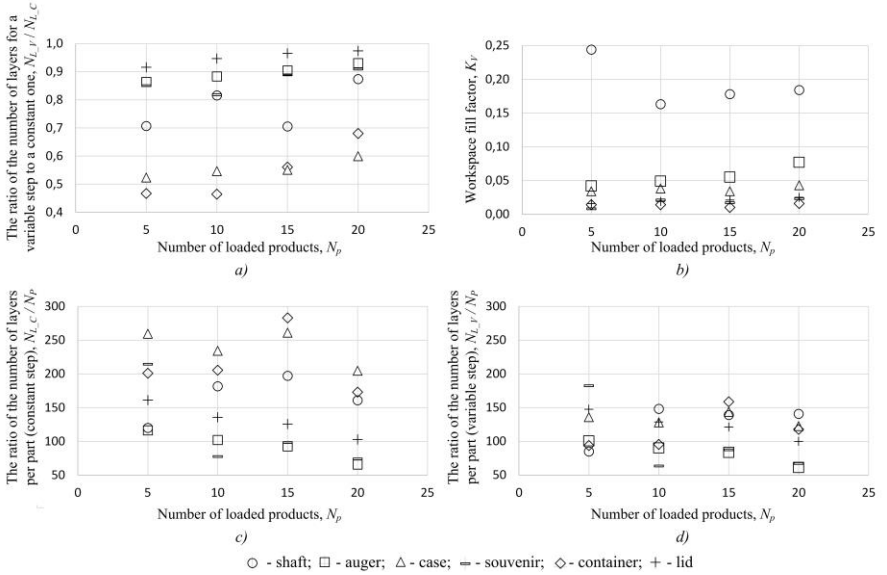

Fig. 2. Dependences of researched features on the number of loaded parts

Ratio dependence of the number of layers obtained by different cutting strategies $N_{L\_V} / NL_{\_C}$ on the number of parts loaded into the workspace N_p, shown in Fig. 2*a*. It allows to you identify the conditions for the greatest efficiency of adaptive slicing in comparison with constant building steps. Using adaptive slicing

for loads of the adaptive machine with a small number of parts is most successful. Best results are obtained for container and case.

Analysis of filling factor of the workspace with models (Fig. 2*b*) shows a significant difference for shaft from other models.

Fig. 2*c*,*d* shows graphs of the influence of loaded models' numbers on a relative number of building layers on one model. It is known, that building time and a number of layers are approximately linearly related (within the framework of using the same slicing strategy with the same parameters) for additive methods such as SLS, SLM, SLA, DLP, etc. [19]. Therefore, obtained dependencies are of interest for identifying conditions for increasing productivity of additive processes. The minimum ratio N_{L_C} / N_p and, accordingly, N_{L_V} / N_p are observed for auger and souvenir. At the same time, increased productivity, i.e. minimization of building time will be ensured with a larger load of these models. In general, for all test 3D models, there is a tendency to increase productivity of layered building processes and fill factor of the workspace of the additive machine.

As a result of research, the following recommendations were obtained to improve the efficiency of using additive installation at stage of placing products in the workspace using a genetic algorithm:

- for products like a shaft and auger, the workspace of the additive machine should not be filled to the maximum;
- greatest efficiency of adaptive slicing is provided for products with complex surface geometry and therefore they should be pre-oriented according to criterion of minimizing surface with greatest deviations;
- for products with complex surface geometry, it is necessary to fill the workspace of the additive machine as much as possible.

Approbation of the algorithm using the example of packing a small group of 3D models of complex products has demonstrated some improvement in researched features due to loading a kit of parts into the workspace of the additive machine. In some cases, it was possible to reduce specific number of construction layers per part within the range of 9.9 ÷ 65.6%. At the same time, the time spent on the implementation of the optimization problem of parts packing increases significantly (preliminary researched results are presented in [16]).

Conclusions. Results of research of genetic algorithm possibilities for effectively solving the problem of packing a group of products 3D models in the workspace to fill it as much as possible showed an increase in productivity of their layered building. At the same time, the time spent does not increase so significantly compared to the task of packing a small 3D models group located directly on the platform of the additive machine.

Based on the analysis of researched features of the workspace with placed 3D models in the workspace, rational quantities of loaded parts have been identified,

depending on their design features. Under certain conditions, it is possible to reduce specific number of building layers per part to 65.6%.

Findings create the basis for further consideration of joint solution of the problems of rational orientation and placement of a large group of complex products in the workspace using a genetic algorithm to expand possibilities of technological preparation of additive manufacturing.

References: 1. *Che Y., Hu K., Zhang Z., Lim A.* Machine scheduling with orientation selection and two-dimensional packing for additive manufacturing. Computers & Operations Research, 2021. 130, 105245. doi: 10.1016/j.cor.2021.105245. **2.** *Chekanin V.A., Chekanin A.V.* Solving the Problem of Dense Packing of Objects of Complex Geometry. In: Evgrafov A.N. (eds) Advances in Mechanical Engineering. Lecture Notes in Mechanical Engineering. Springer, Cham, 2022. doi: 0.1007/978-3-030-91553-7_12. **3.** *Garashchenko Y., Rucki M.* Part decomposition efficiency expectation evaluation in additive manufacturing process planning. International Journal of Production Research, 2021. 14 p. doi: 10.1080/00207543.2020.1824084. **4.** *Psiola V.V.*: Approximate solution of a 3-dimensional packaging problem based on heuristics. Intelligent systems, 2011. Vol. 1, 83-100 [in Russian]. **5.** *Stoyan Y., Gi l N., Scheithauer G.* Packing of convex polytopes into a parallelepiped. Preprint. Dresden. MATH-NM-06-2004, 2004. 32 pages. **6.** *Oh Y., Witherell P., Lu Y., Sprock T.* Nesting and Scheduling Problems for Additive Manufacturing: A Taxonomy and Review. Additive Manufacturing, 2020. 101492. **7.** *Aguilar-Duque J.I., Balderrama-Armendáriz C.O., Puente-Montejano C.A. et al.* Genetic algorithm for the reduction printing time and dimensional precision improvement on 3D components printed by Fused Filament Fabrication. Int J Adv Manuf Technol 115, 2021. 3965–3981. doi: 10.1007/s00170-021-07314-w. **8.** *Li Y.B., Sang H.B., Xiong X., Li Y.R.* An Improved Adaptive Genetic Algorithm for Two-Dimensional Rectangular Packing Problem. Applied Sciences, 11(1), 2021. 413. **9.** *Zhao Y., Rausch C., Haas C.* Optimizing 3D irregular object packing from 3D scans using metaheuristics. Advanced Engineering Informatics, 47, 2021. 101234. **10.** *Araújo L.J.P., Panesar A., Özcan E., Atkin J., Baumers M., Ashcroft I.* An experimental analysis of deepest bottom-left-fill packing methods for additive manufacturing, Int. J. Prod. Res. 0 (0), 2019. 1–17. doi: 10.1080/00207543.2019.1686187 Nov. **11.** *Vanek J., et al.* PackMerger: a 3D Print volume optimizer, Comput. Graph. Forum 33 (6), 2014. 322–332, doi: 10.1111/cgf.12353 Sep. **12.** *Luzon Y., Khmelnitsky E.* Job sizing and sequencing in additive manufacturing to control process deterioration, IISE Trans. 51 (2), 2019. 181–191. doi: 10.1080/24725854.2018.1460518 Feb. **13.** *Fera M., Macchiaroli R., Fruggiero F., Lambiase A.* A modified tabu search algorithm for the single-machine scheduling problem using additive manufacturing technology,", Int. J. Ind. Eng. Comput. 11 (3), 2020. 401–414. **14.** *Li Q., Zhang D., Wang S., Kucukkoc I.* A dynamic order acceptance and scheduling approach for additive manufacturing on-demand production, Int. J. Adv. Manuf. Technol., 2019. doi: 10.1007/s00170-019-03796-x May. **15.** *Yang W., Liu W., Liu L., Xu A.* A genetic algorithm for automatic packing in Rapid prototyping processes, Advanced Intelligent Computing Theories and Applications. With Aspects of Theoretical and Methodological Issues, 2008. pp. 1072–1077. doi: 10.1007/978-3-540-87442-3_132. **16.** *Garashchenko Y., Vitiaziev J., Grimzin I.* Packing 3D-Models of Products in Build Space of Additive Manufacturing Machine by Genetic Algorithm. Advanced Manufacturing Processes III. InterPartner 2021. Lecture Notes in Mechanical Engineering. Springer, Cham, 2022. P. 67-77. doi: 10.1007/978-3-030-91327-4_7. **17.** *Kureichik V., Kureichik V., Gladkov L.* Genetic algorithms. Moscow: Fizmat-lit, 2010. 368 p. [in Russian]. **18.** *Garashchenko Y., Zubkova N.* Adaptive slicing in the additive manufacturing process using the statistical layered analysis. Advances in Design, Simulation and Manufacturing III. DSMIE 2020. Lecture Notes in Mechanical Engineering. Springer, Cham, 2020. P. 253-263. doi: 10.1007/978-3-030-50794-7_25. **19.** *Vitjazev Ju.B.* Rasshirenie tehnologicheskih vozmozhnostej uskorennogo formoobrazovanija sposobom stereolitografii: Dis... kand. tehn. nauk: 05.02.08, Har'kov, 2004. 228 s.

Ярослав Гаращенко, Харків, Україна

ОЦІНКА ЕФЕКТИВНОСТІ ВИКОНАННЯ ЗАДАЧІ РОЗМІЩЕННЯ ГРУПИ ВИРОБІВ У РОБОЧОМУ ПРОСТОРІ АДИТИВНИХ УСТАНОВОК З ВИКОРИСТАННЯМ ГЕНЕТИЧНОГО АЛГОРИТМУ

Анотація. *Представлено результати дослідження можливостей розміщення (упаковки) групи 3D-моделей виробів у робочому просторі пошарової побудови з використанням генетичного алгоритму. Запропоновано визначати ефективність оптимізаційної задачі раціонального розташування групи 3D-моделей у робочому просторі адитивних установок у залежності від кількості завантажених виробів. Умовою ефективного використання робочого простору пошарової побудови є мінімальна кількість шарів на виріб та найбільше відносне заповнення. Такі критерії є важливими для таких технологій як SLS/SLM.*

Розглянуто приклади оцінки ефективності розробленого алгоритму на основі аналізу похідної воксельної 3D-моделі робочого простору з розташованими виробами. В якості тестових 3D-моделей обрано промислові вироби з різною складністю. Такий підхід дозволив виконати порівняльний аналіз результатів в залежності від конструктивних особливостей виробів.

Практична реалізація виконувалась у підсистемі раціонального розташування 3D-моделей у робочому просторі, що входить до системи технологічної підготовки виготовлення складних виробів адитивними методами. Дану систему розроблено на кафедрі «Інтегровані технології машинобудування» ім. М.Ф. Семка НТУ «ХПІ».

Ключові слова: *технологічна підготовка; адитивні технології; тріангуляційна модель; воксельна модель, розміщення групи виробів у робочому просторі.*

UDC 658.511 **doi: 10.20998/2078-7405.2022.96.03**

M.Z. Akkad**,** T. Bányai, Miskolc, Hungary

ANALYSIS AND COMPARISON OF THE WASTE MANAGEMENT DEVELOPMENT IN HUNGARY AND SLOVAKIA

Abstract. *Waste production is an indispensable human process that happens daily in all communities. With the population increase and the industry developments, the waste amounts are growing, and their treating processes are taking a bigger share of the transportation and handling tasks in the city logistics. These waste collection, transportation, and treatment are described as waste management has been investigated and developed especially with the various application, solutions, and developments in the logistics, transportation, and industrial areas. Also, with the higher attention to the environmental impact in the different areas, the green aspect of waste management takes more importance particularly in city logistics where congestion occurs regularly. Within this work, waste management is analyzed in Europe generally and Hungary specifically. Eurostat database is used for that purpose next to previous research work tackling this topic. Also, a comparison between the waste management operations in Hungary and Slovakia is discussed to show the difference of these operations' developments between the two countries between 2014 and 2020.*

Keywords: *waste management; city logistics; data analysis.*

1. INTRODUCTION

The European Union repeatedly formulated aims, plans, and recommendations concerning waste management [1]. A common EU aim is to recycle 65% of municipal waste and 75% of packaging waste by 2030 [2]. The document of "General Union Environment Action Program to 2020; Living well, within the limits of our planet" described a waste management hierarchy according to environmental aspects [1, 3]:

- Prevention,
- reduce waste. To avoid any extra amount of waste,
- reuse. It requires relatively little or no processing where the material can be used again without any structural changes in it,
- recycling, and waste treatment. It means creating usable raw materials from the waste,
- incineration with energy recovery. The released gases and heat are used for power generating. By the end of this process, the gases are released after purification from any contaminated substances,
- another recovery, and disposal. this method remains the worst option that should be avoided as much as possible for its long-time need.

It is possible to describe waste management as the collective process of monitoring, collecting, transporting, treating, recycling, or disposing of waste.

This process takes its importance to lighten the negative effects of waste on the health, environment, and public appearance. Waste can be defined as any excess undesirable material, and it can mean rubbish or trash. Waste collection is a main part of the waste management process. It is the process of transferring the waste to the treatment or landfill facility. Waste treatment refers to the needed processes to ensure that waste has the least possible effect on the environment. The waste treatment methods may vary from a country to another [4]. On one hand, waste management may be considered as a necessary cost that should be paid to reach a clean environment that is not harmful to the health of inhabitants. On the other hand, other authorities give great importance to waste management because it saves raw materials resources. Many developed countries implemented successfully waste treatment projects to get benefits from waste like recycling.

2. WASTE MANAGEMENT DEVELOPMENT

It is observed that there is a shift towards a more holistic approach in the analysis of waste management [5], and reducing environmental impact is the priority for future generations. Waste minimization mechanisms should be implemented as well, taking into consideration the sustainable development principles [6]. Also, sustainable development implementation mustn't cause long-term business disadvantages for companies [7]. Numerous European cities have been using sustainable systems in waste management for a few years, working on optimizing the generated and collected amounts of waste to a minimum. However, the dominant method of waste disposal is landfilling in Hungary [1]. The waste minimization techniques can be used in the waste reduction of municipal waste treatment, but the waste management problem in the European Union is classified by [8]:

- the increase in industrialization and urbanization,
- the increase in the generated waste amount per capita,
- the maintain need of a high level of infrastructure investment (incinerators, landfills, recycling facilities),
- institutional barriers,
- the diversity of interest groups next to the political and legal changes in the field of waste management.

Different waste collection solutions are analyzed in the literature focusing on different aspects of evaluation, like technology, logistics, human resources, policies, and social aspects [9]. The optimal structure of the waste collection system influences the performance of waste collection processes. A Portugal case study shows that strategic expansion plans of waste management companies can be supported by complex mathematical models and heuristic optimization algorithms [10]. The importance of multi-level solutions is highlighted with a three-phase

hierarchical approach in the Spanish region of Galicia [11] and Ankara [12]. the authors focused on routing problems and facility location. Waste collection systems show a broad range of uncertainties, for instance, the design of appropriate infrastructure difficulties for waste collection and recycling were described in a Hong Kong case study [13]. Other case studies from Denmark [14], Kampala City [15], Italy [16], and Taiwan [17] demonstrated the importance of new technologies in municipal waste collection systems.

3. ANALYSIS OF WASTE MANAGEMENT DATA IN EUROPE AND HUNGARY

The used dataset in this chapter was imported from the Eurostat Statistics website, the statistical office of the European Union. Two data were used to be analyzed. The municipal waste management operations [18] and the recycling rate of municipal waste [19]. It should be considered that the collected dataset was based on the municipal waste which is produced by households next to other waste sources like commerce, offices, and public institutions. The generated municipal waste amount data includes the collected waste by or on behalf of municipal authorities and disposed of through the responsible waste management system. According to the OECD/Eurostat Joint Questionnaire municipal [18], waste includes the following materials groups: paper, paperboard and paper products, plastics, glass, metals, food and garden waste, and textiles. As it includes other types of waste such as bulky waste, households, commerce and trade, small businesses, office buildings, and institutions. As well as the collected waste from selected municipal services, for instance, waste from garden and park maintenance, waste from street cleaning services. However, it does not include waste from municipal sewage network and treatment, municipal construction, and demolition waste. The recycling rate of municipal waste indicates how waste from final consumers is used as a resource in the circular economy [19]. The municipal waste recycling rate gives a useful indication of the overall waste management system quality. The Recycling rate indicator measures the share of recycled municipal waste in the total municipal waste generation. Recycling includes material recycling, composting, and anaerobic digestion. The ratio is expressed in percent (%) as both terms are measured in the same unit, namely tons. The following definitions were introduced within the collected data:

- Incineration expresses thermal treatment of waste in an incineration plant,
- Energy recovery is defined as the incineration that fulfills the energy efficiency criteria,
- Recycling means any recovery operation which waste materials are reprocessed into products, materials, or substances whether for the original or other purposes,

- Composting and anaerobic digestion are processes of biological decomposition of biodegradable waste under controlled aerobic (composting) or anaerobic conditions,
- Landfill is defined as the deposit of waste into or onto land; it includes specially engineered landfills and temporary storage of over one year on permanent sites.

The first table shows the annual waste generated in thousands of tons for 37 European countries from 2014 to 2020. It is interesting to see that the waste amount in Hungary is relatively the same except for 2020 where it is 6.5% less than the average of 2014-2019.

Table 1 – annual municipal waste generated in thousands of tons [18]

	2014	2015	2016	2017	2018	2019	2020
Albania	1,229	1,413	1,300	1,254	1,325	1,087	1,048
Austria	4,833	4,836	4,928	5,018	5,119	5,220	:
Belgium	4,762	4,643	4,746	4,672	4,677	4,779	4,800
Bosnia and Herzegovina	1,335	1,249	1,244	1,235	1,244	1,228	:
Bulgaria	3,192	3,011	2,881	3,080	2,862	:	:
Croatia	1,637	1,654	1,680	1,716	1,768	1,812	1,693
Cyprus	513	525	539	537	562	571	543
Czechia	3,261	3,337	3,580	5,177	5,248	5,338	5,419
Denmark	4,558	4,671	4,757	4,728	4,715	4,907	4,927
Estonia	470	473	494	514	535	490	:
Finland	2,630	2,738	2,768	2,812	3,041	3,123	3,296
France	34,260	34,344	35,356	35,817	35,889	37,397	36,154
Germany	51,102	51,625	52,133	51,790	50,260	50,612	52,567
Greece	5,315	5,277	5,367	5,415	5,523	5,613	:
Hungary	3,795	3,712	3,721	3,768	3,729	3,780	3,545
Iceland	175	195	220	225	247	:	:
Ireland	2,619	:	2,763	2,768	2,912	3,086	2,768
Italy	29,652	29,524	30,112	29,572	30,165	30,023	:
Latvia	726	798	802	798	785	840	909
Lithuania	1,270	1,300	1,272	1,286	1,301	1,319	1,350
Luxembourg	348	346	474	476	488	491	498
Malta	273	285	292	312	326	351	332
Montenegro	298	310	307	305	321	339	302
Netherlands	8,894	8,866	8,861	8,792	8,806	8,806	9,321
North Macedonia	765	786	:	:	855	916	913
Norway	2,175	2,187	3,946	3,949	3,927	4,151	3,905
Poland	10,330	10,863	11,654	11,969	12,485	12,753	13,117
Portugal	4,710	4,769	4,891	5,007	5,213	5,281	5,279

Romania	4,956	4,904	5,143	5,333	5,296	5,430	5,534
Serbia	2,130	1,840	1,890	2,150	2,230	2,350	:
Slovakia	1,733	1,784	1,890	2,058	2,254	2,299	2,366
Slovenia	892	926	943	974	1,009	0	1,024
Spain	20,836	21,158	21,542	22,018	22,229	22,262	21,529
Sweden	4,295	4,422	4,439	4,551	4,416	4,611	4,460
Switzerland	6,006	6,030	6,050	5,992	6,012	6,079	6,096
Turkey	31,230	31,283	33,763	34,173	34,533	35,017	:
United Kingdom	31,129	31,475	31,710	30,912	30,786	:	:

The second table shows the annual waste generated in kilograms per capita for the same 37 European countries as it would be easier to compare the numbers in this case. In 2014, Hungary is 24th in the order, while it is the 33rd in 2018, which means a waste amount decrease, and that is harmonious with the previous table.

Table 2 – annual municipal waste generated in kilograms per capita [18]

	2014	2015	2016	2017	2018	2019	2020
Albania	425	491	452	436	462	381	369
Austria	565	560	564	570	579	588	:
Belgium	425	412	419	411	409	416	416
Bosnia and Herzegovina	349	340	354	352	356	352	:
Bulgaria	442	419	404	435	407	:	:
Croatia	387	393	403	416	432	445	418
Cyprus	602	620	633	625	646	648	609
Czechia	310	316	339	489	494	500	507
Denmark	808	822	830	820	814	844	845
Estonia	357	359	376	390	405	369	:
Finland	482	500	504	510	551	566	596
France	517	516	530	535	535	556	537
Germany	631	632	633	627	606	609	632
Greece	488	488	498	504	515	524	:
Hungary	385	377	379	385	381	387	364
Iceland	535	588	655	656	702	:	:
Ireland	562	:	581	576	598	625	555
Italy	488	486	497	488	499	503	:
Latvia	364	404	410	411	407	439	478
Lithuania	433	448	444	455	464	472	483
Luxembourg	626	607	815	798	803	791	790
Malta	628	641	642	666	672	697	643
Montenegro	479	498	493	490	516	545	486
Netherlands	527	523	520	513	511	508	534

North Macedonia	370	380	:	:	412	441	441
Norway	423	422	754	748	739	776	726
Poland	272	286	307	315	329	336	346
Portugal	453	460	474	486	507	513	513
Romania	249	247	261	272	272	280	287
Serbia	299	259	268	306	319	338	:
Slovakia	320	329	348	378	414	421	433
Slovenia	432	449	457	471	486	0	487
Spain	448	456	463	473	475	472	455
Sweden	443	451	447	452	434	449	431
Switzerland	733	728	723	709	706	709	706
Turkey	405	400	426	425	424	424	:
United Kingdom	482	483	483	468	463	:	:

The second table shows the recycling rate of municipal waste as a percentage for 36 European countries. Unfortunately, it shows that Hungary has a very slight rise in the recycling rate between 2014 and 2020 while taking into consideration that the maximum rate was in 2018. By analyzing the data, it is very interesting to notice that Slovakia has a big raise from 10.3 % to 42.2 % in 2020. Considering the similar geographical location and relatively the country area, a comparison of the waste management methods between Hungary and Slovakia is presented in next chapter.

Table 3 – annual recycling rate of municipal waste as a percentage [19]

	2014	2015	2016	2017	2018	2019	2020
Austria	56.3	56.9	57.6	57.7	57.7	58.2	:
Belgium	53.8	53.5	53.5	53.9	54.4	54.7	54.2
Bulgaria	23.1	29.4	31.8	34.6	31.5	:	:
Croatia	16.5	18.0	21.0	23.6	25.3	30.2	34.3
Cyprus	14.8	16.6	16.1	16.2	16.5	16.3	16.4
Czechia	25.4	29.7	33.6	32.0	32.2	33.3	33.8
Denmark	45.4	47.4	48.3	47.6	49.9	51.5	53.9
Estonia	31.3	28.3	28.1	28.4	28.0	30.8	:
Finland	32.5	40.6	42.0	40.5	42.3	43.5	41.6
France	39.7	40.7	42.9	44.1	45.1	43.9	42.2
Germany	65.6	66.7	67.1	67.2	67.1	66.7	67.0
Greece	15.4	15.8	17.2	18.9	20.1	21.0	:
Hungary	30.5	32.2	34.7	35.0	37.4	35.9	33.0
Iceland	29.7	0.0	0.0	0.0	0.0	:	:
Ireland	39.8	:	40.7	40.4	37.6	37.4	40.4
Italy	41.6	44.3	45.9	47.8	49.8	51.4	:
Latvia	27.0	28.7	25.2	24.8	25.2	41.0	39.6

Lithuania	30.5	33.1	48.0	48.1	52.5	49.7	45.1
Luxembourg	47.7	47.4	49.2	48.7	49.0	48.9	52.8
Malta	11.7	10.9	12.7	11.5	10.4	9.1	10.5
Montenegro	:	:	:	:	3.4	5.0	4.6
Netherlands	50.9	51.8	53.5	54.6	55.9	56.9	56.8
Norway	42.2	42.8	38.2	38.8	40.7	40.9	44.9
Poland	26.5	32.5	34.8	33.8	34.3	34.1	38.7
Portugal	30.4	29.8	30.9	29.1	29.1	28.9	26.5
Romania	13.1	13.2	13.4	14.0	11.1	11.5	13.7
Serbia	0.7	0.8	0.3	0.3	0.3	:	:
Slovakia	10.3	14.9	23.0	29.8	36.3	38.5	42.2
Slovenia	36.0	54.1	55.6	57.8	58.9	:	59.3
Spain	30.8	30.0	33.9	36.1	34.8	39.3	36.4
Sweden	49.3	47.5	48.4	46.8	45.8	46.6	38.3
Switzerland	53.5	52.7	52.5	52.5	52.5	53.0	52.8
Turkey	:	:	9.2	9.2	11.5	11.5	:
United Kingdom	43.4	43.3	44.0	43.8	44.1	:	:

4. HUNGARY AND SLOVAKIA DATA COMPARISON

Tables 4 and 5 show the municipal waste management operations in Hungary and Slovakia respectively.

Table 4 – annual municipal waste generated in thousands of tons for Hungary [18]

	2014	2015	2016	2017	2018	2019	2020
Incineration with energy recovery	373	525	554	608	501	515	604
Landfill and other disposal	2,181	1,991	1,888	1,825	1,851	1,918	1,770
Incineration	0	0	0	0	0	0	4
Recycling (material)	923	963	998	1,010	1,085	1,005	788
Recycling (composting and digestion)	236	231	294	309	309	353	383

Table 5 – annual municipal waste generated in thousands of tons for Slovakia [18]

	2014	2015	2016	2017	2018	2019	2020
Incineration with energy recovery	190	191	197	197	187	211	188
Landfill and other disposal	1,158	1,226	1,236	1,246	1,248	1,197	1,175
Incineration	4	0	0	0	30	85	0
Recycling (material)	88	136	291	433	603	616	675
Recycling (composting and digestion)	91	130	143	181	215	269	324

Figures 1 and 2 show the visualization of the waste management operations for Hungary and Slovakia respectively. Energy recovery refers to incineration with energy recovery, A refers to material, and B refers to composting and digestion.

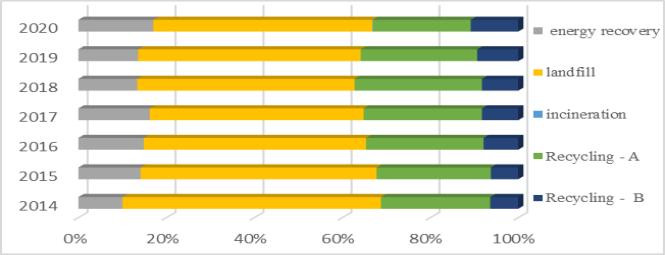

Figure 1 – Waste management operations in Hungary

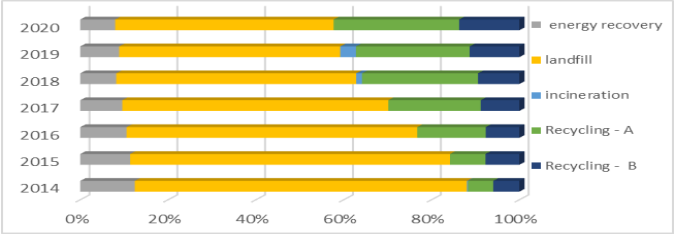

Figure 2 – Waste management operations in Slovakia

While in Hungary, it does not show any main changes in the waste management operations with a slight decrease in the landfilling, Slovakia shows a big increase in the recycling process especially for the material recycling on the share of landfilling mainly. This reflects the green efforts into a more sustainable waste management system in Slovakia in the last few years. However, the recycling rate in Hungary was three doubles than Slovakia in 2014. This shows a big importance to analyze deeply the used methods in both countries in the last decade since it has promising possibility that this study can be used and reflected on the waste management system positively in Hungary, Slovakia, or both.

5. SUMMARY

Taking the importance of the waste management systems that have direct effect on the environmental, social, and sustainability aspects, this work provided an analysis of the annual municipal waste amount, the annual municipal waste generated in kilograms per capita, and the annual recycling rate in Europe

generally and Hungary specifically. The data showed that Hungary does not have noticeable increase in the recycling rate in the last few years, which reflects a possibility and need for further research and developments in this area. Also, the data showed interesting results from the Slovakian data. A comparison between Hungary and Slovakia was presented that showed a big increase in recycling operations in Slovakia compared to Hungary from 2014 to 2020. Considering the nearby geographical location and relatively similar country area, this study suggests a deeper analysis of the waste management operations in Hungary and Slovakia that can be used and reflected on the waste management system positively in Hungary, Slovakia, or both.

ACKNOWLEDGMENT

This work is supported by the ÚNKP-21-3 NEW NATIONAL EXCELLENCE PROGRAM OF THE MINISTRY FOR INNOVATION AND TECHNOLOGY FROM THE SOURCE OF THE NATIONAL RESEARCH, DEVELOPMENT AND INNOVATION FUND.

References: 1. *Mesjasz-Lech, A., Michelberger. P.,* Sustainable Waste Logistics and the Development of Trade in Recyclable Raw Materials in Poland and Hungary, Sustainability (2019) https://doi.org/10.3390/su11154159. **2.** Proposal for a Directive of the European Parliament and of the Council Amending Directive 94/62/EC on Packaging and Packaging Waste. 2015. Available: https://eur-lex.europa.eu/legal-content/EN/TXT/?uri=CELEX:52015PC0596 Accessed: 13/01/2022. **3.** *Bing, X., Bloemhof, J.M., Ramos, T.R.P., Barbosa-Povoa, A.P., Wong, C.Y., Van Der Vorst, J.G.:* Research challenges in municipal solid waste logistics management, Waste Management (2016) pp. 584-592, https://doi.org/10.1016/j.wasman.2015.11.025. **4.** *Akkad, M.Z., Bányai, T.:* Cyber-physical waste collection system: a logistics approach, In: Solutions for Sustainable Development: Proceedings of the 1st International Conference on Engineering Solutions for Sustainable Development (2019) pp.160-168, https://doi.org/10.1201/9780367824037. **5.** *Straka, M., Rosova, A., Malindzakova, M., Khouri, S., Culkova, K.:* Evaluating the waste incineration process for sustainable development through modelling, logistics, and simulation, Polish Journal of Environmental Studies (2018) pp. 2739-2748, https://doi.org/10.15244/pjoes/81062. **6.** *Bing, X., Bloemhof, J.M., Ramos, T.R.P., Barbosa-Povoa, A.P., Wong, C.Y., Van Der Vorst, J.G.:* Research challenges in municipal solid waste logistics management, Waste Management (2016) pp. 584-592, https://doi.org/10.1016/j.wasman.2015.11.025. **7.** *Winkler, H., Kaluza, B.:* Sustainable supply chain networks - A new approach for effective waste management, WIT Transactions on Ecology and the Environment, (2006) pp. 501-510 https://doi.org/10.2495/WM060521. **8.** *Das, S., Lee, S.H., Kumar, P., Kim, K.H., Lee, S.S., Bhattacharya, S.S.:* Solid waste management: Scope and the challenge of sustainability, Journal of Cleaner Production, (2019) pp. 658-678 https://doi.org/10.1016/j.jclepro.2019.04.323. **9.** *Bányai, T., Tamás, P., Illés, B., Stankevičiūtė, Z., Bányai, Á.:* Optimization of municipal waste collection routing: impact of industry 4.0 technologies on environmental awareness and sustainability, International Journal of Environmental Research and Public Health (2019) https://doi.org/10.3390/ijerph16040634. **10.** *Gomes, M.I., Barbosa-Povoa, A.P., Novais, A.Q.:* Modelling a recovery network for WEEE: A case study in Portugal, Waste Management (2011) pp. 1645-1660 https://doi.org/10.1016/j.wasman.2011.02.023. **11.** *Mar-Ortiz, J., Adenso-Diaz, B., Gonzalez-Velarde, J.L.:* Design of a recovery network for WEEE, collection: The case of Galicia, Spain, Journal of the Operational Research Society (2011) pp. 1471-1484 https://doi.org/10.1057/jors.2010.114. **12.** *Demirel, E., Demirel, N., Gokcen, H.:* A mixed integer linear programming model to optimize reverse logistics activities of end-of-life vehicles in Turkey, Journal of Clean Production (2016) pp. 2101-2113 https://doi.org/10.1016/j.jclepro.2014.10.079. **13.** *Chung, S.S., Lau, K.Y.,*

Zhang, C.: Generation of and control measures for e-waste in Hong Kong, Waste Management (2011) pp. 544-554 https://doi.org/10.1016/j.wasman.2010.10.003. **14.** *Grunow, M., Gobbi, C., Alting, L.:* Designing the reverse network for WEEE in Denmark, CIRP Annals (2009) pp. 391-394 https://doi.org/10.1016/j.cirp.2009.03.036. **15.** *Kinobe, J.R., Bosona, T., Gebresenbet, G., Niwagaba, C.B., Vinneras, B.:* Optimization of waste collection and disposal in Kampala city. Habitat International (2015) pp. 126-137 https://doi.org/10.1016/j.habitatint.2015.05.025. **16.** *Gamberini, R., Gebennini, E., Rimini, B.:* An innovative container for WEEE collection and transport: Details and effects following the adoption. Waste Management (2009) pp. 2846-2858 http://dx.doi.org/10.1016/j.wasman.2009.07.006. **17.** *Yu, M.C., Wu, P.S.:* A simulation study of the factors influencing the design of a waste collection channel in Taiwan, International Journal of Logistics Research and Applications (2010) pp. 257-271 https://doi.org/10.1080/13675561003724646. **18.** Eurostat Statistics: Municipal waste by waste management operations. Available: https://ec.europa.eu/eurostat/cache/metadata/en/env_wasmun_esms.htm Accessed: 13/01/2022. **19.** Eurostat Statistics: Recycling rate of municipal waste. Available: https://ec.europa.eu/eurostat/cache/metadata/en/cei_wm011_esmsip2.htm.

Мохаммад Захер Аккад, Тамаш Баньяї, Мішкольц, Угорщина

АНАЛІЗ І ПОРІВНЯННЯ РОЗВИТКУ УПРАВЛІННЯ ВІДХОДАМИ В УГОРЩИНІ І СЛОВАЧЧИНІ

Анотація. *Виробництво відходів є незмінним людським процесом, що відбувається щодня у всіх спільнотах. Зі зростанням населення та розвитком промисловості, обсяги відходів зростають і процеси їх переробки займають дедалі більшу частку транспортних та вантажно-розвантажувальних завдань у міській логістиці. Збори, транспортування та обробка відходів описуються як управління відходами, яке було досліджено та розроблено, зокрема, з різними додатками, рішеннями та розробками в галузі логістики, транспорту та промисловості. Крім того, з підвищеною увагою до впливу на навколишнє середовище у різних галузях, екологічний аспект управління відходами набуває більшого значення, особливо у міській логістиці, де регулярно виникають затори. В рамках цієї роботи аналізується поводження з відходами в Європі загалом та в Угорщині зокрема. База даних Євростату використовується для цієї мети поряд із попередньою дослідницькою роботою, присвяченій цій темі. Крім того, обговорюється порівняння операцій з відходами в Угорщині та Словаччині, щоб показати різницю у розвитку цих операцій між двома країнами у період з 2014 до 2020 року. Зважаючи на важливість систем поводження з відходами, які мають безпосередній вплив на екологічні, соціальні аспекти та аспекти стійкості, у цій роботі був представлений аналіз річної кількості побутових відходів, що утворюються в кілограмах на душу населення, та річного рівня переробки в Європі взагалі та Угорщині зокрема. Дані показали, що в Угорщині за останні кілька років не спостерігається помітного збільшення рівня рециркуляції, що відображає можливість та необхідність подальших досліджень та розробок у цій галузі. Крім того, дослідження показали цікаві результати зі словацьких даних. Було представлено порівняння між Угорщиною та Словаччиною, яке показало значне зростання операцій з переробки відходів у Словаччині порівняно з Угорщиною з 2014 до 2020 року. З огляду на близьке географічне розташування та відносно схожу територію країни, це дослідження пропонує більш глибокий аналіз операцій з відходами в Угорщині. та Словаччини, які можна використовувати та які можуть позитивно позначитися на системі управління відходами в Угорщині, Словаччині або в обох країнах.*
Ключові слова: *керування відходами; міська логістика; аналіз даних*.

UDC 658.511 **doi: 10.20998/2078-7405.2022.96.04**

Á. Francuz**,** T. Bányai, Miskolc, Hungary

OPTIMISATION OF MILKRUN ROUTES IN MANUFACTURING SYSTEMS IN THE AUTOMOTIVE INDUSTRY

Abstract. *The in-plant supply has a great impact on the performance of manufacturing operation, because the manufacturing-related logistics operations influence the efficiency of manufacturing. There are different solutions to perform in-plant supply, in the automotive industry the milkrun and water spider solutions are widely used. Within the frame of this article the authors describe the optimization of milkrun routes in the manufacturing plant of an automotive supplier. The described methodology simplifies the problem for single- and multi-milkrun problems and the solution is demonstrated with an Excel Solver-based methodology. The optimization process and its practicability will be demonstrated through an example.*
Keywords: *milkrun;optimization; logistic process; automobile industry.*

1. INTRODUCTION

The permanently increased demands of customers are significantly changing the role and operation of the automotive industry. Already since the second half of the 20th century, the flexibility of automotive processes and the minimisation of these processes over time become more and more important. In the logistics systems of automotive suppliers, long lead times are linked to production logistics processes, and all companies are therefore trying to find suitable solutions and reduce the lead time of production logistics. Milkrun solutions can be considered as suitable solutions of this problem of automotive industry. Milkrun is a system for the replenishment of raw materials at specific time, in varying quantities but, as a matter of principle, in similar sizes. In fact, it means the scheduled delivery and replenishment of raw materials and components used in production The advantage of milkrun systems is that the trolleys used to implement them can be flexibly extended and, in addition to the supply of raw materials, they can also transport the waste and scrap generated in production, i.e. a raw material cycle can be established [1-3]. In this paper, the authors present an optimization algorithm that is suitable for the design of complex milkrun-based material supply systems in industrial environments. In this paper, a solution method is presented using a practical example of an automotive supplier, which uses the capabilities of Excel Solver for batch execution to determine the optimal design of a large-scale in-plant supply chain for a milkrun system.

2. LITERATURE REVIEW

The literature on the design of milkrun-based material supply systems has expanded over the last decade, due to the increasing application of these solutions in industry, especially in mechatronics assembly and automotive supplier environments [4]. Since the aim of this paper is to present a methodology for the design of milkrun-based material supply systems, in this literature review we briefly review the main sources that provide a survey of the design methods and the main algorithms used in the design. It can be clearly stated that the design of milkrun-based material supply systems can be implemented using essentially heuristic algorithms due to their complexity. An optimization method based on a genetic algorithm is presented using the example of an automotive supplier to illustrate the solution of an NP-hard mixed integer programming problem [5]. A hybrid metaheuristic solution based on a harmony search and simulated annealing forms the basis of the algorithm discussed in [6]. This approach is used to show an example of supply chain optimization involving an off-site milkrun material supply system and a crossdocking facility. An example of the application of the C-W saving algorithm can be found in source [7], where a design method that minimizes the path length of the runs and the operating cost is described. The applicability of the ant colony algorithm is illustrated in [8] through an example of a dynamic optimization problem. In the example presented, minimizing the required time of material supply tasks is included as a main objective function component. A two-phase metaheuristic algorithm based on greedy and tabu search is used as the basis for the design method presented in [9], which aims at selecting optimal vehicles in high density milkrun material supply systems. An example of the application of evolutionary strategies is presented in [10]. The uniqueness of the presented example lies in the fact that the design of the milkrun material supply system integrates the inverse processes of the packaging materials, which is an integral part of both the in-plant and the external milkrun processes [12]. Of course, in addition to heuristic solutions, a number of simulation-based applications can also greatly support the design of milkrun systems [13-16]. Following this brief literature review, the paper presents the optimisation problem. Then, the optimization of the milkrun path for one or more milkrun-routes is described.

3. THE OPTIMISATION PROBLEM

The optimisation algorithm was created in Excel using the Excel Solver extension and the VBA (Visual Basic Application) development environment. Within the frame of this article both the algorithm and a numerical example is described. The parameters of the numerical example are the followings:

- 26 production lines (marked with “A” on the layout),
- 18 junctions (marked with “I” on the layout),

- the departure and arrival locations of the warehouse (marked with "WH" on the layout),
- the straight sections connecting these production lines, junctions and warehouse points.

In this scenario, the algorithm considers the size and capacity of the production lines to be the same. The length of the sections is a ratio without units of measure. The transportation time required per unit section is 3 seconds, and the time required for material handling (loading and unloading) at each production line is 10 seconds.

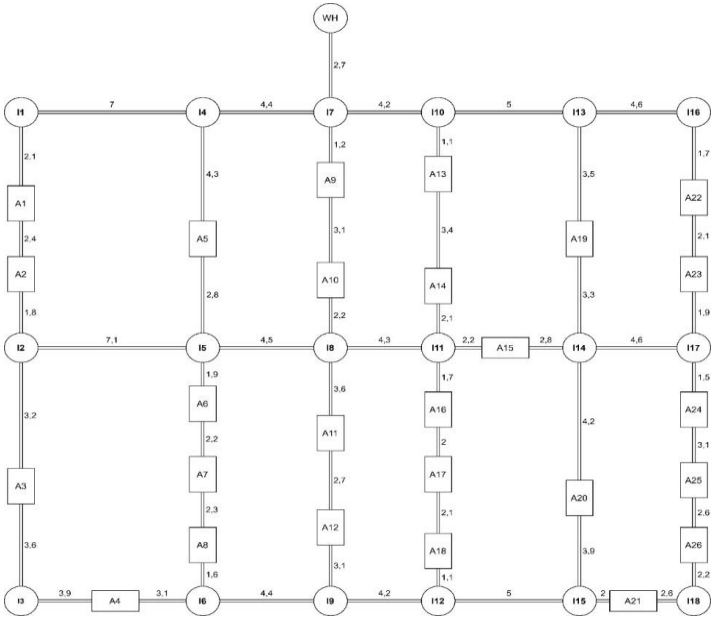

Figure 1 – Layout of the production plant

The main objective function of the optimization is the minimization of required time for the milkrun routes, while this optimised route satisfies the conditions necessary to perform the material handling tasks:

- The time required to travel the generated routes must not exceed the predefined upper time limit of the milkrun system. The predefined time limits may depend on the human resource (e.g. lunch break, end of working hours) or on technical or logistics resources (e.g. low battery). In the present numerical example, the predefined upper limit of the milkrun system is 500 seconds. In case

the time required for the route exceeds the predefined time limit, the number of milkrun routes has to be increased and the optimisation has to be performed again.

- The number of milkrun routes can only be increased until the required quantity of logistics resources (milkrun trolley) does not exceed the available number of milkrun trolleys. In the case where all available trolleys have been used but our time constraint condition is not met, the task is unsolvable because of time- and capacity-related constraints.

To determine a path minimized as a function of time, the extreme value of the single-variable function must be determined, i.e., after derivation, the value of the derived function is 0.

$$f'(t) = 0 \tag{1}$$

There is a direct proportionality between the value of time and the value of distance (1 path unit → 3 s), so the time-dependent function and the distance-dependent function differ only in constant. Since the derivative of the constant is 0, it is sufficient to optimize the path by distance to minimize the time.

$$f(t) = g(s) * c \text{ and } f'(t) = g'(s) \tag{2}$$

Hence, the optimization method works with distance values, only converting the disctane values to time values at the end of the optimisation process.

4. SINGLE-MILKRUN OPTIMISATION

When optimising for a single route, our most important constraints are the followings: (1) the initial location and the final location of each milkrun routes is the warehouse, (2) the required materials are delivered or dropped out at the different production lines exactly once. The first step is to convert the identifiers of the production lines and the warehouse point into numbered identifiers. This is necessary because the Solver extension can only optimize with numeric conditions, not with other identification conditions. The conversion is outlined in Table 1.

Table 1 – Examples for the identification of production lines

ID of production line	WH	A1	A2	A3	A4	A5
No. ID of production line	0	1	2	3	4	5

After the identifiers have been converted, all possible paths connecting two production lines (or a production line and a storage point) should be entered in the Excel spreadsheet. An identifier must also be assigned to these sections, because the optimisation of the milkrun routes is based on the transformation of these

sections. The identifier of the stages is the identifier of the outbound production line and the identifier of the inbound production line, linked by a hyphen. It is important to note that this is a directed graph, so both endpoints of an edge can be head or tail, so each edge must be taken into consideration twice.

Once the data and conditions for the optimisation have been defined, the actual optimisation is carried out.

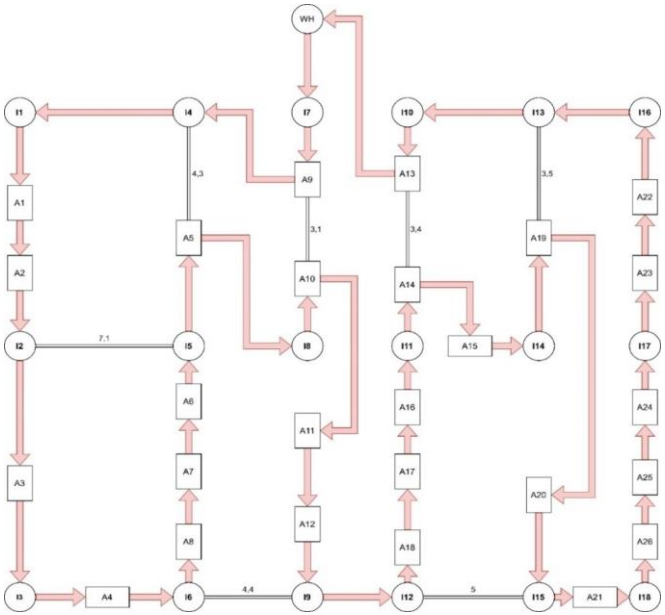

Figure 2 – Results of a single-milkrun optimisation

In the Solver interface, the following parameters are required for the optimisation:

- Value of the objective function: the cell in which the lengths of the given edges are summed.
- Objective: Minimization.
- Variables: The cells that can be varied to achieve the optimal result. In the present case, these variables are the numerical identifiers of production lines, because by changing them we can minimize the length of the route.
- Constraints: Specification of the conditions is necessary to perform the optimisation task. In out numerical example the following conditions are taken into consideration:

- The value of the cells defining the numerical identifiers of production lines is between 0 and 27.
- The required materials are delivered or dropped out at the different production lines exactly once, so each cell must have a different value (permutation representation).
- Solution method: Evolutionary.

Using the evolutionary solution method, the Solver finds the optimal solution of the milkrun routing problem within the frame of *n* phases. In the first phase, it selects the optimal solution from a random set of input values (locale optimum). From this selected set of solutions, in a second phase, it generates new solution sets and selects the optimal value. This algorithm is repeated until the solver cannot refine the solution within a given time parameter (iterative methodology). After all parameters are specified, the Solver outputs the result shown in Figure 2 as the optimal milkrun route. The most important parameters of the optimal route are the followings: length of the route is 141.9 distance unit, required time is 425.7 seconds, idle time is 260 seconds and total required time is 685.7 seconds. The total required time exceeds the predefined upper time limit, so the optimisation process must be extended with more milkrun trolleys.

5. MULTI-MILKRUN OPTIMISATION

Definition of the shortest path

Due to the fact that the result of the optimization for one milkrun route does not meet the predefined milkrun time constraint, the optimization must be performed for two milkrun routes. The first step is to determine the shortest route from the warehouse to each production line. This also requires the use of the Excel Solver extension, but determining the shortest paths to 26 production lines manually would take a lot of time, so VBA is used for batch optimization so that all the shortest paths can be determined in one step.

The optimisation requires a table of all possible routing paths. In contrary to the previous minimisation, in this phase not the edges between two production lines but the edges between the production line and the junction are taken into consideration. For each routing section, we assign its distance and a binary number. This binary number indicates whether or not the section is part of the desired shortest route. The length of the shortest route can be determined from this information multiplying the two numerical values of each route segment. Those sections that are not included in the route are eliminated by multiplying by 0. This value is minimized by the Solver. The minimization is done by varying the binary values of the route sections while constraints are taken into consideration. To specify the constraints, it is necessary to define a new table in which the starting point, the junctions and the production lines are listed. The constraint of the

optimisation problem is that the initial location (the tail of the edge) is set to 1, the arrival point (the head of the edge) is set to -1, and all other production lines and junctions are set to 0.

The value of the points is given by the fact that each departure gives a value of 1 and each arrival a value of -1. The production lines or junctions, through which the route passes are both tail and head of the edges in the graph, so they sum is 0, as do the production lines or junctions through which the route does not pass. We should always give a -1 value to the production line where we want the route to arrive. After setting all the parameters of the Solver, the batch optimisation can be performed.

Definition of production line pairs

In the next step, we use the shortest paths to form pairs of production lines, which are considered as one production line, thus reducing the number of production lines to be taken into consideration.

The pairs of production lines are formed based on the common edges. The production lines that have significant number of common edges are put into a production line pair. This analysis is made for each potential production line pairs.

The common edges can be defined using the the binary values, if the shortest route to both production lines for a given route section is 1, then there is a common edge. Such matches are counted, added together and the total number of possible common edges for all possible pairs of production lines is obtained. However, the finding of a production line pair depends not only on the number of common edges, but also on the distance between the shortest routers to the two production lines. This is necessary because common edges far away from the warehouse have a significantly higher number of common edges than those close to the warehouse, so that taking the distance into account, a much more realistic value is obtained by using it as a ratio.

```
Dim x As Integer, i As Integer, j As Integer
Dim string1 As String, string2 As String


For x = 0 To 25
For i = 4 To 108
For j = 5 To 29

string1 = Cells(2, 4 + x).Value
string2 = Cells(2, j + x).Value


If Cells(i, 4 + x).Value = 1 Then
    If Cells(i, j + x).Value = 1 Then
        Cells(i, j + 30 + 30 * x).Value = 1
    End If
End If

Cells(110, j + 30 + 30 * x).Value = WorksheetFunction.CountIf(Range(Cells(3, j + 30 + 30 * x), Cells(190, j + 30 + 30 * x)), 1)
Cells(111, j + 30 + 30 * x).Value = string1 & "-" & string2

Next j
Next i
Next x
```

Figure 3 – Algorithm to analyse the identity of edges

Definition of production line groups

The next step of the optimization is to use the ratio defined in the previous section to determine the two groups of production line pairs for which the milkrun routes will be optimized separately. Starting with the highest ratio, the common edges are connected in descending order until two large groups of lines are formed.

6. RESULTS

Once we have the two groups of production lines for which we want to optimize the routes, we perform the minimization. The settings of the Solver are exactly the same as for the optimization for one milkrun route. The most important parameters of the optimal route are the followings: length of the routes are 95.1 and 117.4 distance unit, required time is 285.3 and 352.2 seconds, idle time is 140 and 120 seconds and total required time is 425.3 and 472.2 seconds.

The results obtained meet the predefined time-related constraints for the Milkrun trolleys and the times required to cover the route are almost the same, so the optimisation is considered complete. In case the obtained time results do not meet the constraints, the method described for the optimization of multiple milkrun trolleys should be repeated by increasing the number of milkrun trolleys.

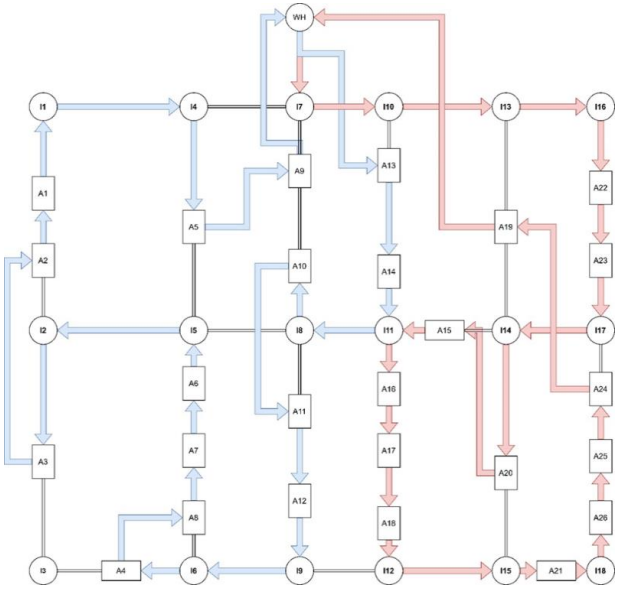

Figure 4 – The optimised milkrun routes in the manufacturing plant

7. SUMMARY

Today, the automotive industry is increasingly influenced by customers' demands. Lead time is a significant part of the processes performing manufacturing. In an automotive supplier's production logistics system, there are many methods to achieve a flexible and well-functioning material flow. One such system is the milkrun system, which implements material flow by creating route among manufacturing objects. The topic of this paper was the optimization of Milkrun systems, where we have presented a methodology to optimize single or multiple milkrun paths. The process has been illustrated through a numerical example. Potential future research direction is the application the mentioned milkrun optimisation method for transportation problems, especially in the case of first-mile problems regarding intermediate storage networks [17], and it is also possible to take the potential of Industry 4.0 technologies [18] for the real-time routing into consideration.

ACKNOWLEDGEMENT

The described article was carried out as part of the NTP-SZKOLL-20-0022 National Talent Program of the Ministry of Human Capacities. The research is supported by the ÚNKP-21-1. New National Excellence Program of the Ministry for Innovation and Technology from the source of the National Research, Development and Innovation Fund.

References: 1. *Lean logistics*: Solutions in production: The milkrun and the waterspider. Available: http://www.leanlogisztika.hu/termeles-kiszolgalo-megoldasok-a-milkrun-es-a-water-spider/ Downloaded: 11/07/2020. **2.** *Mácsay, V., Bányai, T.:* Toyota production system in milkrun based in-plant supply, Journal of Production Engineering vol.9(1) (2017) pp. 141-146. http://doi.org/10.24867/JPE-2017-01-141. **3.** *Bányai, T., Telek, P., Landschützer, C.:* Milkrun based in-plant supply – An automotive approach, Lecture Notes in Mechanical Engineering (2018) pp. 170-185. https://doi.org/10.1007/978-3-319-75677-6_14. **4.** *Kilic, H.S., Durmusoglu, M.B., Baskak, M.:* Classification and modeling for in-plant milk-run distribution systems, International Journal of Advanced Manufacturing Technology vol.62(9-12) (2012) pp. 1135-1146. https://doi.org/10.1007/s00170-011-3875-4. **5.** *Sadjadi, S.J., Jafari, M., Amini, T.:* A new mathematical modeling and a genetic algorithm search for milk run problem (an auto industry supply chain case study), International Journal of Advanced Manufacturing Technology vol.44(1-2) (2009) pp. 194-200. https://doi.org/10.1007/s00170-008-1648-5. **6.** *Hosseini, S.D., Shirazi, M.A., Karimi, B.:* Cross-docking and milk run logistics in a consolidation network: A hybrid of harmony search and simulated annealing approach, Journal of Manufacturing Systems vol. 33(4) (2014) pp. 567-577. https://doi.org/10.1016/j.jmsy.2014.05.004. **7.** *You, Z.L., Jiao, Y.:* Development and application of milk-run distribution systems in the express industry based on saving algorithm, Mathematical Problems in Engineering (2014) 536459. https://doi.org/10.1155/2014/536459. **8.** *Ma, J.H., Sun, G.H.:* Mutation ant colony algorithm of milk-run vehicle routing problem with fastest completion time based on dynamic optimization. Discrete Dynamics in Nature and Society. 2013, 418436. https://doi.org/10.1155/2013/418436. **9.** *Lin, Y., Xu, T.Y., Bian, Z.Y.:* A two-phase heuristic algorithm for the common frequency routing problem with vehicle type choice in the milk run, Mathematical Problems in Engineering (2015) 404868. https://doi.org/10.1155/2015/404868. **10.** *Ranjbaran, F. Kashan, A.H., Kazemi, A.:* Mathematical formulation and heuristic algorithms for optimisation of auto-part milk-run logistics network considering forward and reverse flow of pallets, International Journal of

Production Research vol.58(6) (2020) pp. 1741-1775. https://doi.org/10.1080/00207543.2019.1617449. **11.** *Korytkowski, P., Karkoszka, R.:* Simulation-based efficiency analysis of an in-plant milkrun operator under disturbances, International Journal of Advanced Manufacturing Technology vol.82(5-8) (2016) pp. 827-837. https://doi.org/10.1007/s00170-015-7442-2. **12.** *Fedorko, G., Molnar, V., Honus, S., Neradilova, H., Kampf, R.:* The application of simulation model of a milk run to identify the occurrence of failures, International Journal of Simulation Modelling vol.17(3) (2018) pp. 444-457. https://doi.org/10.2507/IJSIMM17(3)440. **13.** *Tamás, P.:* Decision support simulation method for process improvement of intermittent production systems, Applied Sciences-Basel vol. 7(9) (2017) 950. https://doi.org/10.3390/app7090950. **14.** *Bohács, G., Kovács, G., Rinkács, A.:* Production logistics simulation supported by process description languages, Management and Production Engineering Review vol.7(1) (2016) pp. 13-20. https://doi.org/10.1515/mper-2016-0002. **15.** *Fedorko, G., Vasil, M., Bartosova, M.:* Use of simulation model for measurement of milkrun system performance, Open Engineering vol.9(1) (2019) pp. 600-605. https://doi.org/10.1515/eng-2019-0067. **16.** *Veres, P.; Illés, B.; Landschützer, C.*: Supply Chain Optimization in Automotive Industry: A Comparative Analysis of Evolutionary and Swarming Heuristics, In Vehicle and Automotive Engineering 2; Jármai, K., Bolló, B., Eds.; Springer: Cham, Switzerland, 2018; pp. 666–676. https://doi.org/10.1007/978-3-319-75677-6_57. **17.** *Bányai, Á.:* Optimisation of intermediate storage network of JIT purchasing, Advanced Logistic Systems: Theory and Practice vol.5 (2011) pp. 35-40. **18.** *Nagy, G., Illés, B., Bányai, Á.:* Impact of Industry 4.0 on production logistics, IOP Conference Series: Materials Science and Engineering vol.448(1) (2018) 012013.

Адам Француз, Тамаш Баньяї, Мішкольц, Угорщина

ОПТИМІЗАЦІЯ МАРШРУТІВ MILKRUN У ВИРОБНИЧИХ СИСТЕМАХ АВТОМОБІЛЬНОЇ ПРОМИСЛОВОСТІ

Анотація. *Внутрішньозаводські поставки мають великий вплив на продуктивність виробничих операцій, оскільки логістичні операції, що пов'язані з виробництвом впливають на ефективність виробництва. Існують різні рішення для внутрішньозаводського постачання. В автомобільній промисловості широко використовуються рішення Milkrun та Water Spider. В рамках цієї статті автори описують оптимізацію маршрутів Milkrun на заводі постачальника автомобілів. Описана методологія спрощує завдання для задач з одним і декількома Milkrun, і рішення демонструється методологією на основі Excel Solver. Процес оптимізації та його здійсненність продемонстровано на прикладі. Коли ми маємо дві групи виробничих ліній, для яких ми хочемо оптимізувати маршрути, ми виконуємо мінімізацію. Налаштування «розв'язувача» такі самі, як і для оптимізації для одного маршруту Milkrun. Найбільш важливими параметрами оптимального маршруту є наступні: протяжність маршрутів 95,1 та 117,4 одиниці відстані, необхідний час 285,3 та 352,2 секунди, час простою 140 та 120 секунд та загальний необхідний час 425,3 та 472,2 секунди. Отримані результати відповідають визначеним тимчасовим обмеженням для візків Milkrun, а час, необхідний для проходження маршруту, практично однаковий, тому оптимізація вважається завершеною. У випадку, якщо отримані часові результати не відповідають обмеженням, слід повторити метод, описаний для оптимізації кількох візків для Milkrun, збільшивши кількість візків для Milkrun. Потенційним майбутнім напрямком досліджень є застосування згаданого методу оптимізації Milkrun пробігу для транспортних завдань, особливо у разі проблем першої милі щодо мереж проміжного зберігання, а також можливе використання потенціалу технологій Індустрії 4.0 для вирішення транспортних завдань. враховувати маршрутизацію у реальному часі.*

Ключові слова: *Milkrun; оптимізація; логістичний процес; автомобільна промисловість.*

UDC 621.923 **doi: 10.20998/2078-7405.2022.96.05**

V. Fedorovich, I. Pyzhov, Y. Ostroverkh, Kharkiv, Ukraine

METHODOLOGY OF DEFINITION OF OPTIMAL DIAMOND WHEEL CHARACTERISTICS AT STAGES OF PRODUCTION AND OPERATION

Abstract. *The problem of increase of effectiveness of manufacturing and application of diamond-abrasive tool is still a challenging research subject. Development of computer facilities opens up possibilities for development of three-dimensional (3D) methodology of integrated study of the interconnected processes of manufacturing and exploitation of diamond-abrasive tool and improvement of the single-point tool reliability at the stage of tool sharpening. Creation of the methodology of 3D simulation of processes of diamond-abrasive tool sintering and processes of machining allows to increase essentially validity of the obtained results, to reduce volume of experimental researches for definition of optimum grinding conditions and to develop new technologies, tools and equipment. The developed methodology gives the opportunity to create expert system for assignment of rational characteristics of diamond wheels and grinding modes. The proposed 3D methodology to research processes of diamond-abrasive machining covers all basic stages of life cycle of the tool, including processes of manufacturing and exploitation. Subsystem of computer-generated determination of conditions of manufacturing of defect-free diamond wheels and grinding of superhard materials on the base of 3D simulation of deflected mode of elements of the "SHM crystal grain – metal phase – grain – bond" system at process of diamond wheel sintering and grinding is developed.*

Keywords: *simulation; system "Wheel working surface (WWS)-SHM"; grinding; destruction; system "polycrystal - grain - bond".*

1. INTRODUCTION

It is known that efficiency of diamond grinding process is defined both characteristics of diamond wheels and correct selection of grinding conditions. The former is mostly provided at the stage of manufacture of diamond wheels, the latter - at the stage of their production.

During grinding process of materials, hardness of which does not allow to provide the classic requirement of the cutting theory about twofold exceeding of tool material (TM) hardness above hardness of material to be machined (MM), the relation of «material to be machined - diamond grain – wheel bond» system element strengths can be determinant. For example, at diamond grinding of superhard materials (SHM), when hardness of TM and hardness of MM are practically identical, the efficiency of the process is completely defined by an optimal relation of strengths of SHM, diamond grains and wheel bond [1].

Now there are some hundreds brands of bonds applied in Ukraine for diamond wheels. These bonds essentially differ on strength properties. For example, only metal bonds have rather wide range of strengths from aluminium up to hard-alloys.

Similarly, diamond grinding powders from AC2 up to AC160T are characterized by the same wide range of strength properties which differ on hardness in hundreds time.

However, now there is no methodology for selection of an optimal combination of strength properties of diamond grains and metal bond as applied to processing of particular material to be machined.

The available recommendations on application of any diamond grains and metal bonds are of very common nature and have wide ranges. Such recommendations, taking into account that diamond grains are expensive (cost of diamond grains differs depending on a brand of a grain in hundreds times), lead to low efficiency of their usage and therefore to high production cost of the of diamond grinding process, that essentially restrains diamond grinding application during processing. Insufficiently grounded selection of concentration level of diamond grains in diamond wheels leads to disadvantageous grain usage too. So the concentration of diamond grains (25,50,100,150,200 %), traditionally applied in commercial wheels, should be defined more precisely. Our preliminary investigations have shown, that for processing of particular material to be machined one should select the specific on strength (and price) diamond grains, these grains should be placed in the specific on strength bond and amount (concentration) of the grains in the wheel should be strongly specific (calculated). Thus to save diamond grains their concentration should not be restricted to commercial one. At the same time the task of an optimal combination of strength properties of metal bond and diamond grains should be solved too from the point of view of saving their integrity during diamond wheel sintering.

2. LITERATURE REVIEW

Deliberate attempt has therefore been made in this work to elaborate the calculated methodology for solving given problem. The methodology of calculation is grounded on 3D simulation of deflected mode of grinding zone and analysis of fracture processes occuring in this zone depending on strength properties of diamond grains, bond and material to be machined.

The efficiency of the grinding process with SD and cubic boron nitride wheels using porous metal bonds is shown in [2,3]. In them, the authors studied the design and characteristics of metal-bonded diamond grinding wheels made by selective laser melting, studied the grinding temperature and wear of superabrasive boron wheels on a porous metal bond with highly efficient deep grinding.

The authors [4] found that the ultimate load causing the fracture of diamond grains depends not only on the compressive strength of the diamond grains, but also on the compressive strength of the bond, as well as on the coefficient of embedding of diamond grains in it. The classification of the types of wear of

diamond wheels using various bonds and possible models of fracture of diamond grinding wheels is given in [5, 6].

M. Mahdi and L. Zhang [7] used the finite element method (FEM) to simulate stresses caused by mechanical loading, thermal cycling and phase transitions. H. Sakamoto [8] applied FEM to study the wear and deformation of diamond cutting wheels with different structures by determining the conditions that ensure the minimum temperature during grinding and its uniform distribution. In the works of V. Yadava [9,10] using the FEM, the residual stresses arising during high-speed grinding are determined. The generalization of a large number of experimental data and the results of model experiments [11, 12] made it possible to carry out a comparative analysis of the fracture criteria. The possibilities of using the theory of plastic fracture were considered by K. Iwata (1984), Cockroft and Latham (1968), K. Osakada (1984), R. Mises et al. (1939) [13,14]. When analyzing the behavior of plastic materials, the value of equivalent stresses according to von Mises is most often used as a fracture criterion [15].

To solve nonlinear finite element problems of mechanics of a deformed solid body and heat transfer, it is advisable to use the multipurpose software package LS-DYNA, intended for solving three-dimensional dynamic problems of mechanics of a deformed solid body. [16, 17].

3. RESEARCH METHODOLOGY

Available software packages based on finite element method (FEM) such as «Cosmos», «Nostran» and «Ansys» open new possibilities for study of deflected mode at sintering (production) of diamond wheels and grinding zone. The methodology of 3D simulation of deflected mode (DM) of SHM grinding zone, realized with using of such packages, has allowed to develop expert system of grinding process by calculated way (theoretically), without long-duration and laborious experiments. This expert system permit to predict and to optimize both available defect-free processes of machining of superhard materials, and newly-developed ones [18].

To determine optimal combination of strength properties of diamond grains, material to be machined and metal bond both at the stage of production of diamond wheels, and at the stage of their exploitation the investigations of sintering process of diamond wheels on metal bonds and grinding zone of various hard-to-work materials have been carried out using the developed methodology of 3D simulation of DM (fig. 1).

The task, solved in the process of 3D simulation of DM of sintering zone of diamond-bearing layer of wheel on metal bond is the definition of optimal combination of strength properties of diamond grains and bond, at which integrity retention of diamond grains is provided during diamond wheel sintering.

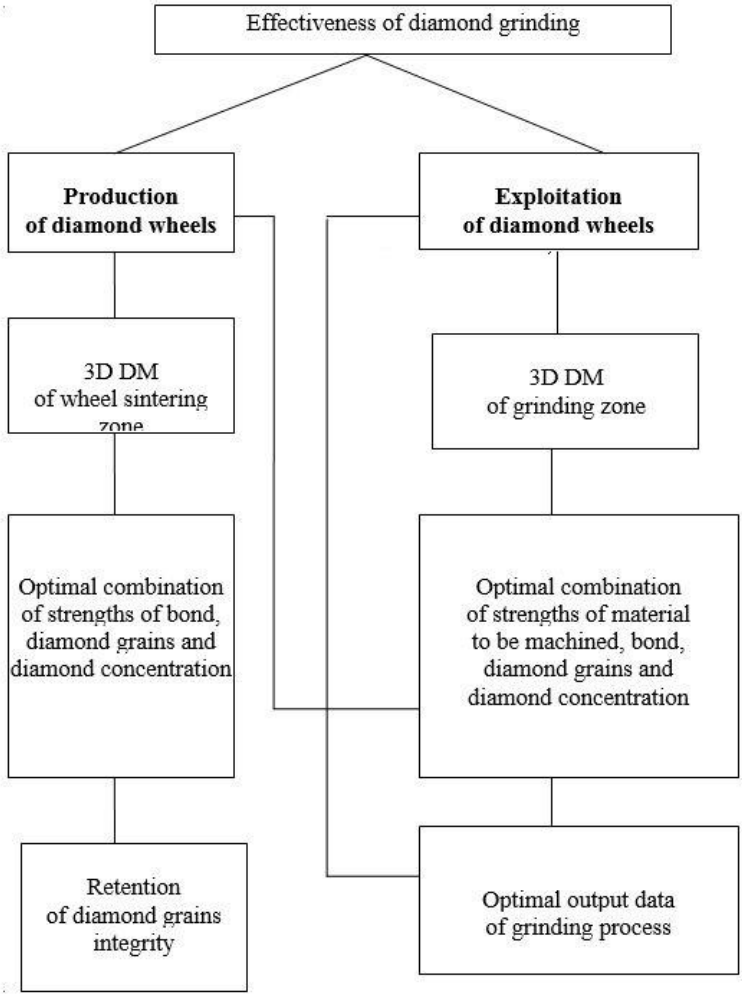

Figure 1 – Finding of optimal combination of strength properties of material to be machined, metal bond, diamond grains and diamond concentration in sequence

Contrary to available ideas, proposed to consider the model of diamond-bearing layer of wheel as perfect one [19,20], we have stated, that the structure of diamond layer of the wheels contains initial defectiveness in the form of damaged

diamond grains, which can be quantitatively defined by damage degree of diamond grains [6].

It is established work [6], that the particle-size analysis of synthetic diamond grains AC50 400/315, extracted by recuperation from tvesal sample, has shown that during sintering only about 10-20 % of grains remain undamaged. So it is shown, that diamond grain concentration influences deeply on damaging rate of diamond grains when sintering composite diamond materials (CDM). The increase of concentration from 50 up to 150 % raises damaging of diamond grains at sintering process in 2,8 times.

Since the technology of sintering of diamond-bearing layer of the wheel, for example, on hard-alloy bond such as BK, is practically identical with the technology of sintering of CDM, we think, that some part of grains at sintering of diamond wheels are damaged.

It is shown [21], that during sintering of diamond wheels the percentage of main fraction (coarse grains) is diminished by 20-30 %.

Apparently, the diamond grains of different strength will be differently fractured during sintering. Certainly, both metal bond composition, and as a consequence, technological parameters of wheel sintering will deeply influence on damaging rate of diamond grains.

At 3D simulation of sintering process the fragment of diamond-bearing layer of wheel was presented as a cube dimensioned 300x300x300 μm, in midpoint of which a diamond grain as an octahedron dimensioned 100x100 μm was placed, that corresponds to 100 % concentration of diamond wheel. At simulation of 50 % diamond grain concentration wheel the size of the cube was redoubled and so on. The model was loaded with stress and temperature appropriate to the real process of diamond wheel sintering. It is accepted, that if the reduced stress in diamond grain exceeds ultimate strength it will be considered as destroyed (defective) one. Sintering process of diamond-bearing layer was simulated for various metal bonds from aluminium up to hard-alloy ones, using diamond grains with various strength from AC2 up to AC160T. Varying combination of diamond grain strength and grain concentration in the wheel for various metal bonds one can determine such their combinations, at which retention of diamond grain integrity was provided i.e. grains should not fracture during sintering. It is established, that not all of commercial wheels with usable combination of brand of diamond grains and brand of metal bond can be manufactured with standard concentration of diamond grains without failure of their integrity. So, for example, at sintering of wheel on bond M6-14 with diamond grains of brand AC6 the grain concentration in the wheel should not exceed 7 %, otherwise grains will fracture as early as wheel sintering. It is shown, that for guaranteed retention of diamond grain integrity practically in all commercial wheels, their concentration should be much less than applied one. Such tendency coordinates well with possibility and necessity of lowering of

diamond grain concentration for wheel up to level of 10-15 % at grinding of superhard materials [22].

4. RESULTS

It is established, that for retention of diamond grain integrity during sintering of the wheels one must observe combinations of brand of diamond grains and brand of metal bond. So diamond grains with strength not less than indicated in table 1 should be included in various metal bonds for the wheel of 100 % grain concentration.

Table 1 – Maximum permissible strength of diamond grains for various bonds

Bond	M1-01	M2-09	M6-14	BK
Grain	AC6	AC32	AC50	AC160

Thus, at the first stage of the investigations the optimal combinations of strengths of metal bond and diamond grains with their maximum concentration limit in the wheel providing retention of diamond grain integrity during diamond wheel production are established. Optimal relation of strengths of bond, diamond grains and grain concentration, obtained at this stage, are only limiting parameters (characteristics) and should be defined more precisely for diamond grinding process depending on strength properties of material to be machined.

After obtaining of the prescribed limits one should determine optimal combination of strengths of material to be machined, bond, diamond grains and grain concentration in the wheel, which provides maximal efficiency of grinding process. During exploitation optimal combination of strengths of bond, diamond grains and grain concentration is determined depending on strength properties of MM. For this purpose the methodology of 3D simulation of DM, only for grinding zone, will be used too.

Optimal combination of strengths of bond, grains and grain concentration should provide such level of DM in grinding zone, when:

- Retention of diamond grains in bond is provided;
- Brittle microfracture of diamond grains (at grinding of "soft" materials) or self-sharpening of grains without forming of wear platforms (at grinding of "hard" materials) are eliminated;
- Maximal stresses in material to be machined (removal of allowance) are provided;
- Formation of inadmissible defect layer is eliminated.

If physico-mechanical characteristics of MM and strength of diamond grains and bond are used as initial data, then outcomes of computation will be concentration of diamond grains. In order to find strength of diamond grains as a

result of computation, one should use physico-mechanical characteristics of MM and strength of bond and concentration of diamond grains, and so on.

Analytical model and example of computation data of 3D DM of the «SHM-grain- bond» system are shown in fig. 2.

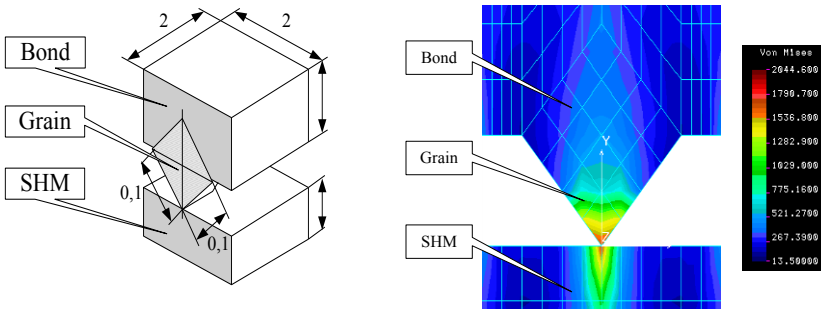

a) b)

Figure 2 – 3D analytical model of grinding area (a) and example of DM computation data of «SHM-grain- bond» system (b)

Thus, space of optimal fracture of units of the «SHM-grain- bond» system elements, where the grain is kept and is not fractured, SHM is fractured in contact, but is not cracked owing to the total loading of all grains (except spoilage) is theoretically defined (fig. 3).

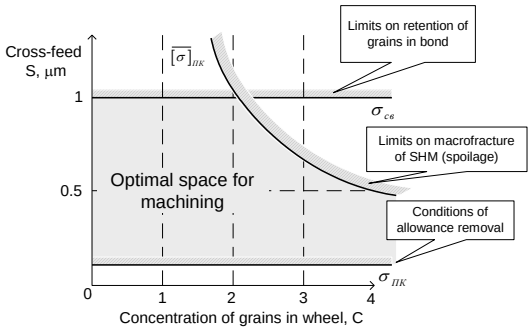

Figure 3 – Computation data of optimal concentration of diamond grains and cross-feed on strength properties of grinding zone elements

The space of optimal conditions of diamond grinding of different brands of SHM, including newly-produced brands can be theoretically defined. The further

experimental researches with the purpose of curtailment of their size, will be carried out in this area.

Optimal characteristics of diamond wheels and conditions of processing (table 2) are defined as applied to diamond grinding of superhard materials

Table 2 – Optimal characteristics of diamond wheels at the stage of their exploitation

SHM to be machined	Strength of diamond grains	Strength of metal bond, GPa	Concentration of diamond grains in wheel	Grinding speed m/s	Normal pressure, MPa
АСПК	АС160	600	5-7	40-50	3-4
АСБ	АС85	500	8-11	35-40	2,5-3
ДАП	АС60	400	12-15	30-35	2-2,5
СКМ	АС32	300	17-22	25-30	1,5-2
Гексанит-Р	АС15	100	25-35	20-30	1-1,5
Эльбор-Р	АС15	100	35-50	20-30	1-1,5

Such relation of strength properties of materials to be machined, bond and diamond grains ensures defect-free processing under conditions of the maximum possible productivity and minimum specific consumption of grains during diamond grinding. One of the substantial reserve for effectiveness increase of given kind of processing is finding of similar optimal relations as applied to the process of diamond grinding not only SHM, but also hard alloys, ceramics, polymers and other materials.

5. CONCLUSIONS

Thus, methodology of definition of the scientifically proved recommendations on application of optimal combination of strengths of bond, diamond grains and grain concentration for effective grinding of materials of different hardness has been worked up. It is established, that strength of wheel bond is the major parameter defining not only degree of diamond retention, but also productivity of the grinding process. Concentration of diamond grains in wheel should be assigned starting from the relation of strength of the «material to be machined-grain-bond» system elements. The defectiveness level at diamond grinding of SHM is defined by relation of strength of SHM, bond, diamond grains and grain concentration in the wheel. Graininess selection of diamond wheel should be carried out taking into consideration strength properties of diamond grains, which differ in size.

References: 1. Effect of hot pressing temperature on microstructure, mechanical properties and grinding performance of vitrified-metal bond diamond wheels / *Dong dong Song, Long Wan, Xiaopan*

Liu, Weida Hu, Delong Xie, Junsha Wang // International Journal of Refractory Metals and Hard Materials. – 2016 . – Vol.54. – pp. 289-294. **2.** *Tian C.C., Li X.K, Zhang S.B., Guo G.Q., Wang L.P., Rong Y.M.* Study on design and performance of metal-bonded diamond grinding wheels fabricated by selective laser melting (SLM) //View ResearcherID and ORCID MATERIALS & DESIGN Volume: 156 pp. 52-61. DOI: 10.1016/j.matdes.2018.06.029 Published: OCT 15 (2018). **3.** *Li Z., Ding W.F., Ma C.Y., Xu J. H.* Grinding temperature and wheel wear of porous metal-bonded cubic boron nitride superabrasive wheels in high-efficiency deep grinding //Proceedings of the institution of mechanical engineers part b-journal of engineering manufacture Volume: 231 Issue: 11 pp. 1961-1971. DOI: 10.1177/0954405415617928 Published: SEP 2017. **4.** *Popov A. V.* Analysis of destruction of diamond grinding wheels (in Russian)/ A. V. Popov // Bulletin of the Tula State University. Technical science. – 2008. – No. 4. – pp. 196–200. **5.** Classification of possible models the diamond grinding wheels destruction/ *A.V. Popov* // III. Mezinárodní konference STROJÍRENSKÁ TECHNOLOGIE – PLZEŇ. 21 – 22. 1. (2009). **6.** *Novikov N.V., Maistrenko A.L., Kulakovsky V.N.* Resistance to fracture of superhard composite materials.(in Russian) – Kyiv: Nauk. Dumka, 1993. – 220 p. **7.** *Mahdi M.* Applied Mechanics in Grinding: residual stress and surface hardening by coupled thermo-plasticity and phase transformation / M. Mahdi, L. Zhang // International Journal of Machine tools Manufacture. – 1998. – № 38. – pp.1289–1340. **8.** *Sakamoto H.* Effects of the Megasonic Coolant on Cylindrical Grinding Performance / [H. Sakamoto, S. Shimizu, K. Suzuki et al.] // Key Engineering Materials. – 2003. – Volume 1. – pp. 189–194. **9.** *Yadava V.* Parametric Study of Temperature Distribution in Electro-Discharge Diamond Grinding / V. Yadava, V. K. Jain, P. M. Dixit // Materials and Manufacturing Processes. – 2004. – Volume 19. – Issue 6. – pp. 1071–1101. **10.** *Yadava V.* Theoretically analysis of Thermal Stress in Electro-Discharge Diamond Grinding / V. Yadava, V. K. Jain, P. M. Dixit // Machining Science and technology. – 2004. – Vol. 8. – № 1. – pp. 119–140. **11.** *Bil H.* Finite Element Modeling of Machining: A Comparison of Different Approaches with Experiments / H. Bil, A. E. Tekkaya, E. S. Kilic // Proceedings of 7th CIRP International workshop on modeling of machining operations: École nationale supérieure d'arts et métiers (ENSAM). – Cluny (France), 04–05 of May, 2004. **12.** Development of a Force Controlled Automatic Grinding System for Actual NC Machining Centers / *Y. Hatamuraa, T. Nagaoa, M. Mitsuishia et al.* // CIRP Annals – Manufacturing Technology. – 1989. – Volume 38.– Issue 1.– pp. 343–346. **13.** *Marusich T. D.* Modelling and Simulation of High-Speed Machining / T. D. Marusich, M. Ortiz // International Journal for Numerical Methods in Engineering. – 1995.– Vol. 38. – pp. 3675–3694. **14.** *Hashemi J.* Finite-Element Modelling of Segmental Chip Formation in High-Speed Machining / J. Hashemi, A. A. Tseng, P. J. Chou // Journal of Materials Engineering and Performance. – 1994. – Vol. 3. – pp. 712–721. **15.** *Mises R.* Mechanic der plastischen Formandenderung von Kristallen / R. Mises // Zeitschrift fur Angewandte Mathematik und Mechanik. – 1928. – Bd. 8.– H.3. – pp. 161–184. **16.** *Böhm A.* FEM-Simulation der Bearbeitung von Faserverbundwerkstoffen mit Hilfe von LS–Dyna / A. Böhm. – Stuttgart: University of Stuttgart, 2010. – 123 p. **17.** *Hallquist J. O.* LS-DYNA Theoretical manual / J. O. Hallquist. – Livermore: LSTC, 1998. – 498 p. **18.** *Fedorovich V.A.* Development of scientific grounds and methods of practical realization of adaptability control at diamond grinding of superhard materials, Kharkiv DSc dissertation (2002) 466 p. (In Russian). **19.** *B. Denkena, A. Krödel, R. Lang.* Fabrication and use of Cu–Cr–diamond composites for the application in deep feed grinding of tungsten carbide/Diamond & Related Materials 120 (2021). **20.** *Chen J.B., Fang Q.H., Wang C.C., Du J.K., Liu F.* Theoretical study on brittle–ductile transition behavior in elliptical ultrasonic assisted grinding of hard brittle materials. Precis Eng. 2016, 46. pp. 104-117. **21.** *Kyratsis, P., Tzotzis, A., Markopoulos, A., Tapoglou, N.* CAD–based 3D–FE modelling of AISI–D3 turning with ceramic tooling. In: Machines. Volume 9, Issue 1, January 2021, Article number 4, pp. 1–14. DOI: 10.3390/machines9010004 (2021). **22.** *Samuel, R., Asadi, M., Tarda, A., Simbotin, G., Markopoulos, A.P.* Validating dynamic crush response of unidirectional carbon fibre tube via finite element analysis method using LS-DYNA. In: IOP Conference Series: Materials Science and Engineering, Volume 1037, Issue 1, 11 February 2021, DOI: 10.1088/1757-899X/1037/1/012027 (2021).

Володимир Федорович, Іван Пижов, Євгеній Островерх,
Харків, Україна

МЕТОДОЛОГІЯ ВИЗНАЧЕННЯ ОПТИМАЛЬНИХ ХАРАКТЕРИСТИК АЛМАЗНОГО КРУГА НА ЕТАПАХ ВИРОБНИЦТВА ТА ЕКСПЛУАТАЦІЇ

Анотація. *Проблема підвищення ефективності виготовлення та застосування алмазно-абразивного інструменту залишається актуальною темою досліджень. Розвиток обчислювальної техніки відкриває можливості для розробки тривимірної (3D) методики комплексного дослідження взаємопов'язаних процесів виготовлення та експлуатації алмазно-абразивного інструменту та підвищення надійності одноточкового інструменту на етапі його заточування. Створення методики тривимірного моделювання процесів спікання алмазно-абразивного інструменту та процесів механічної обробки дозволяє суттєво підвищити достовірність отриманих результатів, скоротити обсяг експериментальних досліджень для визначення оптимальних режимів шліфування та розробити нові технології, інструменти та обладнання. Розроблена методика дає можливість створити експертну систему для завдання раціональних характеристик алмазних кругів та режимів шліфування. Пропонована 3D-методика дослідження процесів алмазно-абразивної обробки охоплює всі основні етапи життєвого циклу інструменту, включаючи процеси виготовлення та експлуатації. Таким чином, розроблено методику визначення науково обґрунтованих рекомендацій щодо застосування оптимального поєднання міцності зв'язки, алмазних зерен та концентрації зерен для ефективного подрібнення матеріалів різної твердості. Встановлено, що міцність зв'язки круга є найважливішим параметром, визначальним і як ступінь алмазоутримання, і як продуктивність процесу шліфування. Концентрацію алмазних зерен у крузі слід задавати виходячи із співвідношення міцності елементів системи «матеріал–зерно–зв'язка». Рівень дефектності при алмазному шліфуванні НТМ визначають за співвідношенням міцності НТМ, зв'язки, алмазних зерен та концентрації зерен у крузі. Підбір зернистості алмазного круга слід проводити з урахуванням властивостей міцності алмазних зерен, що різняться за розміром.*

Ключові слова: *моделювання; система "робоча поверхня круга – оброблюваний матеріал"; шліфування; руйнування; система "полікристал – зерно – зв'язка".*

UDC 621.9.04 **doi: 10.20998/2078-7405.2022.96.06**

I.T. Christodoulou, V.E. Alexopoulou, N.E. Karkalos,
E.L. Papazoglou, A.P. Markopoulos, Athens, Greece

ON THE SURFACE ROUGHNESS OF 3D PRINTED PARTS WITH FDM BY A LOW-BUDGET COMMERCIAL PRINTER

Abstract. *As additive manufacturing machines price is decreasing, while, at the same time, the expertise in the relevant field is rising, it is essential to test and evaluate the low-budget machines that are available for commercial use. Whilst low-budget machines are widely utilized for rapid prototyping and experimentation, they are not capable of producing parts with high surface quality and achieve high levels of repeatability due to low quality hardware and not optimized software. Having said that, the main aim of the current study is to experiment with a low budget Fused Deposition Modeling (FDM) 3D-Printer, and evaluate the surface roughness of the printed parts in respect to the angle from the print plate. Polylactic Acid (PLA) was chosen as filament material, while the printed parts surface roughness was measured according to the ISO ASTM 52902-2021 standard. The surface roughness was estimated in terms of the R_a and R_z values, while a statistical analysis was implemented in order some interesting conclusions to be deduced regarding the correlation between part orientation and surface quality.*

Keywords: *additive manufacturing machines; rapid prototyping; Fused Deposition Modeling; surface roughness; 3D-Printer.*

1. INTRODUCTION

Over the last decades, Additive Manufacturing (AM) processes have become a hot topic for both the researching and the industrial world, as they can give highly customized and geometrically complex products. In AM, a 3D-CAD model is virtually broken down into 2D-cross sections and the final product is built by consecutive layers [1]. Many AM techniques have been developed, such as vat polymerization (SLA), powder bed fusion (SLS, SLM) and material extrusion (FDM).

Specifically, in Fused Deposition Modeling (FDM), a thermoplastic filament (such as PLA, ABS, PEEK, etc.), which is stored in a reservoir, is heated up to the melting temperature and then it is extruded through a nozzle tip on the 3d-printing bed [2]. Several parameters affect the characteristics and the quality of the building part. Some of them are the build orientation, the layer height, the raster angle, the air gap, the printing speed, the infill density, the infill pattern, the extrusion temperature and the nozzle diameter [3].

Most of the published papers study the impact of these parameters on the mechanical properties of the final products. Es-Said et al.[4] carried out experiments with FDM-produced ABS samples with 0^o, 45^o and 90^o raster angle. The results showed that the highest ultimate, yield and bending strength are

reached for 0°, whereas 45° and 90° are much weaker orientations and may lead to delamination of the layers. Ashtankar et al. [5] tested FDM-processed ABS samples in five different orientations (0°, 30°, 45°, 60°, 90°) and concluded that both maximum tensile and compressive strength reduce as the build orientation varies from 0° to 90°. Baich et al. [6] investigated the effect of infill density on the tensile, compressive and bending strength of FDM-manufactured ABS specimens. Specifically, three different infill densities were tested and compared with solid ABS specimens: low density, high density and double density. In compression and bending tests the results showed that double dense samples achieved higher properties, as expected. On the other hand, the result of the tensile test was counter-intuitive, as the high dense sample achieved higher strength compared to the double dense sample. De Toro et al. [7] investigated the impact of layer height, printing pattern, infill density and nozzle diameter on the tensile and bending behavior of FDM-printed CRF-Nylon parts. The results showed that infill density is the most crucial parameter in order to achieve good tensile and bending behaviors. Moreover, lower layer heights result in better bending properties, whereas the printing pattern influences more the tensile behavior of the component. On the other hand, nozzle diameter had not a significant influence on the tensile and bending properties. As follows from the analysis of this paragraph, a great number of experiments have been done in order to study the impact of the different FDM parameters on the mechanical properties of the final products. However, in Mechanical Engineering, strength is not the only property that judges the quality of a product. For this reason, tests should not only be limited on mechanical properties, but they should also take into consideration the surface roughness of the products, as well.

Although, surface roughness is a crucial factor when studying FDM processes, yet the experimental work that has been carried out is limited. Lin et al. [8] processed with FDM methods the following three materials: 1% alginate/7% gelatin hydrogel, 3% alginate/7% gelatin hydrogel and poloxamer paste. The results showed that conical nozzles, high pressures and large nozzle-to-platform gap generally reduce the surface roughness. However, there is a need for calibration of these three parameters for each material. Moreover, a slight limitation of this study is the fact that extrusion stress caused by these parameters is not taken into consideration. Sandhu et al. [9] carried out experiments with FDM-processed PLA samples. Specifically, they tested the impact of layer thickness (0.16mm, 0.2mm, 0.28mm), raster angle (30°, 45°, 60°) and infill pattern (octet, quarter-cubic, cubic) on the surface roughness of the samples, along *X* and *Y* axis. They concluded that the surface roughness in both *X* and *Y* axis lies in, approximately, the same range and the best result is given for the combination of 0.16mm layer thickness, 60° raster angle and cubic infill pattern.

Several researchers have studied the impact of build orientation on the surface roughness. Kozior et al. [10] pointed out the significant impact of build orientation on the surface roughness of SLM-processed 316L Stainless Steel parts. However, these observations should be ratified and for other material, such as thermoplastics in order to achieve a more general view of the build orientation-surface roughness correlation. Buj-Corral et al. [11] and Alsoufi et al. [12] carried out some very interesting experiments in order to find out the build orientation-surface roughness correlation in FDM-printed PLA parts. However, both their studies are based on case-sensitive (cylindrical FDM-processed samples) and the measurements are not according to a standard regulation, so their results cannot be generalized. For this reason, there is a need to carry out experiments, with the strict specifications that the ISO standards recommend. By following these regulations, the experiments will be much more consistent, which will be very valuable when it comes to understanding and simulating these phenomena.
The target of this paper is to calculate the build orientation-surface roughness correlation of FDM-printed PLA samples, according to ISO ASTM 52902-2021. The novelty of this paper is the use of a low-cost FDM-printer in order to ascertain whether low-budget 3D-printers can give parts with acceptable (according to ISO ASTM 52902-2021) surface roughness.

2. MATERIALS AND METHODS

The material used in this paper is PLA with its properties listed in the Table 1, while the utilized

Table 1 – PLA properties and technical specifications

PLA Properties – specifications	
Manufacturer	Real Filament
Manufacturer's preferred hot-end temperature	205 ℃
Manufacturers preferred heating bed temperature	40 ℃
Specific gravity	1.24 g/cc
Tensile strength	16 kpsi (machine direction, MD) / 21 kpsi (traverse direction, TD)
Elongation at break	160% (MD) 100% (TD)
Tensile modulus	480 *MPa* (MD) 560 *MPa* (TD)
Impact strength	2.5 *J*
Melt temperature	210 ^{o}C +/- 8 ^{o}C
Melting point	145-160 ^{o}C
Vicat softening temperature	60 ^{o}C

Figure 1 – PLA Filament that was utilized

The low-budget 3D-Printer used in this case is the Ender 3 with direct drive extruder set up, whilst the Cura 4.12 was chosen as the slicer software. The basic settings that been utilized are presented in the Table 2, while the full detailed list of Cura Software Settings can be provided and will be in CSV format.

Table 2 – 3D printing main parameters

3D Printing main parameters	
Layer Height	0.16 *mm*
Wall Line Count	4
Infill Density	45.0%
Printing Temperature	205
Build Plate Temperature	67
Print Speed	50 *mm/s*
Retraction	Enabled
Fan Speed	75%
Build Plate Adhesion Type	Brim

In Figures 2 and 3 the Cura GUI environment is depicted, as well as the respective roughness test prints.

The measurements were taken on both sides of the test prints, with these sides were named “UP” and “DOWN” respectively. For the surface roughness measurements, a Taylor Hobson Surtronic 3+ profilometer was employed (see Figure 4). Based on the ISO ASTM 52902-2021, on each specimen side three

roughness measurements were taken at different locations, in a direction perpendicular to the lay pf the texture (i.e., along the samples' length). The evaluation length was set 12.5 *mm* and the sampling length (λ_C) at 2.5 *mm*.

The suggested number of samples for this test is five according to the AS ISO ASTM 52902-2021. The measured values are the arithmetical mean deviation of the assessed profile known as Ra and the average distance between the highest peak and lowest valley in each sampling length known as Rz, which are calculated by the equations shown below [13,14]:

$$R_a = \frac{1}{l_r}\int_0^{l_r}|z(x)|dx \quad (1)$$

where lr is the length where measurements are taken, *X* is the length axis, and *Z* is the height from valleys to peaks.

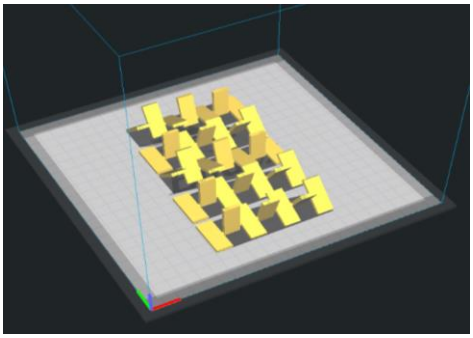

Figure 2 – Cura GUI Environment, Settings, and the part arrangement on the build plate of the 3D-Printer are visible

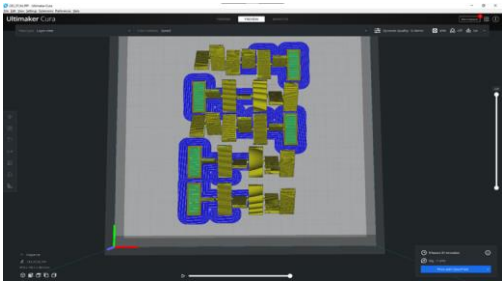

Figure 3 – Printing lines orientations are perpendicular to the long side of the parallelogram with 0° angle from the bed

Figure 4 – Taylor Hobson Surtronic 3+

$$R_Z = \frac{1}{s}\sum_{i-1}^{s} R_{t_i} \quad (2)$$

where s is the number of sampling lengths and R_{ti} is R_t of the ith sample. The assessment of the surface roughness is done based on the mean values of R_a and R_z for each angle, and the respective coefficient of variation as well. The coefficient of variation considers the mean value and the standard deviation, and is calculated by eq. 3 [14]:

$$c_v = \frac{\sigma}{\mu} \quad (3)$$

where σ is the standard deviation and μ the average of the sample.

3. RESULTS AND DISCUSSION

The parts geometry and the obtained prints based on the AS ISO ASTM 52902-2021 is presented in Figure 5.

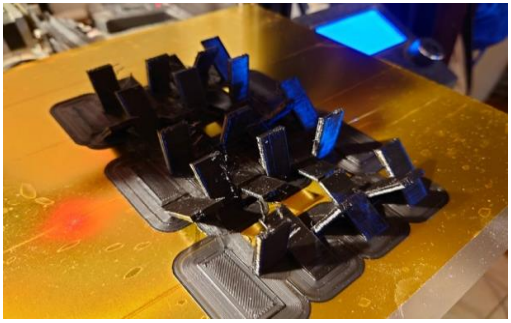

Figure 5 – 3D-Printed parts

In Tables 3 – 6 the surface measurements of R_a and R_z are listed along with the respective mean values, standard deviations, and the coefficients of variation.

Table 3 – Ra measurements for the Up surface

R_a – Up Surface								
# of spec.	# of meas.	0°	15°	30°	45°	60°	75°	90°
1	1	0.00	15.00	30.00	45.00	60.00	75.00	90.00
	2	13.80	32.20	26.00	26.80	24.80	20.80	14.20
	3	11.60	31.60	25.80	26.20	22.60	16.40	15.40
2	1	12.20	33.20	28.40	26.20	25.60	18.00	15.00
	2	18.60	33.40	27.60	25.80	27.40	19.60	19.80
	3	19.00	35.20	27.80	25.80	26.20	20.80	19.60
3	1	19.80	35.20	27.40	24.80	30.80	22.00	19.00
	2	14.00	37.80	30.60	23.60	31.60	x	15.20
	3	15.80	36.60	29.00	23.60	23.20	x	15.00
4	1	14.60	43.20	33.00	23.80	21.60	x	14.00
	2	17.00	9.20	25.60	22.80	21.60	20.00	18.40
	3	16.60	9.20	25.80	23.40	19.00	18.40	18.60
5	1	17.20	9.00	25.40	22.60	20.20	23.00	17.20
	2	7.80	38.80	27.40	25.00	22.40	22.60	18.60
	3	7.80	36.80	26.40	24.80	21.20	21.00	19.40
Mean value in μm			8.80	38.40	26.00	25.40	21.40	20.40
Standard deviation in μm			14.31	30.65	27.48	24.71	23.97	20.25
Coefficients of variation			3.97	11.51	2.11	1.33	3.73	1.93

Table 4 – R_z measurements for the Up surface

R_z – Up Surface								
# of spec.	# of meas.	0°	15°	30°	45°	60°	75°	90°
1	1	85.00	168.00	139.00	156.00	144.00	132.00	81.00
	2	80.00	169.00	137.00	160.00	133.00	97.00	91.00
	3	86.00	168.00	161.00	160.00	156.00	110.00	85.00
2	1	105.00	164.00	156.00	146.00	153.00	122.00	129.00
	2	112.00	175.00	168.00	144.00	151.00	124.00	123.00
	3	124.00	174.00	164.00	139.00	181.00	133.00	106.00
3	1	91.00	181.00	166.00	139.00	195.00	x	93.00
	2	99.00	178.00	153.00	136.00	133.00	x	94.00
	3	96.00	220.00	174.00	135.00	133.00	x	82.00
4	1	117.00	51.00	132.00	129.00	122.00	116.00	109.00
	2	119.00	54.00	130.00	136.00	113.00	108.00	110.00

	3	117.00	45.00	131.00	128.00	116.00	145.00	96.00
5	1	55.00	211.00	142.00	142.00	132.00	132.00	111.00
	2	62.00	197.00	140.00	134.00	125.00	119.00	126.00
	3	60.00	205.00	140.00	143.00	135.00	118.00	106.00
Mean value in μm			93.87	157.33	148.87	141.80	141.47	121.33
Standard deviation in μm			22.53	58.09	14.97	10.12	22.88	13.05
Coefficients of variation			0.24	0.37	0.10	0.07	0.16	0.11

Table 5 – R_a measurements for the Down surface

R_a – Down Surface								
# of spec.	# of meas.	0º	15º	30º	45º	60º	75º	90º
1	1	x	x	x	15.60	18.20	18.20	14.60
	2	x	x	x	15.40	14.80	17.80	17.20
	3	x	x	x	15.60	16.00	19.40	13.60
2	1	x	x	x	15.60	16.80	19.40	16.40
	2	x	x	x	16.40	19.00	17.80	15.40
	3	x	x	x	17.80	17.80	18.40	14.20
3	1	x	x	x	16.20	16.00	13.40	14.00
	2	x	x	x	18.40	15.80	14.00	14.40
	3	x	x	x	20.80	20.20	14.20	13.60
4	1	x	x	x	14.60	3.60	18.80	16.80
	2	x	x	x	14.60	7.40	17.40	15.00
	3	x	x	x	15.40	5.60	19.80	14.20
5	1	x	x	x	20.40	x	18.00	16.00
	2	x	x	x	20.20	x	21.80	17.40
	3	x	x	x	21.00	x	18.40	16.20
Mean value in μm			-	-	-	17.20	14.27	17.79
Standard deviation in μm			-	-	-	2.36	5.53	2.30
Coefficients of variation			-	-	-	0.14	0.39	0.13

Table 6 – R_z measurements for the Down surface

R_z – Down Surface								
# of spec.	# of meas.	0º	15º	30º	45º	60º	75º	90º
1	1	x	x	x	90.00	106.00	114.00	84.00
	2	x	x	x	89.00	94.00	115.00	94.00
	3	x	x	x	92.00	101.00	124.00	99.00
2	1	x	x	x	86.00	97.00	113.00	97.00
	2	x	x	x	97.00	108.00	104.00	91.00

	3	x	x	x	105.00	101.00	100.00	87.00
3	1	x	x	x	99.00	88.00	75.00	85.00
	2	x	x	x	107.00	96.00	75.00	94.00
	3	x	x	x	118.00	124.00	85.00	84.00
4	1	x	x	x	82.00	25.00	114.00	106.00
	2	x	x	x	80.00	40.00	100.00	86.00
	3	x	x	x	89.00	23.00	120.00	83.00
5	1	x	x	x	120.00	x	103.00	103.00
	2	x	x	x	114.00	x	132.00	111.00
	3	x	x	x	126.00	x	100.00	108.00
Mean value in μm			-	-	-	99.60	83.58	104.93
Standard deviation in μm			-	-	-	14.65	34.12	16.74
Coefficients of variation			-	-	-	0.15	0.41	0.16

Based on the experimental data of Tables 3 – 6, the charts for R_a and R_z depending on the angle to the build plate can be drawn, which are presented in Figures 6 and 7.

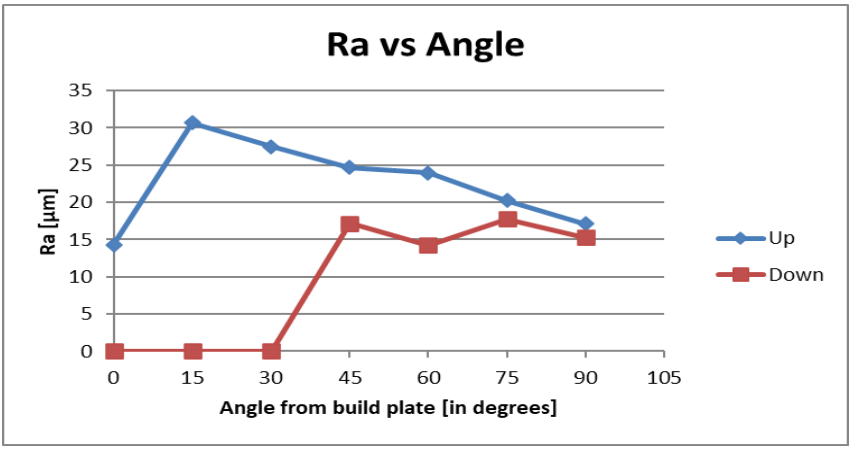

Figure 6 – R_a to Angle Degrees from build plate

Based on the charts of Figure 5, it can be deduced that mean R_a values on the up side are low for the 0o angle, then they increased up to 30.65 μm for the 15°, and finally they descend to 17.09 for the 90°. The mean R_a for the Down surface has a more vague behavior, since it has only a small variation depending on the angle, while, this deviation is not monotonous. Another interesting observation

regarding the correlation between the surface roughness of the Up and Down side of the printed part can be also deduced. The values are getting more similar as the printed part orientation changes to be perpendicular to the build surface, where the roughness of each side should be equal. Unfortunately, due to measurement errors, 3D-printer accuracy and other parameters, the measurements cannot be exactly similar for the 90°. Moreover, it is visible that the Up side of the parts are rougher than the other Down side for all the angles.

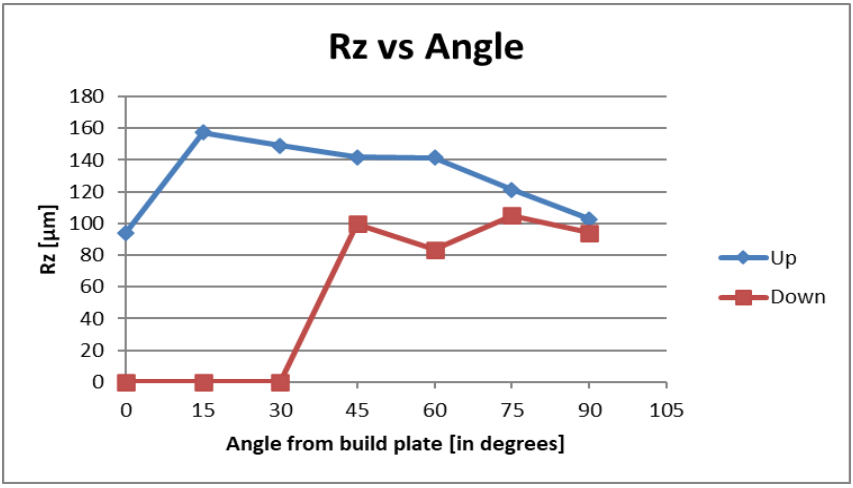

Figure 7 – R_z to Angle Degrees from build plate

Regarding the R_z values, and based on the diagrams of Figure 6, it is visible that the mean R_z values follow the same trend as the R_a. For the up side, at first, mean R_z is as low as 93.86 µm, then it peaks to 157.33 µm at 15 degrees and it is gradually descending to 102.8 µm for the 90°. For the down side, again the samples for 0, 15 and 30 degrees could not be measured due to overrange values at 15 and 30 degrees, or because (for the 0°) the surface was in touch with the building plate. Other than that, the downside has smaller values for the 45, 60 and 75 degrees and at 90 degrees the values of R_z are very close, almost similar. It can be said that non measurable values for 15 and 30 degrees at the Down side has been created due to lack of sufficient cooling and inaccuracy of the printer. The same conclusion can be reasonably deduced for the high R_z values at 15° on the up side of the parts.

Finally, by the plots for the coefficient of variation of Figure 8, it is possible to get to some interesting conclusions regarding the repeatability. The 45 degrees

have significantly low coefficient of variation, meaning that the surface finish was very similar in all the samples and in both surfaces (i.e., Up and Down). A big difference between the coefficient is visible on the Up side of the part and the Down side of the part for the 60°. This is due to reasons such as lack of structural supports and not sufficient and proper cooling. In all the samples the worst scenario is the samples that were printed in 15 degrees from the build plate, which also have a very high coefficient of variation. This is expected reasonable since, for the 15° the unsupported surface is even bigger, and the not fully cooled material is pulled by the gravity, creating a rough and nonuniform surface.

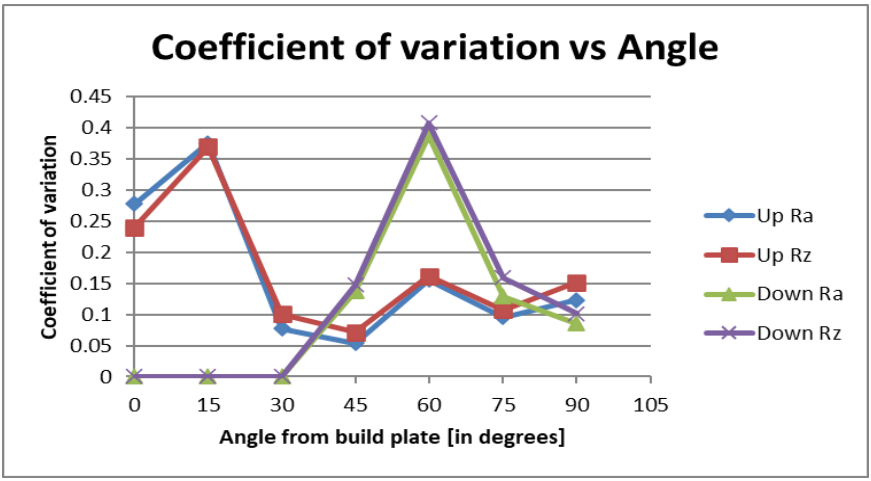

Figure 8 – Coefficient of variation *vs* Angle degrees from build plate for the R_a and R_z for the Up and Down surfaces

Last but not least, it is visible that even though 30 and 45 degrees have the smallest coefficient of variation, meaning that in these angles the produced parts will have similar surface roughness, they do not have the smallest R_a or R_z values. This is a trade-off the user of such a machine must accept as he can choose to reliably create parts of bigger surface roughness or create parts with smaller surface roughness unreliably.

4. CONCLUSIONS

In the current study, an experimental investigation of surface roughness in 3D printed parts manufactured by a low budget 3D-print machine was studied. The

creation of the 3D-printed parts was performed according to ISO AS ISO ASTM 52902-2021, as well all the measurements. For each angle, 5 specimens were built and the surface roughness was measured on the Up and Down surface. The assessment of the surface roughness was made based on the R_a and R_z mean values, as well the respective coefficient of variation. The main deduced conclusions are:

- A low budget machine cannot produce parts with low R_a and R_z values reliably.
- A trade-off should be conducted between reliably producing parts with big R_a and R_z values or unreliably and unrepeatably producing parts with small R_a and R_z values.
- This machine due to lack of cooling, lack of second extruder for water soluble support and not so high quality of the hardware, as well as not optimized software and firmware, cannot produce reliably parts with good surface roughness on both sides, i.e., Up and Down.

References: 1. *A. Rashid*, "Additive Manufacturing Technologies," *CIRP Encycl. Prod. Eng.*, pp. 1–9, 2019, doi: 10.1007/978-3-642-35950-7_16866-1. **2.** *S. Vyavahare, S. Teraiya, D. Panghal, and S. Kumar*, "Fused deposition modelling: a review," *Rapid Prototyp. J.*, vol. 26, no. 1, pp. 176–201, 2020, doi: 10.1108/RPJ-04-2019-0106. **3.** *I. J. Solomon, P. Sevvel, and J. Gunasekaran*, "A review on the various processing parameters in FDM," *Mater. Today Proc.*, vol. 37, no. Part 2, pp. 509–514, 2020, doi: 10.1016/j.matpr.2020.05.484. **4.** *O. S. Es-Said, J. Foyos, R. Noorani, M. Mendelson, R. Marloth, and B. A. Pregger*, "Effect of layer orientation on mechanical properties of rapid prototyped samples," *Mater. Manuf. Process.*, vol. 15, no. 1, pp. 107–122, 2000, doi: 10.1080/10426910008912976. **5.** *K. M. Ashtankar, A. M. Kuthe, and B. S. Rathour*, "IMECE2013-63146," pp. 1–7, 2016. **6.** *L. Baich, G. Manogharan, and H. Marie*, "Study of infill print design on production cost-time of 3D printed ABS parts," *Int. J. Rapid Manuf.*, vol. 5, no. 3/4, p. 308, 2015, doi: 10.1504/ijrapidm.2015.074809. **7.** *E. V. De Toro, J. C. Sobrino, A. M. Martínez, and V. M. Eguía,* "Analysis of the influence of the variables of the fused deposition modeling (FDM) process on the mechanical properties of a carbon fiber-reinforced polyamide," *Procedia Manuf.*, vol. 41, pp. 731–738, 2019, doi: 10.1016/j.promfg.2019.09.064. **8.** *Z. Lin, T. Jiang, J. M. Kinsella, J. Shang, and Z. Luo*, "Assessing roughness of extrusion printed soft materials using a semi-quantitative method," *Mater. Lett.*, vol. 303, no. July, p. 130480, 2021, doi: 10.1016/j.matlet.2021.130480. **9.** *G. S. Sandhu, K. S. Boparai, and K. S. Sandhu*, "Effect of slicing parameters on surface roughness of fused deposition modeling prints," *Mater. Today Proc.*, no. xxxx, 2021, doi: 10.1016/j.matpr.2021.09.047. **10.** T. Kozior and J. Bochnia, "The influence of printing orientation on surface texture parameters in powder bed fusion technology with 316L steel," *Micromachines*, vol. 11, no. 7, 2020, doi: 10.3390/MI11070639. **11.** *I. Buj-Corral, A. Domínguez-Fernández, and R. Durán-Llucià,* "Influence of print orientation on surface roughness in fused deposition modeling (FDM) processes," *Materials (Basel).*, vol. 12, no. 23, 2019, doi: 10.3390/ma122333834. **12.** *M. S. Alsoufi, A. El-Sayed, and A. E. Elsayed, "How Surface Roughness Performance of Printed Parts Manufactured by Desktop FDM 3D Printer* with PLA+ is Influenced by Measuring Direction," *Am. J. Mech. Eng.*, vol. 5, no. 5, pp. 211–222, 2017, doi: 10.12691/ajme-5-5-4. **13.** *Whitehouse, David* (2012). *Surfaces and their Measurement*. Boston: Butterworth-Heinemann. ISBN 978-0080972015. **14.** *Everitt, Brian* (1998). *The Cambridge Dictionary of Statistics*. Cambridge, UK New York: Cambridge University Press. ISBN 978-0521593465.

Іоаніс Т. Христодулу, Василікі Е. Алексопулу, Ніколаос Е. Каркалос,
Емануїл Л. Папазоглу, Ангелос П. Маркопулос, Афіни, Греція

ПРО ШОРСТКІСТЬ ПОВЕРХНІ ДЕТАЛЕЙ ДРУКОВАНИХ ЗА ТЕХНОЛОГІЄЮ FDM З ВИКОРИСТАННЯМ МАЛОБЮДЖЕТНОГО КОМЕРЦІЙНОГО 3D ПРИНТЕРА

Анотація: *Оскільки ціни на машини для адитивного виробництва знижуються, а досвід у відповідній галузі зростає, важливо тестувати та оцінювати малобюджетні машини, доступні для комерційного використання. Хоча малобюджетні верстати широко використовуються для швидкого прототипування та експериментів, вони не здатні виробляти деталі з високою якістю поверхні та досягати високого рівня повторюваності із-за низькоякісного обладнання та неоптимізованого програмного забезпечення. При цьому основною метою поточного дослідження є проведення експериментів з малобюджетним 3D-принтером для моделювання методом наплавлення (FDM) та оцінка шорсткості поверхні надрукованих деталей в залежності від кута відносно друкованої форми. В якості філаментного матеріалу була обрана полімолочна кислота (PLA), а шорсткість поверхні друкованих деталей вимірювалася відповідно до стандарту ISO ASTM 52902-2021. Шорсткість поверхні оцінювалася з огляду значень R_a і R_z, а також був проведений статистичний аналіз, щоб зробити деякі цікаві висновки щодо кореляції між орієнтацією деталі та якістю поверхні. Для кожного кута виготовляли по 5 зразків та вимірювали шорсткість поверхні на верхній та нижній поверхнях. Оцінку шорсткості поверхні проводили за середніми значеннями R_a і R_z, а також відповідним коефіцієнтом варіації. Основними висновками є такі: малобюджетний верстат не може надійно виробляти деталі з низькими значеннями R_a та R_z; необхідно знайти компроміс між надійним виробництвом деталей з великими значеннями R_a та R_z або ненадійним та неповторним виробництвом деталей з малими значеннями R_a та R_z; дана машина через відсутність охолодження, відсутність другого екструдера для водорозчинної підкладки і не настільки високої якості апаратної частини, а також не оптимізованого програмного забезпечення та прошивки, не може надійно виробляти деталі з гарною шорсткістю поверхні з обох боків, тобто зверху та знизу.*

Ключові слова: *машини для адитивного виробництва; швидке створення прототипів; моделювання плавленого осадження; шорсткість поверхні; 3D-принтер.*

UDC 621.941.04 **doi: 10.20998/2078-7405.2022.96.07**

V. Molnár, Miskolc, Hungary

WEAR RESISTANCE OF HARD TURNED SURFACES

Abstract. *The quality of working surfaces plays an important role in automotive industrial components. One of the main characteristics of such surfaces is their wear resistance. In this study external cylindrical surfaces were analyzed. A Design of Experiment methodology was applied and hard turning experiments were carried out to analyze the effects of the cutting parameters on the 3D surface roughness values of reduced peak height, skewness and kurtosis. The study confirmed earlier findings that at lower feed the wear resistance is higher based on the analyzed roughness parameters. The cutting speed and the depth-of-cut do not influence these parameter values significantly.*
Keywords: *hard turning; wear resistance; 3D surface roughness.*

1. INTRODUCTION

A working surface means that it has motion relative to another surface. One of the most important phenomena in this relationship is the wear of surfaces. In the automotive industry many components incorporate working surfaces. Most of them have to be hardened in order to increase the wear resistance and therefore the life of the components [1, 2]. Machining of these hard materials is challenging. Not only the conventional grinding but the use of single-point tools is also possible [3]. Hard turning is a good choice to machine hardened surfaces by a relatively high material removal rate and can result in an efficient procedure. However, turning hard materials requires a machine tool with rigid structure and superhard tool materials [4, 5] in order to reach the expected accuracy and surface quality [6]. Hard turning results in a periodic surface topography. If random topography is required, grinding is the recommended technology [7].

Due to the complex requirement system of working surfaces, topography and therefore surface roughness characterization have become highlighted topics in machining [8–10]. Wear resistance is of the tribological properties of surfaces. There are numerous roughness parameters that aim to provide information about the wear resistance of a surface, for example the peak height (S_p), reduced peak height (S_{pk}), peak material portion (S_{r1}), peak material volume (V_{mp}), skewness (S_{sk}), kurtosis (S_{ku}), and surface bearing index (S_{bi}). These parameters are defined in different ways, for example S_{sk} and S_{sk} are dimensionless parameters, V_{mp} measures specific volume and S_{pk} measures a certain part of the profile height. These differences make comparison difficult. In one study it was stated that the orders of wear resistance of surfaces machined by different technological data are different in the cases of the differently defined roughness parameters [11].

In this study the results of hard turning experiments are demonstrated. The technological data (cutting speed, feed, depth-of-cut) were varied. According to the tool manufacturer's recommendation the lowest and the highest values of these data were applied and a design of experiment (DoE) was carried out, which resulted in 8 setups. Among the above mentioned parameters the relatively widely used S_{pk} and two statistical-based parameters, S_{sk} and S_{ku}, were analyzed. It has to be noted that the industrial use of the 3D roughness parameters is not widespread yet because of the relatively high time consumption; however, the accuracy of these parameters is considered better than that of their 2D counterparts [12–14].

The novelty of the experiments is that more than one roughness parameter was considered at the same time for the analysis of wear resistance and the experiments were designed for the total range of technological parameters. The results can provide useful information for the research of the tribological characteristics of machined surfaces.

2. EXPERIMENTAL SETUP

In the experiments external cylindrical surfaces were machined by hard turning. The technological data of the machining are summarized in Table 1, which also details the DoE setups.

Table 1 – Setups of the experiment and the applied technological data

Surface / Setup	depth-of-cut a_p [mm]	cutting speed v_c [m/min]	feed f [mm/rev]
A	0.05	60	0.05
B	0.05	60	0.2
C	0.05	150	0.05
D	0.05	150	0.2
E	0.3	60	0.05
F	0.3	60	0.2
G	0.3	150	0.05
H	0.3	150	0.2

The machining experiments were carried out on a CNC lathe type Optiturn S 600. In the machining experiment a Mitsubishi CNGA 120408TA4 type insert was used. The workpiece material was 16MnCr5, its hardness was 63 HRC. The lengths of the machined surfaces were 40 mm and their diameters were 70 mm.

The surface topography was analyzed by 3D roughness parameters. In the measurements 2.05×2.05 mm areas were scanned by using a measurement machine type Altisurf 520. A 0.8 mm cut-off and Gauss filter were applied. The scanning was carried out using an optical sensor (type CL2). The x- and y-direction resolutions were 2 µm, therefore one million points were scanned. The z-direction resolution was 0.012 µm. The nominal measurement range was 0–300 µm. For the analysis of the roughness parameters the standard ISO 25178 was used

3. DISCUSSION

The arithmetical mean heights (S_a) were analyzed to get information about the surfaces based on a parameter which is widely used in industry. S_a values vary between 0.11 and 1.08 µm. The machine tool proved to be good; no resonances were experienced during the machining process. In Fig.1 examples are demonstrated for the analyzed surfaces. In Table 2 the analyzed roughness parameter values are summarized for the 8 setups.

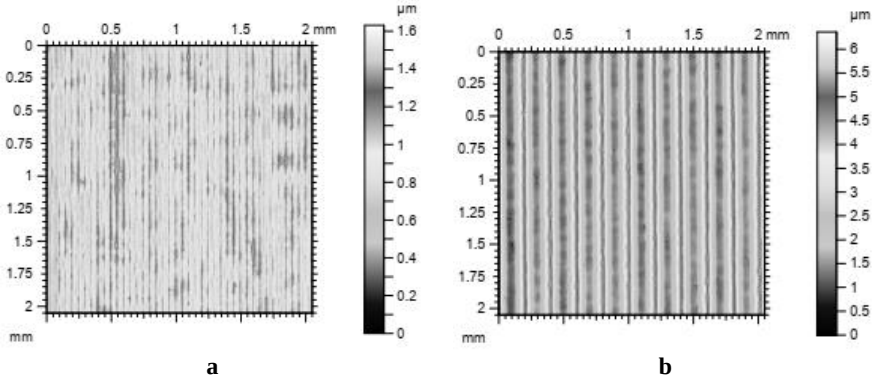

Figure 1 – Examples for hard turned topographies; (a) setup A, a_p=0.05 mm, v_c=60 m/min, f=0.05 mm/rev, (b) setup F, a_p=0.3 mm, v_c=60 m/min, f=0.3 mm/rev

The reduced peak height is defined according to Fig. 2. A lower value indicates better wear resistance. In Fig. 3 the values of this parameter are demonstrated. It can be observed that the feed influences this value to a relatively high extent. At 0.05 mm depth-of-cut (d-o-c), by increasing the feed from 0.05 to 0.2 mm/rev the S_{pk} values are 11 and 9 times higher at cutting speeds of 60 and 150 m/min, respectively. At 0.3 mm d-o-c, by increasing the feed from 0.05 to 0.2 mm/rev the S_{pk} values are 7 and 19 times higher at cutting speeds of 60 and 150 m/min, respectively. The lower feed results in better S_{pk} values. The depth-of-

cut does not influence the value. It is not obvious how the cutting speed influences the parameter values. In the case of higher d-o-c S_{pk} increases with the cutting speed when higher feed is applied but in the case of lower d-o-c the opposite can be observed.

Table 2 – Measured roughness values

Surface / Setup	S_a	S_{pk}	S_{sk}	S_{ku}
A	0.12	0.14	-0.03	3.14
B	0.94	1.56	0.65	2.39
C	0.13	0.11	-0.26	3.20
D	0.65	1.09	0.59	2.10
E	0.21	0.21	0.05	2.64
F	1.04	1.53	0.54	2.11
G	0.11	0.10	-0.20	3.13
H	1.08	1.88	0.62	2.21

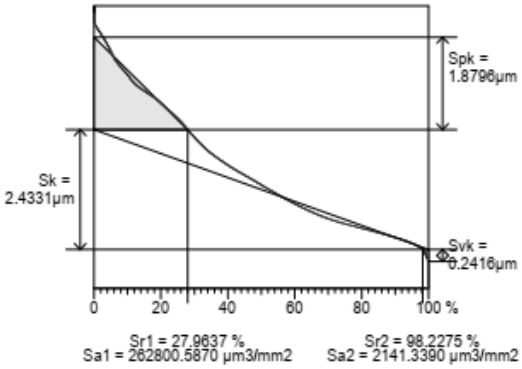

Figure 2 – Calculation of the Spk parameter (setup H)

In Fig. 4 the value ranges for the 2D R_{sk} and R_{ku} parameters are demonstrated for easier visualization.

The skewness gives information about the wear resistance, among other things. A negative or zero value belongs to a greater bearing area, therefore the wear resistance is better. In all the experimental setups the values do not exceed 0.7 (Fig. 5). When lower feed was applied, the values were around or below zero. The

reason for this is that by such low feed the tool 'burnishes' the surface. At 0.05 mm d-o-c, by increasing the feed from 0.05 to 0.2 mm/rev the S_{sk} values increase by 0.68 and by 0.85 at cutting speeds of 60 and 150 m/min, respectively. At 0.3 mm d-o-c, by increasing the feed from 0.05 to 0.2 mm/rev the S_{sk} values increase by 0.51 and by 0.82 at cutting speeds of 60 and 150 m/min, respectively.

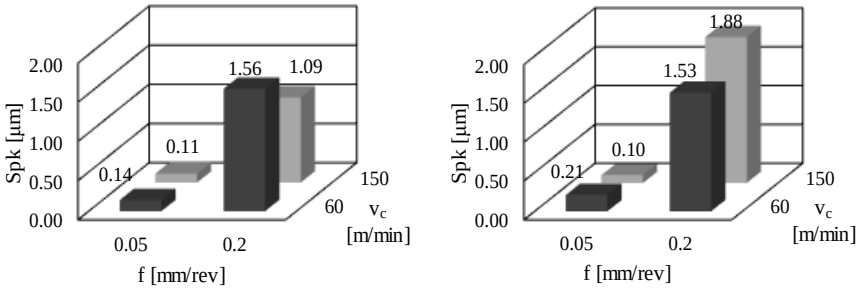

a **b**

Figure 3 – Reduced peak height: (a) a_p=0.05 mm, (b) a_p=0.3 mm

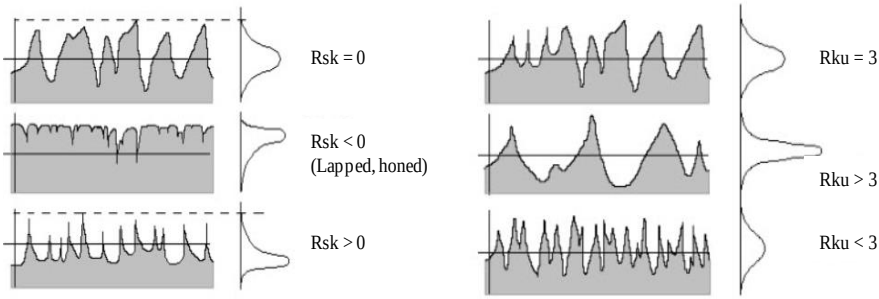

Figure 4 – The values of Rsk and Ssk parameters [15]

If the kurtosis value is 3 or lower, the wear resistance increases. When a lower feed was applied, the values were around 3. At higher feed the values decreased. At 0.05 mm d-o-c, by increasing the feed from 0.05 to 0.2 mm/rev the S_{ku} values decrease by 0.75 and by 1.10 at cutting speeds of 60 and 150 m/min, respectively. At 0.3 mm d-o-c, by increasing the feed from 0.05 to 0.2 mm/rev the S_{ku} values decrease by 0.53 and by 0.92 at cutting speeds of 60 and 150 m/min,

respectively. The d-o-c has no significant influence on the S_{ku} value. The role of the cutting speed is again not obvious.

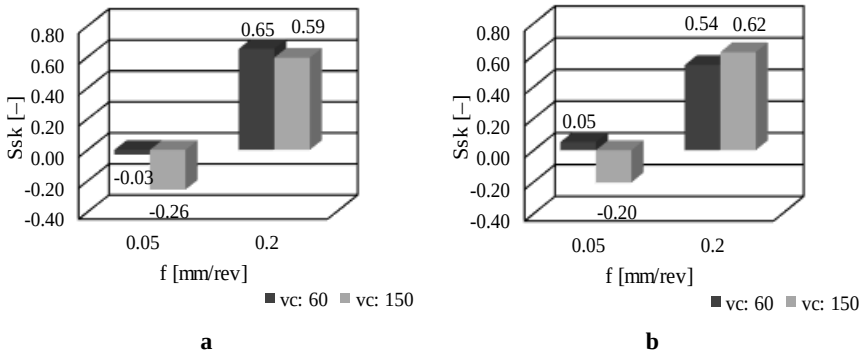

Figure 5 – Skewness values: (a) a_p=0.05 mm, (b) a_p=0.3 mm

Analyzing the three roughness parameters the following order can be stated among the setups (better wear-resistance from left to the right):

- S_{pk}: H→B→F→D→E→A→C→G
- S_{sk}: B→H→D→F→E→A→G→C
- S_{ku}: D→F→H→B→E→C→A→G

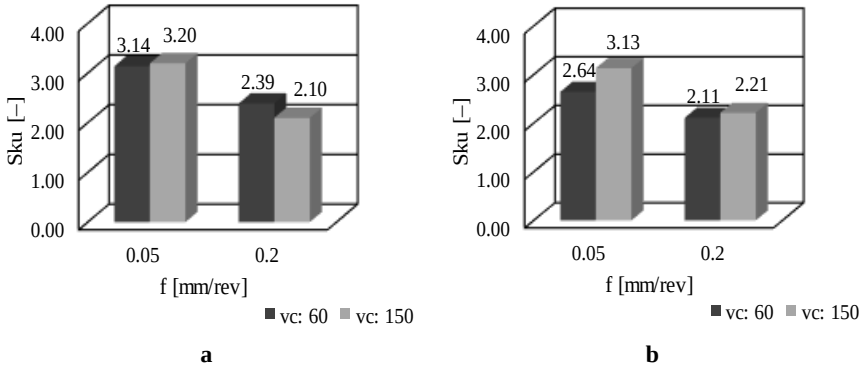

Figure 6 – Kurtosis values: (a) a_p=0.05 mm, b) a_p=0.3 mm

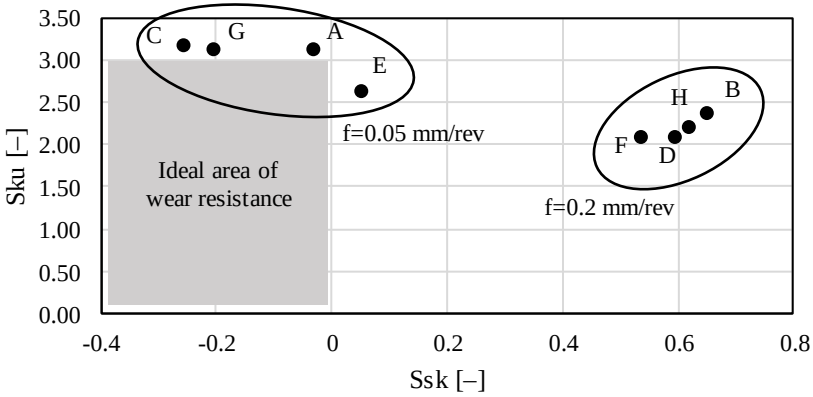

Figure 7 – Tribological topography map

The second four setups belong to the feed 0.05 mm/rev in all the three cases. The reason for this clear order is that because of the lower feed a relatively 'filled' topography is formed by the cutting tool. Concerning the other two technological parameters no clear tendency can be identified. It has to be noted that the surface topography is mainly determined by the feed. This can be seen also in Fig. 7.

CONCLUSIONS

Hard turning experiments were carried out for 8 setups by varying the technological parameter values of the cutting speed, the depth-of-cut and the feed. S_{pk}, S_{sk} and S_{ku} 3D surface roughness parameters were analyzed. The change of the d-o-c and the cutting speed do not influence the analyzed values. The only clear statement of the experiments is that the feed influences the analyzed roughness parameters. When lower feed (0.05 mm/rev) was applied, the wear resistance was clearly better than in the case of higher (0.3 m/rev) feed. All the three roughness parameters support this statement.

References: **1.** *Linins, O., Krizbergs, J., Boiko, I.:* Surface texture metrology gives a better understanding of the surface in its functional state, Key. Eng. Mater., No.527, 2013, pp.167–172, DOI: 10.1016/j.precisioneng.2016.06.001. **2.** *Karpuschewski, B., Kundrak, J., Emmer, T., Borysenko, D.:* A new strategy in face milling-inverse cutting technology, Solid State Phen., No. 261, 2017, pp.331–338. **3.** *Grzesik, W., Rech, J., Zak, K.:* High-precision finishing hard steel surfaces using cutting, abrasive and burnishing operations, Procedia Manuf., No.1, 2015, pp. 619–627, DOI: 10.1016/j.promfg.2015.09.048. **4.** *Zawada-Tomkiewicz, A.:* Analysis of surface roughness parameters achieved by hard turning with the use of PCBN tools, Estonian J. Eng., No.17, 2011, DOI: 10.3176/eng.2011.1.09. **5.** *Kundrak, J., Nagy, A., Markopoulos, A.P., Karkalos, N.E.:* Investigation of surface roughness on face milled parts with round insert in planes parallel to the feed at various cutting speeds, Cut. Tools Technol. Syst., 2019, pp.87–96, DOI: 10.20998/2078-7405.2019.91.09. **6.** *Mamalis, A.G., Kundrak, J. Horvath M:* On a

novel tool life relation for precision cutting tools, J. Manuf. Sci. Eng., No.127, 2005, pp.328–332, DOI: 10.1115/1.1794158. **7.** *Grzesik, W., Zak, K., Kiszka, P.:* Comparison of surface textures generated in hard turning and grinding operations, Procedia CIRP, No.13, 2014, pp.84–89, DOI: 10.1016/j.procir.2014.04.015. **8.** *Blawucki, S., Zaleski, K.:* The effect of the aluminium alloy surface roughness on the restitution coefficient, Adv. Sci. Technol. Res. J, No.9, 2015, pp.66–71, DOI: 10.12913/22998624/59086. **9.** *Gogolin, A., Wasilewski, M., Ligus, G.; Wojciechowski, S.; Gapinski, B.; Krolczyk, J.; Zajac, D.; Krolczyk, G.:* Influence of geometry and surface morphology of the U-tube on the fluid flow in the range of various velocities, Measurement, No.164, 2020, art. no.108094, DOI: 10.1016/j.measurement.2020.108094. 10. **10.** *Varga, G., Ferencsik, V.:* Analysis of surface topography of diamond burnished aluminium alloy components, Lecture notes in mechanical engineering, 2017, pp.143–154. **11.** *Molnar, V.:* Tribology and Topography of Hard Machined Surfaces, Rezanie i instrumenty v tekhnologicheskih sistemah, No. 94, 2021, pp.49–59. **12.** *Gadelmawlaa, E.S., Kourab, M.M., Maksoucf, T.M.A., Elewaa, I.M., Solimand, H.H.:* Roughness parameters, J. of Mat. Proc. Techn., Vol. 123, 2002, pp.133–145. **13.** ISO 25178-2:2012 Geometrical product specifications (GPS) - Surface texture: Areal - Part 2: Terms, definitions and surface texture parameters. 2012. **14.** *Stout, K., Blunt, L.:* Three-dimensional Surface, Topography. 2 ed. London: Penton Press, 2000. **15.** *Bitelli, G., Simone, A., Girardi, F., Lantieri, C.:* Laser Scanning on Road Pavements: A New Approach for Characterizing Surface Texture, Sensors, No.12, 2012, pp.9110-9128, DOI: 10.3390/s120709110.

Віктор Мольнар, Мішкольц, Угорщина

ЗНОСОСТІЙКІСТЬ ПОВЕРХОНЬ ЗАГАРТОВАНИХ ДЕТАЛЕЙ ПІСЛЯ ОБРОБКИ ТОЧІННЯМ

Анотація. *Обробка загартованих матеріалів є складним завданням. Можливе як звичайне шліфування, так і використання одноточкових інструментів. Жорстке точіння - хороший вибір для обробки загартованих поверхонь за рахунок відносної швидкості знімання матеріалу і може забезпечити ефективну процедуру. Однак токарна обробка твердих матеріалів вимагає верстат з жорсткою структурою та інструменти з надтвердих матеріалів для досягнення очікуваної точності та якості поверхні. Жорстке точіння призводить до періодичного рельєфу поверхні. Через складну систему вимог до робочих поверхонь, топографія і, отже, характеристика шорсткості поверхні стали пріоритетними темами при обробці. Зносостійкість – це трибологічні властивості поверхонь. Існує безліч параметрів шорсткості, які покликані надати інформацію про зносостійкість поверхні. У цьому дослідженні демонструються результати експериментів із твердим точінням. Технологічні параметри (швидкість різання, подача, глибина різання) змінювалися. Відповідно до рекомендацій виробника інструменту були застосовані найнижчі та найвищі значення цих даних, і було проведено планування експерименту, в результаті якого було отримано 8 налаштувань. Новизна експериментів у тому, що з аналізу зносостійкості одночасно враховувалися більше одного параметра шорсткості, а експерименти проводилися для усього діапазону технологічних параметрів. Експерименти по жорсткому точінню проводилися для 8 установок з варіюванням значень технологічних параметрів швидкості різання, глибини різання та подачі. Були проаналізовані 3D параметри шорсткості поверхні S_{pk}, S_{sk} та S_{ku}. Зміна глибини різання та швидкості різання не впливає на аналізовані значення. Єдина чітка констатація експериментів – подача впливає на аналізовані параметри шорсткості. Коли застосовувалася нижча подача (0,05 мм/об), зносостійкість була явно кращою, ніж у разі більш високої (0,3 м/об) подачі. Усі три параметри шорсткості підтверджують це твердження. Результати можуть надати корисну інформацію для дослідження трибологічних характеристик оброблених поверхонь.*

Ключові слова: *жорстке точіння; зносостійкість; 3D шорсткість поверхні.*

UDC 621.941.01 **doi: 10.20998/2078-7405.2022.96.08**

I. Sztankovics, J. Kundrák, Miskolc, Hungary

THEORETICAL VALUE AND EXPERIMENTAL STUDY OF ARITHMETIC MEAN DEVIATION IN ROTATIONAL TURNING

Abstract. *The calculation method of the Arithmetic Mean Deviation (R_a) is presented for rotational turning. The necessary equations for the calculation of R_a are given beginning from the equation of the cut surface theoretical profile, and we determine the theoretical values in the studied range of the technological parameters. Cutting experiments with these data were performed and the roughness values of the machined surfaces were measured. Then we carried out a comparative analysis of the measured and the calculated values of the arithmetic mean deviation.*
Keywords: *arithmetic mean deviation; rotational turning; theoretical and experimental study.*

1. INTRODUCTION

In the production of surfaces and parts, which meet the prescribed roughness requirements, several types of procedures with different kinematic and/or geometric relation are applied in finishing operations [1,2]. The variety of kinematics comes from the different translational or rotational movements of the workpiece and tool [3,4], while the diversity of geometry is given by the number of edges, the design and position of the cutting edge (for example: linear or helical), the shape of the removed chip (constant or varying) and the characteristic of material removal (continuous or intermittent) [5,6]. The selection of the machining procedure is determined by the prescribed accuracy and roughness (quality) requirements among others [7,8], furthermore the more productive one should be chosen for several optional procedures [5,6,7]. However, the increasing costs with the increase in tool wear should be considered as well [9,10]. Longitudinal turning is most widespread in the machining of cylindrical surfaces [11,12].

We study rotational turning, where a helical edged cutting tool with slow rotations removes the allowance from a fast-rotating workpiece with constant chip cross-section and continuous material removal [13,14]. In the studied procedure the machining is done by one cutting edge with constant circular feed and depth of cut. The non-linear (helical) cutting edge and the applied circular feed alter the characteristics of chip removal from the longitudinal cutting; the extent and ratio of cutting force components is different due to the applied edge geometry and kinematics. The contact length between the cutting edge and the workpiece is longer, which is caused by the 0° major cutting edge angle and the inclination angle determined by the helix angle. Therefore, the topography of the machined surface is different. The contact point between the machined surface and the tool moves continuously in one direction along the cutting edge during the cutting.

Hence not just one point of the cutting edge comes into contact with the workpiece during material removal. The usage, load and tool wear will be even along the entire cutting edge. These differences must be taken into consideration in the determination of the process parameters. The effects of the influencing parameters must be known in different machining procedures which can achieve the prescribed roughness values on the part surfaces. The study of these can be done by theoretical (mathematical deduction or modelling [15,16]) and/or experimental analyses, or the comparative analysis of the two [17].

The theoretical values of the roughness parameters give important information on the effect of cutting edge geometry of feed alteration by helping estimate the expected roughness. Therefore, we worked out the calculation method of the Arithmetic Mean Deviation (R_a) for turning with circular feed, and the outcome is compared with experimental results.

2. THEORETICAL VALUE OF ARITHMETIC MEAN DEVIATION

When determining the machined surface roughness, it must be taken into consideration that the theoretically determinable and the practically measurable values are usually different, although a strict correlation can be observed between the two. The theoretical roughness is defined by the position of the cutting edge in the tool reference plane and the feed that is generating the surface periodicity. In rotational turning, the former results from the machined surface radius (r_m), the radius (r_s) and the inclination angle (λ_s) of the helical cutting edge. The periodicity of the surface is given by the tool and workpiece revolutions or angular speed (ω_s and ω_m), the additional axial feed rate ($v_{s,a}$), the inclination angle and the radius of the cutting tool.

In our study, the highlighted section (I-III) of the cut surface must be evaluated for the determination of the arithmetic mean deviation, due to the symmetric nature of the periodically repeating cut surface.

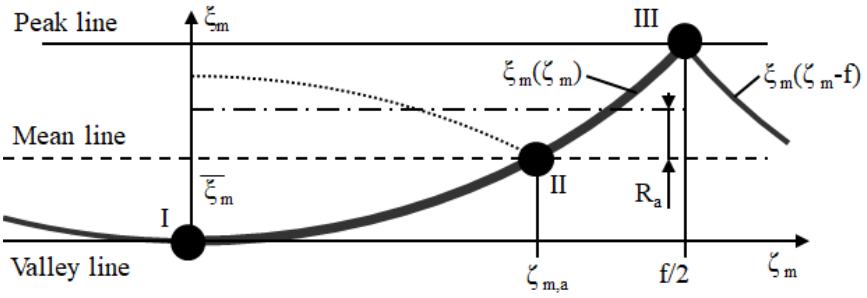

Figure 1 – Arithmetic Mean Deviation (R_a) in the theoretical machined surface

The Arithmetic Mean Deviation can be given by the solution of Equation (1) according to the standard [18] for the theoretical profile (f_a: axial feed, ξ_m: dependant variable, ζ_m: independent variable, $\bar{\xi}m$: value of the mean line).

$$R_a = \frac{1}{f_a}\int_{-f_a/2}^{f_a/2} |\xi_m - \bar{\xi}_m| d\zeta_m \tag{1}$$

The determination of the cut surface equation is presented in our earlier work [19]; one variable $\xi_m(\zeta_m)$ form can be seen in Equation (2).

$$\xi_m(\zeta_m) = \sqrt{r_s^2 - \left((r_s + r_m)sin\frac{\zeta_m \omega_m tan(\lambda_s)}{\omega_m r_m + \omega_s r_s + \frac{v_{s,a}}{tan(\lambda_s)}}\right)^2} - \\ -(r_s + r_m)cos\frac{\zeta_m \omega_m tan(\lambda_s)}{\omega_m r_m + \omega_s r_s + \frac{v_{s,a}}{tan(\lambda_s)}} \tag{2}$$

The equation of the line parallel to the horizontal axis (mean line) is $\xi_m = \bar{\xi}m$, where the areas below and above the curve are the same. The sought value results from the quotient of the integral on the ζ_m axis of the analysed curve (I-III) and the length of the assessed profile. This results in Equation (3) for the case presented in Figure 1.

It follows from the interpretation above that Equation 1 can be transformed here. Due to the symmetric nature of the studied profile, the lower limit of the integration is 0 instead of $-f_a/2$. The interval can be divided into two sections since the area below (I-II) and above (II-III) the mean line can be calculated separately. The I-III interval is divided into two section by coordinate $\zeta_{m,a}$, where the mean line intersects the analysed curve(point II in Figure 1). This condition can be written as $\xi_m(\zeta_{m,a}) = \xi_m$. Hence the theoretical value of R_a is the solution of Equation (4).

$$\bar{\xi}_m = \frac{2}{f_a}\int_0^{f_a/2} \xi_m(\zeta_m) d\zeta_m \tag{3}$$

$$R_a = \frac{2}{f_a}\left[\int_0^{\zeta_{m,a}} (\bar{\xi}_m - \xi_m) d\zeta_m + \int_{\zeta_{m,a}}^{f/2} (\xi_m - \bar{\xi}_m) d\zeta_m\right] \tag{4}$$

The next step in our study is the determination of the mean line position in the roughness profile of the machined surface. Equation (1) was approximated to perform the designated integration. 6th Taylor polynomial is calculated due to the shape and attributes of the function. The result can be seen in Equation (5). After the evaluation of Equation (3) with the function in Equation (5), the vertical position of the mean line is deduced in Equation (6).

$$\xi_m(\zeta_m) = \frac{\omega_m^2 \zeta_m{}^2 r_m (r_s + r_m)}{2r_s \left(v_{s,a} + (r_s\omega_s + r_m\omega_m) cot(\lambda_s) \right)^2} \tag{5}$$

$$\bar{\xi}_m = \frac{r_m \pi^2 \left(v_{s,a} + r_s\omega_s cot(\lambda_s) \right)^2 (r_s + r_m)}{6r_s \left(v_{s,a} + (r_s\omega_s + r_m\omega_m) cot(\lambda_s) \right)^2} \tag{6}$$

The next step is the determination of $\zeta_{m,a}$ from the given condition ($\xi_m(\zeta_{m,a}) = \bar{\xi}m$). After the substition of Equations (5) and (6) into the condition, the sought value is given in Equation (7).

$$\zeta_{m,a} = \frac{\pi\sqrt{3}}{3\omega_m} \left(\frac{r_s\omega_s}{tan\lambda_s} + v_{s,a} \right) \tag{7}$$

The evaluation of the equations leads us to the theoretical value of the Arithmetic Mean Deviation in the form of Equations (8)-(9).

$$R_a = \frac{\frac{2\sqrt{3}}{27}\pi^2 \left(r_m + \frac{r_m^2}{r_s} \right) \left[\frac{r_s^2\omega_s^2 - v_{s,a}^2}{2} cos^2\lambda_s + r_s\omega_s A + \frac{v_{s,a}^2}{2} \right]}{\frac{(r_s\omega_s + r_m\omega_m)^2 - v_{s,a}^2}{2} cos^2\lambda_s + (r_s\omega_s + r_m\omega_m)A + \frac{v_{s,a}^2}{2}} \tag{8}$$

$$Av_{s,a} sin(\lambda_s) cos(\lambda_s) \tag{9}$$

3. CONDITIONS OF THE CUTTING EXPERIMENTS

The main aim of the cutting experiments was the comparison of the measured and calculated values of R_a. A Perfect-Jet MCV-M8 machining centre was chosen for our studies. The helical edged rotational turning tool was clamped on the machine table parallel with the workpiece placed in the spindle of the machine tool. The rotary feed is caused from the circular interpolation of the tool and the cutting

speed is resulted from the rotational movement of the workpiece. The position of the tool and the workpiece can be seen in Figure 2.

The experiments are carried out on heat-treated C45 cylindrical steel workpieces with Ø40 mm diameter and 12 mm length. The material removal is done by a Fraisa P5300682 cutting tool with 30° inclination angle. 200 m/min cutting speed and 0.1 mm depth of cut were adjusted. We analysed the effect of the feed alteration with 7 kinds of values: 0.1 mm/rev., 0.2 mm/rev., 0.4 mm/rev., 0.6 mm/rev., 0.8 mm/rev., 1.0 mm/rev., 1.2 mm/rev. 2D surface roughness was measured by a Mitutoyo SurfTest SJ-301 device on 3 different generatrix of the machined surfaces. The evaluation and cut off lengths were chosen according to the DIN EN ISO 4288 standard.

Figure 2 – Position of the tool and the workpiece

4. EXPERIMENTAL RESULTS AND DISCUSSION

The theoretical and experimental R_a values were evaluated within the studied range. The theoretical values of the Arithmetic Mean Deviation ($R_{a,c}$) were calculated for the different setups using Equation (8). The averages of each of the 3 measured values ($R_{a,m}$) were also determined for the 7 parameter combinations after the cutting experiments. The results of the evaluation are shown in Table 1. Typically, the calculated values of R_a are lower than the measured values.

It can be seen based on the depiction of the theoretical and experimental values in function of the feed (Figure 3) that the roughness alteration caused by the

increasing feed is well described by the theoretical curve, the tendency is the same. The coefficient of determination in the studied range is $R^2 = 0.8543$.

Table 1 – Results of the roughness measurement and calculations

f	a	v_c	$R_{a,1}$	$R_{a,2}$	$R_{a,3}$	$R_{a,m}$	$R_{a,c}$
[mm]	[mm]	[m/min]	[µm]	[µm]	[µm]	[µm]	[µm]
0.1	0.1	200	0.47	0.45	0.48	**0.466**	**0.016**
0.2	0.1	200	0.47	0.48	0.49	**0.480**	**0.063**
0.4	0.1	200	0.54	0.55	0.57	**0.553**	**0.255**
0.6	0.1	200	0.73	0.69	0.74	**0.720**	**0.578**
0.8	0.1	200	1.2	1.39	1.28	**1.290**	**1.034**
1	0.1	200	1.15	1.08	1.14	**1.123**	**1.627**
1.2	0.1	200	2.78	2.86	2.79	**2.810**	**2.361**

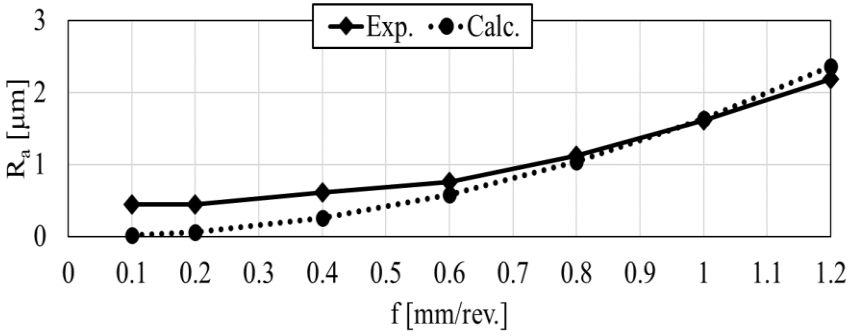

Figure 3 – Measured and calculated values of R_a

Based on the measured and calculated values, if the feed is below 0.6 mm/rev, the difference between the two is proportionally higher than the difference in higher feeds. This caused by that phenomenon that at lower feeds the geometry of the tool has a weaker effect, with the machined surface roughness being influenced more by the material composition, the attributes of the surface layer and the deformation in the cut zone. The latter effects remain nearly constant at different feeds; however, the periodical profile generating effect of the cutting edge geometry becomes dominant. This finding can be clearly seen in Figure 4.

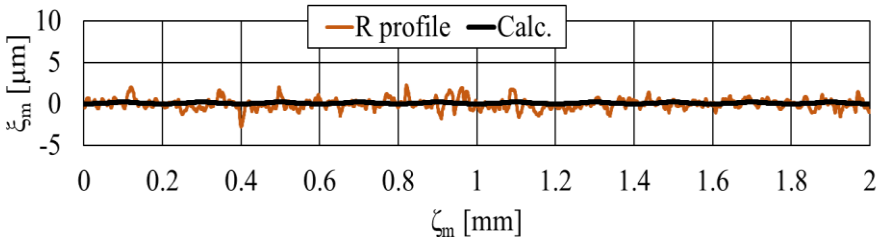

Figure 4a – Measured and calculated roughness profiles (f = 0.2 mm/rev.)

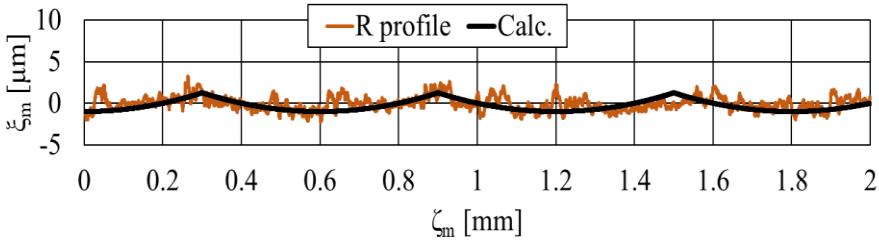

Figure 4b – Measured and calculated roughness profiles (f = 0.6 mm/rev.)

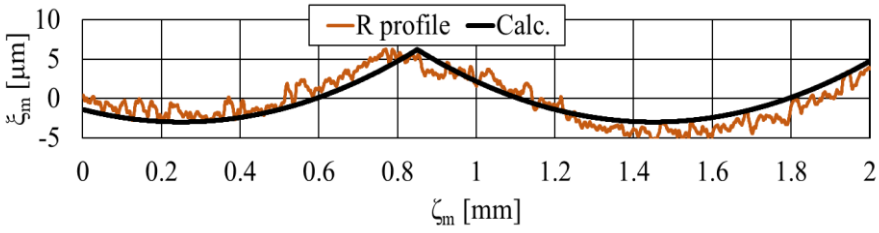

Figure 4c – Measured and calculated roughness profiles (f = 1.2 mm/rev.)

5. SUMMARY

The effect of feed alteration in rotational turning is studied based on the theoretical and experimental values of Arithmetic Mean Deviation in this paper. We presented a method for the determination of the theoretical value of the

analysed roughness value. Based on the equation of the cut surface deducted using by constructive tool geometry, we described the equation necessary for the calculation of R_a in function of the influencing kinematic and geometric parameters. For the chosen technological parameters in the studied range, we calculated the theoretical values, which are validated through cutting experiments.

It was found that the theoretical values of R_a are typically lower than the measured roughness values in the 0.1-0.2 mm/rev feed interval. The change in roughness with the increasing feed is described well by the calculated values, the trends are the same. Roughness profiles are also showed that with the increase of the feed, the periodic profile generating effect of the tool edge geometry becomes dominant, while the proportion of other topography affecting mechanisms becomes lower.

References: 1. *Byrne, G., Dornfeld, D., Denkena, B.:* Advancing Cutting Technology. CIRP Annals - Manufacturing Technology Vol 52, Issue 2, pp. 483-507, 2003. **2.** *Savas V., Ozay C.:* Analysis of the surface roughness of tangential turn-milling for machining with end milling cutter. Journal of Materials Processing Technology, ISSN: 0924-0136, Vol 186, pp. 279-283, 2007. **3.** *Armarego, E. J. A., Karri, V., Smith, A. J. R.:* Fundamental studies of driven and self-propelled rotary tool cutting processes – I. Theoretical investigation. International Journal of Machine Tools and Manufacture, ISSN: 0890-6955, Vol 34, No 6, pp. 785-801, 1994. **4.** *Childs, T. H. C., Sekiya, K., Tezuka, R., Yamane, Y., Dornfeld, D.:* Surface finishes from turning and facing with round nosed tools. Cirp Annals 57, 2008. pp. 89-92. **5.** *Tschätsch, H.*: Applied Machining Technology. Springer Science & Business Media. 2010. **6.** *Shaw, M. C.*: Metal Cutting Principles, Oxford University P, New York, 651 p., 2005. **7.** *Brechner, C., Esser, M., Witt, S.*: Interaction of manufacturing process and machine tool. CIRP Annals - Manufacturing Technology Vol 58, pp. 588-607, 2009. **8.** *Struzikiewicz, G., Otko, T.:* Dependence of shape deviations and surface roughness in the hardened steel turning. Key Engineering Materials, 581, pp. 443-448. 2014. **9.** *Paprocki, M., Wygoda, M., Wyczesany, P., Bazan, P.*: Symptoms of wear HSS cutting tools in different wear stages. Manufacturing Technology 21(3), pp. 387-397. 2021. **10**. *Klymenko, G., Vasylchenko, Y., Kvashnin, V.*: Modeling of cutting tools wear for lathes. Cutting & Tools in Technological System Vol. 93, pp. 138–148. 2020. **11.** *Beňo, J., Maňková, I., Vrábel, M., Karpuschewski, B., Emmer, T., Schmidt, K.*: Operation Safety and Performance of Milling Cutters with Shank Style Holders of Tool Inserts. Procedia Engineering, 48, pp. 15-23. 2012. **12.** *Zębala, W., Gawlik, J., Matras, A., Struzikiewicz, G., Ślusarczyk, Ł.*: Research of surface finish during titanium alloy turning. Key Engineering Materials, 581, pp. 409-414. 2014. **13.** *Klocke, F., Bergs, T., Degen, F., Ganser, P.*, Presentation of a novel cutting technology for precision machining of hardened rotationally symmetric parts, Production Engineering: Research and Development, vol. 7, pp. 177-184, 2013. **14.** *Degen, F., Klocke, F., Bergs, T., & Ganser, P.*: Comparison of rotational turning and hard turning regarding surface generation. Production Engineering, 8(3), pp. 309-317., 2014. **15.** *He, C.L. Zong, W.J. Zhang, J.J.:* Influencing factors and theoretical modeling methods of surface roughness in turning process: State-of-the-art. International Journal of Machine Tools and Manufacture, Volume 129, pp. 15-26, 2018. **16.** *Dyadya, S., Kozlova, Y., Germashev, A., Logominov, V.:* Simulation of the machined surface after end milling with self-oscillations. Cutting & Tools in Technological System Vol 94, pp. 19–27, 2021. **17.** *Guo, H., Kang, M., Zhou, W.:* Prediction of Surface Roughness and Optimization of Process Parameters for Slow Tool Servo Turning. Manufacturing Technology 21(5), pp. 616-626., 2021. **18.** *ISO4287:1997*: Geometrical Product Specifications (GPS) — Surface texture: Profile method — Terms, definitions and surface texture parameters, 1997. **19.** *Sztankovics, I.:* A forgácsolt felület analitikus meghatározása rotációs esztergálásnál. ("Analytical description of the cut

surface in rotational turning", in Hungarian) Multidiszciplináris Tudományok: A Miskolci Egyetem Közleménye 11: 4 pp. 102-110., 9 p. (2021).

Іштван Станкович, Янош Кундрак, Мішкольц, Угорщина

ТЕОРЕТИЧНА ЗНАЧИМІСТЬ І ЕКСПЕРИМЕНТАЛЬНЕ ДОСЛІДЖЕННЯ СЕРЕДНЄАРИФМЕТИЧНОГО ВІДХИЛЕННЯ ПРИ РОТАЦІЙНОМУ ТОЧІННІ

Анотація. *Наведено метод розрахунку середнього арифметичного відхилення R_a для ротаційного точіння. Наведено необхідні рівняння для розрахунку R_a, виходячи з рівняння теоретичного профілю поверхні різання, та визначено теоретичні значення у досліджуваному діапазоні технологічних параметрів. З цими даними були проведені експерименти з різання та вимірювання значень шорсткості оброблених поверхонь. Потім було проведено порівняльний аналіз виміряних та розрахованих значень середнього арифметичного відхилення. При визначенні шорсткості обробленої поверхні необхідно враховувати, що значення, що теоретично визначаються і практично вимірювані, зазвичай різні, хоча між ними може спостерігатися строга кореляція. Теоретична шорсткість визначається положенням різальної крайки в базовій площині інструменту та подачею, що створює періодичність поверхні. При ротаційному точінні перший визначається радіусом обробленої поверхні (r_m), радіусом (r_s) та кутом нахилу (λ_s) гвинтової різальної крайки. Періодичність поверхні задається обертами інструменту та заготівки або кутовою швидкістю (ω_s і ω_m), додатковою осьовою подачею ($v_{s,a}$), кутом нахилу та радіусом різального інструменту. На основі виміряних і розрахованих значень, якщо подача нижче 0,6 мм/об, різниця між ними пропорційно більша, ніж різниця при більш високих подачах. Це викликано тим явищем, що при менших подачах геометрія інструменту має менший вплив, а на шорсткість поверхні, що обробляється, більший вплив надають склад матеріалу, властивості поверхневого шару і деформації в зоні різання. Останні ефекти залишаються майже постійними при різних подачах; проте переважаючим стає вплив геометрії різальної крайки у створенні періодичного профілю. Було виявлено, що теоретичні значення R_a зазвичай нижчі за виміряні значення шорсткості в інтервалі подач 0,1-0,2 мм/об. Зміна шорсткості зі збільшенням подачі добре описується розрахунковими значеннями, тренди ті ж самі. Профілі шорсткості також показали, що зі збільшенням подачі переважаючим стає ефект формування періодичного профілю геометрії різальної крайки інструменту, тоді як частка інших механізмів, що впливають на топографію, знижується.*

Ключові слова: *середнє арифметичне відхилення; ротаційне точіння; теоретичне та експериментальне дослідження.*

UDC 621.923 **doi: 10.20998/2078-7405.2022.96.09**

V. Fedorovich, I. Pyzhov,Y. Ostroverkh,
L. Pupan, Ya. Garachenko, Kharkiv, Ukraine

METHODOLOGY FOR DEVELOPING AN EXPERT SYSTEM FOR THE GRINDING OF SUPERHARD MATERIALS

Abstract. *An expert system of the grinding process has been developed, which makes it possible to predict and optimize the process of defect-free processing of both existing and newly created superhard materials. The expert system consists of two interconnected modules - theoretical and experimental. The theoretical module of the expert system allows, at a given level of significance, to determine the values of the output indicators and the kinetics of their change in the process of adaptability, depending on the physical and mechanical properties of the interacting materials and processing conditions. The experimental module of the expert system allows you to coordinate and correct the results of theoretical calculations when determining the optimal grinding and operating conditions for processing various grades of superhard materials. When optimizing the sharpening process of a blade tool, processing efficiency, consumption of diamond wheels, cost price and various quality indicators of its cutting elements can be selected as a criterion. The use of the expert system significantly reduces the amount of expensive and laborious researches in determining the optimal processing conditions for various grades of superhard materials (SHM), including newly created ones.*
Keywords: *Diamond grinding wheel; Finite element method; Knowledge base and database; grinding process optimization; grinding rate; Stress-Strain State; Tool Sharpening; Surface Roughness.*

1. INTRODUCTION

The main purpose of the expert system is to predict the level of output indicators when grinding various grades of SHM, including newly created ones, and to optimize the processing.

At certain stages of work, the expert system provides for the participation of an expert. The expert has knowledge of the process and how to influence its effectiveness.

2. LITERATURE REVIEW

An expert system is a computer program that uses expert knowledge to provide highly efficient problem solving in a narrow subject area [1]. When creating the expert system, a procedural knowledge base was used, that is, the author of the work acts as a knowledge engineer and subject expert.

The expert system uses both a database and a knowledge base in the subject area of diamond abrasive processing and blade processing with a SHM tool. The database contains reference data on the characteristics of diamond wheels (bond, grain grades, concentration, grain size, etc.), physical and mechanical properties of various grades of diamond grains and processed SHM. The expert system is

developed on the basis of a procedural knowledge base. The knowledge base operates with such concepts as the reliability of a SHM blade tool, defects during its sharpening, the weight contribution of various factors to the efficiency of the processing and is built according to the proposed algorithm for determining the optimal conditions for micro-fracture of the elements of the "SHM - grain – bond" system, based on ensuring the load on single grain. Borland Delphi 5 was used as a programming language. The expert system includes a finite element method (FEM) software such as Cosmos and Ansys.

3. RESEARCH METHODOLOGY

Combining the elements of the grinding area into a single technical 3D system "SHM-grain-bond" made it possible to establish the mutual influence of their physical and mechanical properties and geometrical parameters on the intensity and nature of mutual micro-fracture [2]. On the basis of 3D modeling of the stress-strain state (SSS) of the grinding area, a scientifically grounded systematics of the destruction mechanisms of its elements is proposed, taking into account the degree of contact between the bond and the processed material. The systematics includes the types of interaction of elements and the types of their destruction. Fracture mechanisms during diamond grinding of superhard materials are determined by the anisotropy of the properties of diamond crystallites, the ratio in the contact of "soft" and "hard" faces of crystallites and grains. It has been proved that when calculating the processes of fracture of polycrystalline materials consisting of anisotropic elements, one should use not averaged physical and mechanical properties, but their most characteristic values, taking into account the specifics of a particular problem being solved. The fatigue-cyclic nature of mutual micro-fracture of both the processed superhard material and diamond grains has been confirmed by model and experimental studies. The number of cycles to fracture is determined by the degree of defectiveness of the interacting structures and the values of the crack resistance coefficient.

4. RESULTS

The structural and logical diagram of the expert system algorithm is shown in Fig. 1.

According to the diagram, the expert system consists of several interconnected modules and subsystems, each of which solves its own specific problem. The operation of the expert system is based on the results of research carried out in previous works of the authors [2, 3,4].

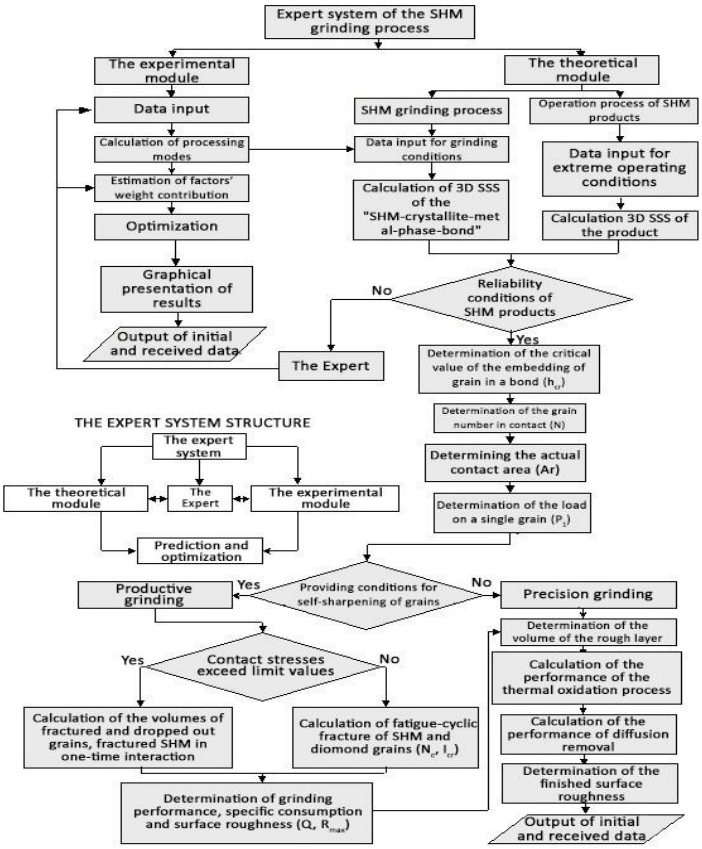

Figure 1 – Structural and logical diagram of the expert system of the grinding process

After entering the initial data into the expert system - physical and mechanical properties of SHM, grains and bonds, normal pressure or transverse feed, grinding speed, grain size and concentration of diamond grains, parameters of the working surface of the wheel (which can be controlled during grinding [2]), preliminary check of ensuring the defect-freeness of the processing. For this, the calculation of 3D SSS of the system "Bond - crystallite - metal phase – grain" is carried out. At this stage, 3D modeling of the stress-strain state of the SHM - grain - bond system, the level of thermal stress and / or strain energy in the polycrystal is analyzed and it is checked whether they do not exceed the critical values. An analytically similar problem was solved by N.V. Novikov. [5] in relation to the

fracture of composite superhard materials, but without taking into account the force factor.

If the operating conditions of a SHM product are known (for example, a blade tool), then the calculation of the 3D SSS of a cutting wedge of an SHM blade tool is carried out under extreme operating conditions to ensure the reliability of an SHM blade tool at the stage of its manufacture.

The theoretical module includes subsystems: determination of the critical value of the embedding of grains in the bond (by the 3D SSS method); determining the number of working grains; determination of the relative value of the actual contact area in the WWS - SHM system; determination of the load on a single grain. If the load on the grain is sufficient to ensure its self-sharpening (micro-fracture), a productive process is implemented, if not, a precision one, where thermally activated processes are responsible for the rough tolerance removal. The volume of fractured SHM and diamond grains is calculated in two ways. If the loads in the grain - SHM contact are sufficient for their microfracture in one-step interaction, the calculation is carried out by the finite element method [6], if the load is not sufficient, the fatigue-cyclic contact problem is solved. In productive grinding, the process of microfracture of SHM and grains can be carried out with one-step (in one contact) interaction of a grain with a polycrystal or in the mode of fatigue-cyclic microfracture. In the first case scenario, the volumes of fractured SHM and grains are determined during 3D modeling of the stress-strain state of the system by the value of supercritical reduced stresses and / or deformation energy in individual elements. Based on these calculation results, the productivity of tolerance removal, specific consumption and wear of diamond grains are estimated.

If it is necessary to calculate the process of thermally activated finishing (precision processing) - the decision is made by an expert, the sequence of the subsystems includes: calculation of the intensity of thermo-oxidative and diffusion removal of the rough surface layer of SHM, during thermal-force interaction with an iron-containing metal bond obtained after preliminary treatment of SHM; determination of productivity and time required for removal of the volume of material located in a layer corresponding in thickness to the maximum roughness of the preliminary treated surface (determined by laser scanning).

In the case of processing a new superhard material (experimental data are absent), the initial data are entered directly into the theoretical module, and the output indicators of the diamond grinding process or finishing of new SHM obtained as a result of its operation can be corrected using the experimental module.

The theoretical module of the expert system allows, without costly and time-consuming experiments, to quantitatively evaluate the grinding performance, specific wear, roughness of the processed surface depending on the SHM grade, grain grade, grain size and concentration, normal pressure, load on a single grain,

grinding speed, actual contact area, the relative support area of the wheel's working surface (WWS). Since the process of diamond grinding is carried out with a combined control of the parameters of the WWS, based on the metered removal of the bond and the forced formation of a cutting submicrorelief on diamond grains, it is necessary to determine the control parameters [7]. When assigning technological parameters for the forced formation of a submicrorelief on the areas of grain wear under ultrasonic action with an impactor tool, the grade of grains and grain size of the WWS and impactor and their bond are taken into account [2]. The concentration of the impactor is determined by the physical and mechanical properties and grain sizes of the WWS and the impactor. The grain size of the impactor should be 2 - 3 times less than the grain size of the WWS, the grain grade is as strong as possible (AS160T, $K_{IC} \geq 10$ MPa·m$^{1/2}$).

The experimental module of the expert system based on computer processing of a wide range of experimental studies allows, with / or without an expert, to determine the optimal conditions for the diamond grinding process of various SHM under specific limiting factors, i.e., under certain real production capabilities. The weighted contribution of various input parameters of the processing was determined by the method of regression analysis, which allows the system to make a decision without the participation of an expert.

The order of operation of the expert system in the general case for various options for its use determines the following sequence of user actions:

- If there are results of experimental studies for the processed SHM, we enter the initial data into the experimental module of the expert system, we obtain the optimal conditions (modes) for processing this SHM grade.

- If the product made of SHM is a blade tool, then data on the extreme conditions of its specific operation are entered into the theoretical module. For these conditions (cutting force, temperature), the calculation of 3D thermo-force SSS of the cutting edge is carried out. Then the inverse problem is solved for 3D thermo-force stress-strain state of the system "Crystallite of SHM - metal phase - grain – bond" and the loading conditions of this system (force and temperature) are determined, at which these stresses will slightly exceed operating ones during the sharpening of the tool.

- If the obtained modes of diamond grinding or thermally activated finishing in the experimental expert system cause defects during processing, the command "change modes" is issued; at this stage, the expert decides which input data should be changed. Subject to fulfillment of this requirement (which ensures the reliability of the SHM blade tool already at the stage of its manufacture), the calculation according to the theoretical module continues.

- In the event that the reduced thermal and force stresses and / or the deformation energy exceed the ultimate stress of SHM, there is a high probability of the formation of microcracks on the processed surface of the mesh, i.e., scrap,

for example, when sharpening a blade tool. In this case, it is necessary to change the initial data, for example, to reduce the value of the transverse feed or to intensify the process of controlling the parameters of the WWS [8]. If no defects are formed, then using the same technique in the package for the finite element method by calculating the reduced stresses in the "Grain – bond" contact, we determine the critical value of the embedding of grains in the bond with the selected initial data. Knowing the critical value of the embedding of grains in the bond, using the theoretical dependences obtained by us [9] and corrected by the experimental correction factor obtained when studying the parameters of 3D topography of the surface of the WWS and SHM by laser scanning, we determine the number of grains in the contact and the value of the actual contact area. For this purpose, a system developed by V.L. Dobroskok of 3D modeling of the working surface of the wheel is also applied [10]. Using the obtained results, we determine the load on a single diamond grain. If the load on the grain is sufficient for its micro-fracture (self-sharpening) or the process of forming a cutting submicrorelief on the grains is carried out purposefully by superimposing ultrasonic vibrations [11], (determined by the expert), then further calculations are carried out along the "productive grinding" branch. The process of productive grinding is analyzed in two stages. At the first stage, by the method of 3D modeling of the stress-strain state of the "SHM - grain – bond" system by the finite element method, elements are determined in which either the reduced stresses or the deformation energy exceed the critical values for STM and grains, predetermining their destruction. At the second stage, the fatigue-cyclic problem of microfracture of elements of the "grain – SHM" system is solved [2].

5. CONCLUSIONS

Thus, on the basis of a comprehensive theoretical and experimental study of the 3D topography of the processed surface and the working surface of the grinding wheel by laser scanning, modeling the 3D stress-strain state of the system "processed material - working surface of the abrasive diamond tool" and the dynamics of wear of its elements, an expert system of the grinding process has been developed. The expert system for the grinding process of superhard materials allows predicting and optimizing the process of defect-free processing of both existing and newly created superhard materials. The development of the expert system was carried out at the level of the finished software product.

References: 1. *Waterman D. A* guide to expert systems / Transl. from Eng. - M.: Mir, 1989. - 369 p. **2.** *Fedorovich V.A.* (2002) Elaboration of scientific fundamentals and methods of practical realization of adaptability control at diamond grinding of superhard materials: Thesis, Doct. Techn. Sc.: 05.03.01. Kharkov, 469 p. **3**. *Grabchenko, A., Fedorovich V., Pyzhov I., Babenko E., Klimenko V.:* Simulation of Grinding Process of Polycrystalline Superhard Materials. In: Key Engineering Materials, Vol. 581, pp. 217 – 223, (2014). Trans Tech Publications, Switzerland. **4**. *Mamalis A.G., Grabchenko A.I., Fedorovich V.A., Kundrák J.:* Methodology of 3D simulation of processes in technology of diamond-composite materials. In: International Journal Of Advanced Manufacturing Technology, Vol. 43, Issue: 11-12, pp. 1235 – 1250, DOI: 10.1007/s00170-008-1802-0 (2009). **5**. *Novikov N.V., Maistrenko A.L.,*

Kulakovsky V.N. Resistance to fracture of superhard composite materials. - Kiev: Nauk. dumka, 1993.— 220 p. **6**. *Wang J.M., Tong F.Y., Li* XX (2013) 3D Dynamic Finite Element Simulation Analysis of Single Abrasive Grain during Profile Grinding with Axial Feed. Advanced Materials Research 680: 410-416 DOI 10.4028/www.scientific.net/AMR.680.410 **7.** *Mamalis, A.G., Grabchenko, A.I., Fedorovich, V.A., Paulmier, D., Horvath, M.:* Development of an expert system of diamond grinding of superhard polycrystalline materials considering grinding wheel. In: International Journal of Advanced Manufacturing Technology, 17(7), pp. 498 – 507, (2001). **8.** *Kundrák, J., Fedorenko, D.O., Fedorovich, V.O., Fedorenko, E.Y., Ostroverkh, E.V.:* Porous diamond grinding wheels on ceramic binders: Design and manufacturing. In: Manufacturing Technology, Vol. 19, No. 3, pp. 446 – 454, (2019). **9**. *Mamalis A.G., Grabchenko A.I., Fedorovich V.A., Kundrak J, Babenko E.A.* (2012) Ways of simulation-based improvement in the performance of diamond-abrasive tools. Journal of Machining and Forming Technologies 4: 1-11 53. **10.** *Dobroskok V.L.* Scientific foundations of the formation of the working surface of wheels on conductive bonds in the process of grinding: Disc...Doc. of engineering: 05.03.01 - Kharkov, 2001. – p. 447. **11**. *Fedorovich V.A.* Controlling the parameters of the submicrorelief of diamond grains when grinding superhard materials // Vysoki tekhnolohii v mashynobuduvanni: Collection of scientific articles NTU "KhPI". - Kharkiv. - 2001.- Ed. 1(4). - pp. 50-54.

Володимир Федорович, Іван Пижов, Євгеній Островерх,
Лариса Пупань, Ярослав Гаращенко, Харків, Україна

МЕТОДОЛОГІЯ РОЗРОБКИ ЕКСПЕРТНОЇ СИСТЕМИ ДЛЯ ШЛІФУВАННЯ НАДТВЕРДИХ МАТЕРІАЛІВ

Анотація. *Розроблено експертну систему процесу шліфування, що дозволяє прогнозувати та оптимізувати процес бездефектної обробки як існуючих, так і новостворюваних надтвердих матеріалів. Експертна система складається з двох взаємопов'язаних модулів – теоретичного та експериментального. Теоретичний модуль експертної системи дозволяє на заданому рівні значущості визначати значення вихідних показників та кінетику їх зміни у процесі пристосовуваності залежно від фізико-механічних властивостей взаємодіючих матеріалів та умов обробки. Експериментальний модуль експертної системи дозволяє узгоджувати та коригувати результати теоретичних розрахунків при визначенні оптимальних умов шліфування та управління для обробки різних марок надтвердих матеріалів. При оптимізації процесу заточування лезового інструменту як критерій може бути обрана продуктивність обробки, витрата алмазних кругів, собівартість та різні показники якості їх ріжучих елементів. Використання експертної системи істотно скорочує обсяг дорогих і трудомістких досліджень щодо оптимальних умов обробки різних марок надтвердих матеріалів (НТМ), зокрема новостворених. Таким чином на базі комплексного теоретико-експериментального вивчення 3D топографії оброблюваної поверхні та робочої поверхні шліфувального круга методом лазерного сканування, моделювання 3D напружено-деформованого стану системи "оброблюваний матеріал – робоча поверхня абразивно-алмазного інструменту" та динаміки зносу була створена експертна система. Експертна система процесу шліфування надтвердих матеріалів дозволяє прогнозувати та оптимізувати процес бездефектної обробки як існуючих, так і новостворюваних надтвердих матеріалів. Розробка експертної системи виконано на рівні готового програмного продукту.*

Ключові слова: *алмазний шліфувальний круг; метод кінцевих елементів; база знань і база даних; оптимізація процесу шліфування; продуктивність шліфування; напружено-деформований стан; заточка інструменту; шорсткість поверхні.*

UDC 621.91.01 **doi: 10.20998/2078-7405.2022.96.10**

B. Varga; B. Mikó, Budapest, Hungary

THE EFFECT OF THE POINT SAMPLING TO THE RESULT OF COORDINATE MEASURING OF FREE-FORM SURFACE

Abstract. *The coordinate measuring technique appropriates to measure dimensional and geometric properties of a machine part. The result of the measuring is effected by several parameters, like the measuring method, the point sampling technique, and the mathematical processing of the measured coordinates. The current article investigates the effect of the point sampling methods in case of a free-form surface. Two methods are compared: the uniform matrix method, and the Halton-Zaremba quasi-random method. The number of measured points is investigated also. The free-form test surface was produced by ball-end milling, and the radius, the cylindricity and the surface profile error were assessed.*

Keywords: *free-form milling; geometric tolerances; point sampling; form deviation.*

1. INTRODUCTION

The free-form surfaces are widely used in die and mould industry. The accuracy of the surfaces is critical in this application, because the shape of the mould is copied to the product. The geometric accuracy of the free-form surface is the result of the cutting technology, but the measuring method ensures the feedback to the production.

The coordinate measuring technique appropriates to measure dimensional and geometric properties of a machine part. The measuring process is defined by several parameters and circumstances, which have effect on the measured results. The measuring method (contact or non-contact), the point sampling method, the mathematical method of the data processing are the most characteristic questions in case of coordinate measuring of free-form surfaces [1].

During the point sampling, the number of measured points a distribution of them are defined. Regular, random, quasi-random and adaptive point sampling method can be used.

Kawalecz and Magdziak [2] investigates the accuracy of the curve reconstruction in function of the number of measured points. The numerical simulation shown, than the accuracy do not change over 50 points. Zhao et al. [3] investigates the similar approach in case of four case studies. They found, that over 50 points, the deviation of the theoretical and constructed surface decreases.

Zahmati et al. [4] suggest a new adaptive point sampling method, which consider the CAD model of the free form surface. The positions of the points are determined by a swarm algorithm. Rajamohan et al. [5] investigates uniform and adaptive point distribution methods. In case of 25 points, the patch size ranking

method ensured the smallest error of the rebuild surface.

The aim of the research is to investigate the effect of the tool path strategies of ball-end milling on the micro and macro accuracy of a free form surface. During the research not only the machining circumstances, but also the selection of the appropriate measuring methods means challenges. The detailed definition of the measuring method is important from the viewpoint of the accuracy of the result, the comparison of the different parts, and the time of the measuring process.

In this paper, the coordinate measuring method is analysed. The aim of the paper is to present the effect of the point sampling methods and the number of measure points (NoP) on the dimensional and geometric error in case of free form surface. The results will be the base of the measuring process of the further research for investigate the effect of the tool path and the cutting parameters to the dimensional and geometric accuracy.

2. MATERIALS AND METHODS

Four convex (CX) and four concave (CV) test parts were manufactured by ball-end milling. The radius of the cylindrical test surface was 45 mm. The overall size of the test part is 80x80 mm. The material of the part was 42CrMo4 (1.7225; Rm = 1000 MPa) low alloy steel. The four teeth ball-end milling cutter was used with 10 mm diameter, the tool was Fraisa X7450.450 solid carbide milling cutter.

The machining was performed by a Mazak 410 A-II CNC machining centre, and the CNC programs were generated by CATIA v5 CAD/CAM systems. The tool path was parallel with the *y*-axis, and the zigzag strategy was used. The spindle speed (n) was 5100 1/min, the depth of cut (a_p) 0.3 mm. The feed per tooth (f_z), the feed speed (v_f) and the width of cut (ae) were varied based on the Table 1.

Table 1 – The cutting parameters

	n 1/min	f_z mm	v_f mm/min	a_p mm	a_e mm
CV-1	5100	0.08	1630	0.3	0.35
CX-1	5100	0.08	1630	0.3	0.35
CV-2	5100	0.08	1630	0.3	0.25
CX-2	5100	0.08	1630	0.3	0.25
CV-3	5100	0.12	2450	0.3	0.15
CX-3	5100	0.12	2450	0.3	0.15
CV-4	5100	0.16	3260	0.3	0.15
CX-4	5100	0.16	3260	0.3	0.15

The coordinates of the surface points were measured by the Mitutoyo Crysta-Plus 544 coordinate measuring machine. The 441 points were measured in an

equidistant, 21x21 matrix. During the analyses, the current point pattern was generated by the selection of these points.

Two point sampling methods were investigated, the uniform matrix pattern (maked by X) and the Halton-Zaremba method (marked by HZ). The uniform matrix pattern covers the whole surface with the same point density. However, in case of low number of points, some regions are not covered exactly. The problem is, that the character of the surface should be consider during determining the point pattern, but then the preliminary processing of the investigated surface is required. The quasi-random methods, like the Halton-Zaremba pattern, cover the surface with better sampling. The random point patterns eliminate the problems of periodical errors also.

In case of Halton-Zaremba method the relative coordinates of the point can be defined as following [6]:

$$x_i = \frac{i}{NoP} \tag{1}$$

$$y_j = \sum_{j=0}^{k-1} {b_{ij}}' \cdot 2^{(-j-1)} \tag{2}$$

where

i: the number of the points (*0* to *(NoP-1)*)

b_{ij}: the j^{th} bit of the binary representation of i

b_{ij}': the transformed value of b_{ij}

$b'_{ij} = b_{ij}$, if j is even,

$b'_{ij} = 1 - b_{ij}$, if j is odd,

For example, if 36 points were determined (*NoP = 36*) the i is between *0* and *35*. The binary representation of *i=35* and the b_{ij}' are:

j	*5*	*4*	*3*	*2*	*1*	*0*
bij	*1*	*0*	*0*	*1*	*0*	*0*
bij'	*0*	*0*	*1*	*1*	*1*	*0*

Fig. 1 shows the 36 points in case of concave and convex test parts. The first picture shows the uniform matrix pattern, and the second shows the Halton-Zaremba pattern. In case of matrix pattern, there are several points on the horizontal sections, but no points on the small radius. In case of the Halton-Zaremba pattern, there are points on every regions.

The number of measured points were NoP = 16, 25, 36, 49, 64, 100, 121. The seven matrix patterns and Halton-Zaremba patterns are shown on the fig. 2 and fig. 3. During the research two types of surface were investigated (CV/CX), which were machined by 4 different sets of parameters, 7 sets of points were measured based on 2 patterns, so the number of data was 2x4x7x2 = 112.

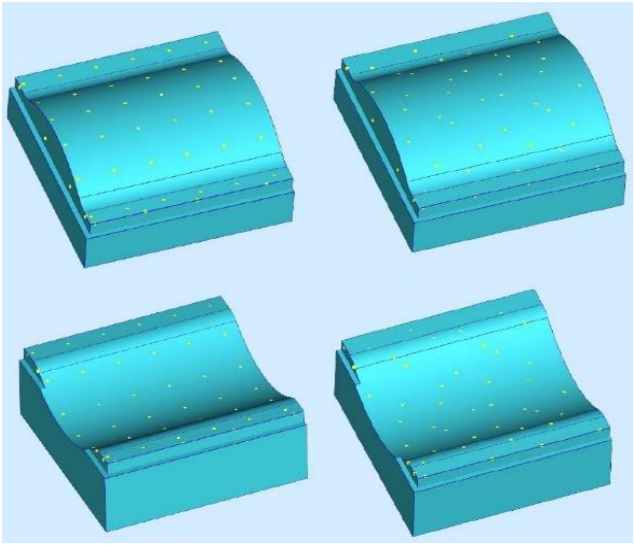

Figure 1 – Example for point sampling in case of 36 points

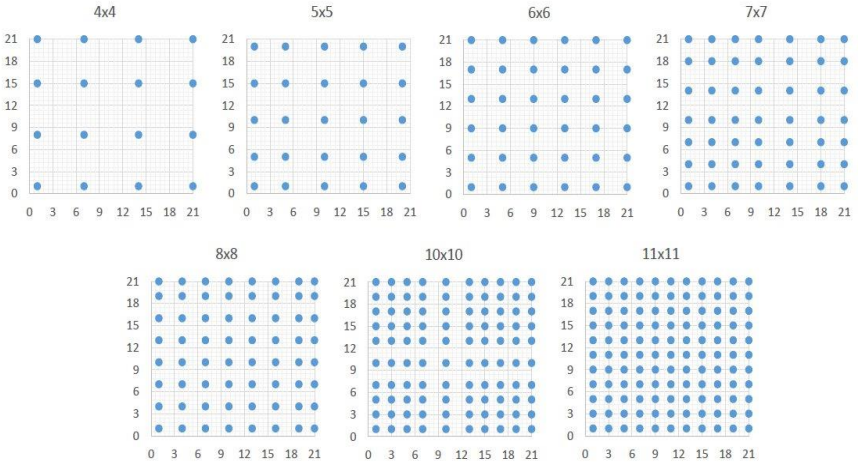

Figure 2 – Matrix point sampling patterns

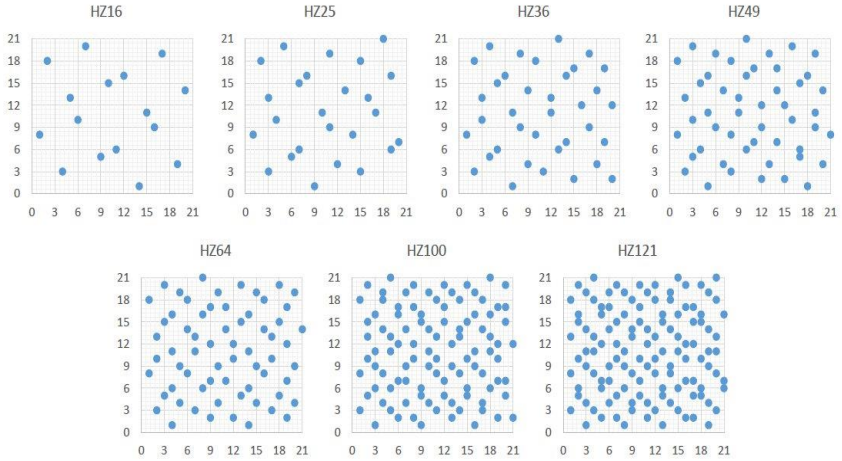

Figure 3 – Halton-Zaremba point sampling patterns

Based on the measured point data the radius of the cylindrical surface (R), the cylindricity error (Cyl) and the surface profile error of the whole surface (SP) were determined. The reference values are the result of the evaluation of 441 points. The dimensional and geometric error were determined by Evolve Smart Profile v7. The data analysis was performed by Excel and MiniTab v14.

3. RESULTS

The measured data of the radius, cylindricity error and surface profile error in function of number of measured points can be seen on the fig. 4. The value of the radius is very different in case of convex and concave parts (~0.09-0.14 mm) and in case of small number of points, the value is inaccurate, the changing is large. The HZ pattern ensures better stability of the evaluated radius, while the matrix pattern results very different radius comparing with the reference values.

In case of geometric errors, the effect of the nature of the surface is smaller, but the importance of the number of measured point is evident. Small number of measured points result smaller geometric error, but the HZ patterns reach the near reference value earlier. Based on the diagrams the point number 49 is the lower limit in case of the investigated geometry.

The effect of the measuring pattern can be seen on the error map also. Fig. 5 shows the four error maps of surface profile error in case of 36 measured points. The left pictures show the result of the matrix pattern and the right ones show the

maps of the Halton-Zaremba method. In case of matrix pattern, there is no point on the small radiuses, so it cannot be taken into account.

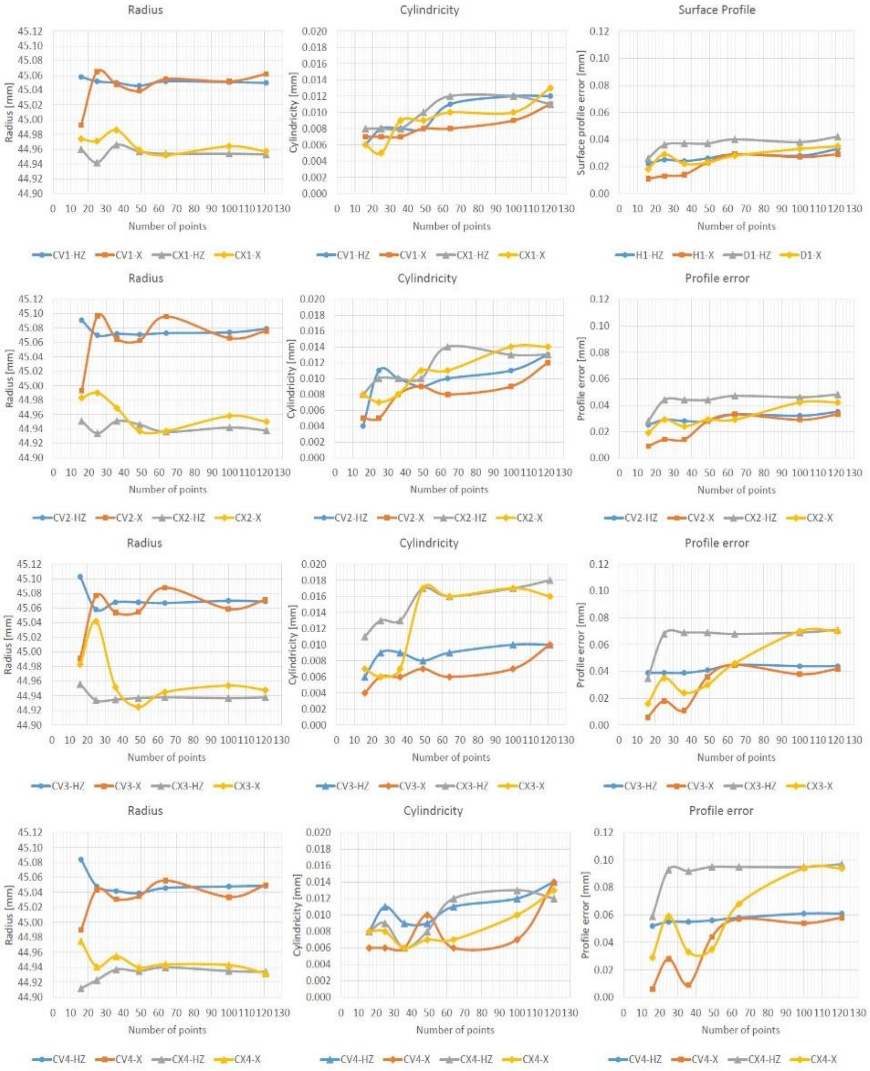

Figure 4 – The measured dimensional and geometric data

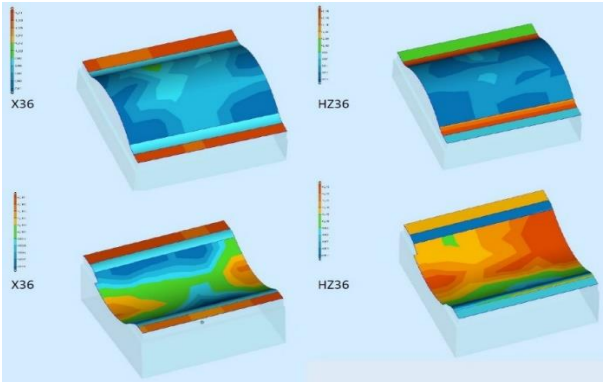

Figure 5 – The surface profile error in case of NoP=36 (CX-1; CV-1)

In order to deeper analysis of the factors, main effect plots were generated. The main effect plot shows the average value of the investigated parameter, in function of the selected input parameter.

Fig. 6 shows the results of the analysis of the value of the radius. The rR means the ratio of the measured and the reference value. The ideal value is one, when the measured value is equal with the reference value.

The character of the surface has the largest effect on the radius, the cutting parameter sets, the number of points and the point sampling method has just a little effect. Nevertheless, in case of convex and concave surfaces the values of the radius are very different, the average values can balance each other, so the separated database was analysed too (fig. 7). In these cases, the effect of the number of points is well recognised. The value of the radius approaches the reference value. The effect of the point sampling method is clearer: the Halton-Zaremba method ensures more accurate results.

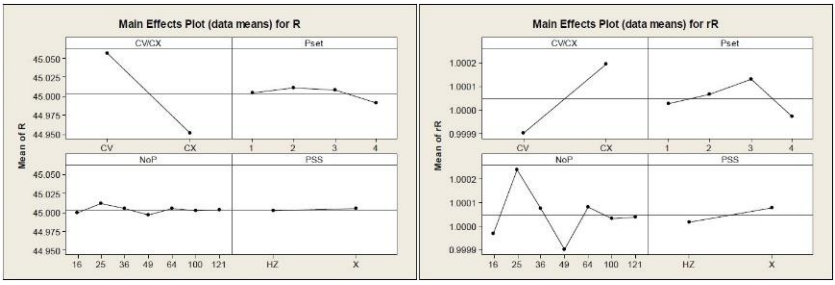

Figure 6 – The main effect plots of the radius

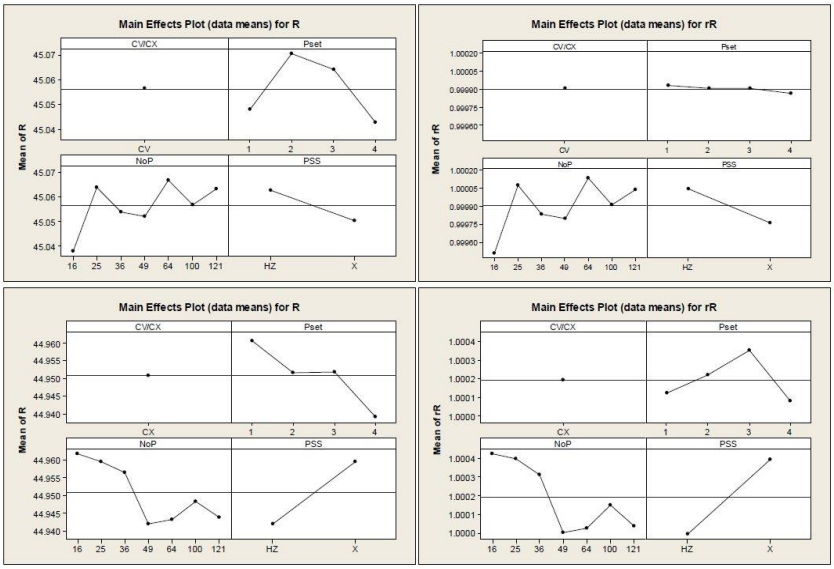

Figure 7 – The main effect plots of the radius in case of separated data

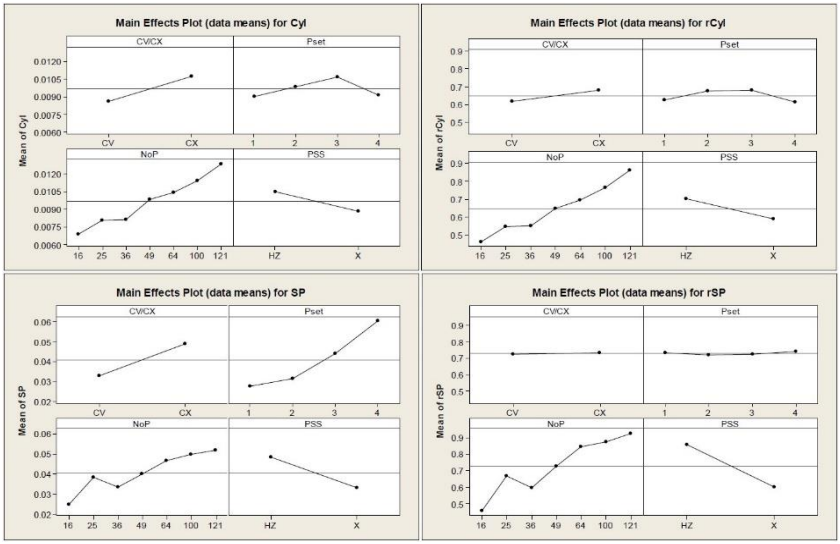

Figure 8 – The main effect plots of the geometric errors

The main effect plots of the cylindricity and the surface profile error show (fig. 8), that the character of the surfaces has effect on the geometric error. The convex surfaces have smaller error, but in case of relative values, the effect is small. The number of measured points improves the results. The cylindricity and the surface profile error are close to the reference values. However the cutting parameters modify the geometric errors, they have no effect on the relative values. The Halton-Zaremba point sampling method ensures more accurate results in this case too.

4. CONCLUSION

The geometric errors are receiving increasing attention in the machine and tool design and manufacturing. During the tolerancing process, not only the functional and manufacturing aspects have to be considered, but the measuring process also. The parameters of the measuring process have effect on the results, so the standard measuring process ensures the repeatability and comparability.

The effect of the number of measured points and the point sampling method were investigated in case of free form surface milling. Two methods were compared, the uniform matrix method and the Halton-Zaremba quasi-random method.

In case of the dimensional error (value of the radius), the number of points and the point sampling method have only a little effect on the measured values.

In case of cylindricity and surface profile error, the character of the surface (convex or concave) and the cutting parameters have no effect on the relative values of the errors. The increasing number of points correct the values and the Halton-Zaremba method ensures better results.

Based on the measured data, under 49 points, the results can change a lot. Therefore, the 49 points can be a lower limit of the number of measured points with Halton-Zaremba pattern in case of the test geometry.

The regression analysis [7] can improve the accuracy of the assessment of the geometric error, so the further aim is to apply this method in case of surface profile error of free form surfaces.

References: 1. *Li Y; Gu P.* (2004) Free-form surface inspection techniques state of the art review. Computer-aided design 36:1395-1417 doi: 10.1016/j.cad.2004.02.009. **2.** *Kawalec A; Magdziak M.* (2011) An influence of the number of measurement points on the accuracy of measurements of free-form surfaces on CNC machine tool. Advances in Manufacturing Science and Technology 35(2):17-27. **3.** *Zhao D; Wang W.; Zhou J.; Jiang R.; Cui K.; Jin Q.* (2018) Measurement point sampling method for inspection of parts with free-form surfaces. Advances in Mechanical Engineering 10(11):1-12 doi: 10.1177/1687814018809577. **4.** *Zahmati J.; Amirabadi H.; Mehrad V.* (2018) A hybrid measurement sampling method for accurate inspection of geometric errors on freeform surfaces. Measurement 122:155-167 doi: 10.1016/j.measurement.2018.03.013. **5.** *Rajamohan G.; Shunmugam M.S.; Samuel G.L.* (2011) Practical measurement strategies for verification of freeform surfaces using coordinate measuring machines. Metrology and Measurement Systems 18(2):209-222 doi: 10.2478/v10178-011-

0004-y. **6.** *Moroni G, Petro S*. (2011) Coordinate measuring machine measurement planning. Colosimo B, Senin N (eds) Geometric Tolerances. Springer, London pp.111-158 doi: 10.1007/978-1-84996-311-4_4. **7.** *Mikó B*. (2021) Assessment of flatness error by regression analysis. Measurement 171:108720 doi: 10.1016/j.measurement.2020.108720.

Балінт Варга, Балаш Міко, Будапешт, Угорщина

ВПЛИВ ТОЧКОВОЇ ВИБІРКИ НА РЕЗУЛЬТАТ КООРДИНАТНИХ ВИМІРЮВАНЬ ПОВЕРХНІ ДЕТАЛІ ДОВІЛЬНОЇ ФОРМИ

Анотація. *Координатно-вимірювальна техніка призначена для вимірювання розмірних та геометричних параметрів деталей машини. На результат вимірювання впливають кілька параметрів, таких як метод вимірювання, метод вибірки точок та математичне оброблення вимірюваних координат. У цій статті досліджується вплив методів точкового відбору проб у випадку поверхні вільної форми. Порівнюються два методи: метод однорідних матриць та квазівипадковий метод Холтона-Заремби. Досліджується також кількість точок, що вимірюваються. Випробувана поверхня довільної форми була виготовлена за допомогою торцевого фрезерування, і були оцінені радіус, циліндричність та похибка профілю поверхні. Геометричним похибкам приділяється все більше уваги при проектуванні та виробництві машин та інструментів. У процесі визначення допусків необхідно враховувати як функціональні і виробничі аспекти, так і процес виміру. Параметри процесу вимірювання впливають на результати, тому що стандартний процес вимірювання забезпечує відтворюваність та сумісність. У разі розмірної помилки (значення радіусу) кількість точок та метод вибірки точок мало впливають на виміряні значення. У разі помилки циліндричності та профілю поверхні, характер поверхні (опукла або увігнута) та параметри різання не впливають на відносні значення помилок. Збільшення кількості точок коригує значення, а метод Холтона-Заремби забезпечує найкращі результати. На основі виміряних даних, менше 49 балів результати можуть сильно змінитися. Таким чином, 49 точок можуть бути нижньою межею кількості виміряних точок з діаграмою Холтона-Заремби у разі тестової геометрії. Регресійний аналіз може підвищити точність оцінки геометричної похибки, тому метою є застосування цього методу у разі похибки профілю поверхонь довільної форми.*

Ключові слова: *фрезерування довільної форми; геометричні допуски; точковий відбір проб; відхилення форми.*

UDC 621.923 **doi: 10.20998/2078-7405.2022.96.11**

V. Lavrinenko, Kyiv, Ukraine,
V. Solod, Kamianske, Ukraine

THE RALATIONSHIP BETWHEEN THE PARAMETERS OF ROUGHNESS AND FEATURES OF SURFACE FORMATION WITH A SPECIAL MICROPROFILE

Abstract. *This article shows the regularities of the formation of the relationship between the parameters of the roughness of the treated surface under the conditions of processing with a tool made of superhard materials. Features of formation of the ratio of height parameters of roughness R_{max}/R_a for conditions of diamond-abrasive processing are shown. In general, in relation to R_{max}/R_a we have a kind of "roughness arc", when first for a normal untreated rough source surface it is close to 4, then abrasive-diamond treatment of this surface raises this ratio to 6 and then to 8, but further methods of abrasive finishing and polishing reduce the ratio to 6 and then chemical-mechanical polishing to a high-quality surface returns this ratio to values close to 4. This means that if the initial cost of grinding the original surface affects the increase in the ratio, then the subsequent cost of finishing and polishing work reduces the value of the ratio R_{max}/R_a to the original. The peculiarities of obtaining a treated surface with a special microprofile, which is a flat protrusions with recesses (a kind of "pockets") for placing oil to increase the service life of such a surface.*
Keywords: *parameters of the roughness; the ratio of height parameters of roughness Rmax/Ra; special microprofile.*

1. INTRODUCTION

An arithmetical average deviation from the mean line R_a is a surface roughness parameter most widely accepted and used in scientific and technical publications. We point out that at one time GOST 2789-73 "Roughness of the surface. Parameters, characteristics and designations" indicated that the roughness parameters (one or more) are selected from the following nomenclature: R_a – arithmetic mean deviation of the profile; R_z is the height of the profile irregularities at 10 points; R_{max} is the highest profile height; S_m is the average step of inequalities; S – the average step of the local protrusions of the profile; t_p is the relative reference length of the profile, where p is the value of the cross-sectional level of the profile. Generalized data on the influence of various machining methods and modes using tools of superhard materials (SHM) on these parameters have not been adequately presented in the literature. Therefore, it is not clear which criteria should be used when deciding upon the machining processes in order to achieve the required R_a value. Furthermore, the experience in commercial operation of products suggests [1] that for various applications more than one surface roughness parameter of contacting surfaces should be monitored:

- R_a and the relative reference length of the profile irregularities t_p for the parts that operate under the conditions of sliding and rolling frictions and for low-wear parts,
- R_a and t_p for the parts prone to contact stresses,
- R_a for press-fit joints,
- maximum height of irregularities R_{max}, maximum peak height R_p and mean spacing of the profile irregularities S_m for the parts subjected to variable loads,
- R_a and t_p for the parts that form tight joints.

In this case, it is also stated that the parameter R_a is preferred. Thus, using this parameter, in [2] the classification of methods of abrasive processing (roughness) – grinding (when R_a is from 100.000 *Å* to 1.000 *Å* or from 10 μ*m* to 0.1 μ*m*), lapping (when R_a is from 1.000 *Å* to 100 *Å* or from 0.1 μ*m* to 0.01 μ*m*), polishing (when R_a is from 100 *Å* to 1 *Å* or from 0.01 μ*m* to 0.0001 μ*m*).

2. THE PURPOSE OF RESEARCH

Note that there are such persistent misconceptions that the above parameters seem to exist independently and it is possible to obtain any desired value of one parameter and any desired value of another, or, for example, you can act on one parameter, and others will not change. The consequence of such misleading judgments is that researchers separately study the influence of processing regimes and conditions on specific roughness parameters, which introduces a system error, because in fact for the same processing conditions all roughness parameters are interconnected and affect only one parameter is impossible, because others will change. Therefore, the purpose of this article was to identify the features of the relationship between the roughness parameters and to establish how this may affect the achievement of a special microprofile of the treated surface.

3. RESEARCH DATA

We will illustrate this with a number of existing relationships between the parameters cited in the literature. Note that roughness is a statistical process, so such relationships are largely correlated. In [1], it was shown that the magnitude of the relationship or relationship between the parameters R_z and R_a can vary. The magnitude of this ratio depends on the profile of the roughness combs. Thus, for the triangular profile $R_z/R_a = 4$. For convex and concave profiles, this ratio is larger and can reach up to 8 depending on the degree of convexity and concavity. Thus, the more the profile of the combs differs from the triangular one, the greater the R_z/R_a ratio. Therefore, this ratio can be called as the coefficient of profile shape or the coefficient of completeness of the profile. It is known that the parameter R_z cannot carry information about the shape of the comb. The parameter R_a contains

such information in an implicit form and only the ratio R_z/R_a gives a numerical characteristic [1]. For specific processing conditions in a number of works the values of such relation are shown. Thus, to calculate the height characteristics of the roughness of the workpiece, you can use the following relations: $R_{max} = kR_z$, where k=1.25 for irregular and k=1.15 for regular roughness. In this case, $R_z \approx 4R_a$ for the rough surface and $R_z \approx 5R_a$ for the surface in the range R_a = 1.25–0.02 μ*m*. For conditions of processing by diamond-abrasive wheels: $R_z = 5R_a$. For turning with cutters: $R_z = 5R_a$ [1].

Let us now consider the correlation between R_a and R_{max}. Thus, for the conditions of diamond abrasive tool processing – $R_{max}=(8–10)R_a$ [3]. For grinding conditions of coarse-grained CBN (160/125) steels 40X (HRC 53) and SHX15 (HRC 60) – $R_{max}=(6.472\pm0.225)R_a$. For EDM conditions: $R_{max} = 5.40625R_a$ [1].

Additionally, we pay attention to the correlation between the parameters: altitude R_a and R_{max} and step S_m. In [3] it was shown that for most methods of machining at an average height of microroughnesses the step of roughness S_m does not exceed $40R_{max}$ (grinding, planing, milling, boring of steel and cast iron parts), and for inequalities with a smaller height, their step values can reach $300R_{max}$. For the conditions of EDM: $S_m=14,1R_a$ [1].

As we can see, the analysis of the literature refutes the constant misleading judgments about the independence of the roughness parameters. But there are other misleading judgments: about the constancy of the ratio R_{max}/R_a or that the step of microroughness S_m increases with increasing parameter R_a. Let's look at these misleading judgments in more detail below.

The first misleading judgment is that the R_{max}/R_a ratio is constant and equal to 5 [4]. The theory of calculation of roughness parameters at grinding is based on this value of the relation. It would be possible to agree with this judgment, because the number 5 is quite decent, which we will show later, but why it is a constant, it is unclear. The identity of the slice thickness and the R_{max} parameter is even more unclear.

The second misleading judgment is that the R_{max}/R_a ratio is not constant and can vary in a wide range: very wide from 1.36 to 109.6 [5], or moderate from 1.42 to 18 [6]. The authors of [5] also indicated that the practice of abrasive treatment has shown that the ratio R_{max}/R_a during grinding mainly takes the value 4…6. This somehow explains the figure above in the first sentence – 5, as the average between 4 and 6. But a little further in [5], its authors point out that in the case of abrasive polishing, the R_{max}/R_a ratio can take the value 30. Let's understand - why such ranges and what it means.

Let's start with work [5]. It performs a theoretical analysis of the nature of the change in the ratio R_{max}/R_a for different conditions of abrasive treatment, and the grains are modeled in the form of a cone and a sphere. The authors assumed that the parameter R_{max} physically determines the slice thickness a_z by a single grain.

Further, the authors argue that during the transition from the cutting process to the process of grain friction with the processed material, the ratio of the height parameters of roughness R_{max}/R_a can vary widely – from 56 to 14. It follows that the process of abrasive polishing can take place under these conditions at R_{max}/R_a = 30, and, accordingly, R_{max}/R = 0.07, where R is the radius of the abrasive grain, μ*m*. When grinding, as we mentioned above, the ratio R_{max}/R_a takes smaller values (4…6), which corresponds to the values of R_{max}/R >0,6. It is in these conditions, according to the authors [5], is a steady cutting process. That is, the lower the R_{max}/R_a ratio, the better the high-performance material removal. And when the transition from the cutting process to the process of friction of the grain with the processed material, the ratio R_{max}/R_a can take quite large values. Note that the assumptions of this work are certainly interesting and have a right to life. We will analyze them in more detail below. However, the results of theoretical studies of the ratio R_{max}/R_a from 1.36 to 109.6 are surprising.

Now let's deal with the work [6]. Here, too, we are faced with a fairly wide range of R_{max}/R_a ratios from 1.42 to 18. But it should be noted that when the authors of [6] present the results of experimental studies of roughness, they are quite conscious and logical. Thus, with fine diamond grinding of glass, the ratio R_{max}/R_a is 7.2…8.5. When polishing stone with bound abrasive R_{max}/R_a is 4.2…18. When polishing glass *K*8 R_{max}/R_a = 7.8…15.0. But when we encounter in this work with modeling in the framework of the physical-statistical model, the results of calculations of the ratio R_{max}/R_a are surprising. Thus, for monocrystalline silicon carbide, this ratio is 1.5±0.1. For the polishing of single-crystal sapphire the R_{max}/R_a ratio was 1.8…2.0 [6].

What is the conclusion from the above? Let's pay attention to R_{max}. This is the highest altitude parameter. It is usually greater than R_z. In turn, R_z is greater than R_a. How big? It is known: $R_z \square 4R_a$ for a rough surface and $R_z \square 5R_a$ for a polished surface. Can R_{max} and R_z match? They can. However, R_{max} can never be less than $4R_a$ for polished and polished surfaces, and in fact for all finishing surfaces. That is, the lower value of the ratio R_{max}/R_a = 4. And what is the upper value? In order to answer this question, we need to return to the conclusions of the work [5]. The authors of this work accepted that the parameter R_{max} physically determines the slice thickness a_z by a single grain. Let's deal with this. If we accept the above statement, then when grinding, according to the authors [5] the value of R_{max}/R >0.6, where *R* is the radius of the abrasive grain, μ*m*. Let's see if this is so. To do this, take from work [1] table. 8.2 and slightly refine it (Table 1).

Table 1 – Influence of the concentration of AC4 diamonds with MA coating in circles on the BC-E polymer bond on the roughness indices during electrochemical grinding of TH20 alloy with a productivity of 525 mm^3/min

Characteristics of the wheel	Roughness indicators			R, μm	R_{max}/R
	R_a, μm	R_{max}, μm	R_{max}/R_a		
100/80–100	0,36	2,75	7,64	45	0,061
(100/80–100)+(50/40–25)	0,63	2,99	4,75	40	0,075
100/80–150	0,40	3,29	8,23	45	0,073

As you can see, the ratio R_{max}/R when grinding from table. 1 are significantly lower than 0.6, and the ratio R_{max}/R_a correspond to those characteristic of grinding. So what determines the value of the ratio R_{max}/R_a when polishing up to 30 [5], or up to 18 [6]? Determines not a_z [5], but scratches that occur during polishing on the treated surface. And these scratches occur due to the fact that, as we pointed out above, abrasive grains are not homogeneous. Any grain size has only 75… 80% of the main fraction, and up to 10% are grains of higher grain size. Similarly, the strength of SHM grains is not the same, because this indicator is subject to the logarithmically normal distribution law [1], and therefore the grain sample necessarily contains grains of higher grain size and greater strength, and therefore they cause scratches when polishing. In order to get rid of this, it is necessary to either further classify the powders of SHM grains, or to carry out the polishing process in several stages with a decrease in the grain size of the polishing paste.

Let us return to our R_{max}/R_a ratio. And what do the authors themselves suggest? Let's deal with this.

According to our data, this connection is generally reduced to simple relationships. For example, for the sintered and untreated surface of hard alloys, this dependence is close to the form $R_{max} \approx 4R_a$. At blade processing of steels (40X, SHX15, X12M) with cutters from Hexanite-P the ratio corresponds more to the form of $R_{max}/R_a \approx 6$.

For abrasive treatment the most characteristic in this case will be the ratio close to the form of $R_{max}/R_a \approx 8$. This is typical both for the processing of tool materials: high-speed steels, tool ceramics, hard alloys (tungsten and tungsten), and for the processing of stainless steels, titanium alloys and joint processing of hardened and not Hardened steel (steel 10 + 9HF). And can there be other variants of this relation for abrasive processing? We found that they can. The ratio $R_{max}/R_a \approx 6$ is characteristic for abrasive processing of high-speed steels by circles of electrocorundum and diamond processing of magnetohard alloys, when a rougher surface is formed or its contribution to the height parameters are introduced by porosity. In general, it would probably be more correct to assume that for abrasive treatment (in a sufficiently wide range) the ratio R_{max}/R_a is closer to the form $R_{max}/R_a \approx 6–8$, and larger values are also characteristic of pure abrasive treatment

methods. But when proving ceramics and coatings, the ratio is close to the form $R_{max}/R_a \approx 10$. In the latter case, the porosity of these materials contributes to the relative increase in the value of R_{max}, because it already matters when proving it. The above allowed us to formulate the following position: the rougher the surface, the smaller the ratio between R_{max}/R_a, and the more perfect the surface obtained by proving, polishing or other finishing methods, the greater the ratio. That is, for example, the sintered surface and the surface after abrasive treatment with conventional abrasives have the ratio R_{max}/R_a in the range (4-6). Processing with grinding wheels with SHM, when the surface has a lower roughness than after the above methods, and in fine grinding is mainly characterized by the ratio $R_{max}/R_a \approx 8$. In the case of finishing operations on porous materials, when the values of R_a are small, this ratio R_{max}/R_a is already close to 10. Just in this case, the defects of the treated surface in the form of pores or scratches and is the reason for the increase in the value of this ratio.

Meanwhile, a number of further studies have shown that this conclusion is incomplete, as it reflects only the first part of this trend. It turns out that if we need to get an even more perfect surface after grinding, for example, polishing to obtain values of roughness values up to 5–10 *nm*, ie the cost of the process of obtaining the surface increases, the value of the ratio R_{max}/R_a begins to decrease and reaches the situation when the above ratio becomes close to the form $R_{max}/R_a \approx 4$. That is, we have a kind of return to the original data in relation.

We will demonstrate the above on the example of forming a polished and polished surface of lithium tetraborate single crystal, a new promising material for functional electronics, the processing of which is very expensive, as it requires a final roughness for parameter R_a within 1 *nm* [1]. After cutting the single crystal, its grinding was performed with a free abrasive with a decrease in the grain size of the abrasive and it would be logical to assume that the ratio R_{max}/R_a, based on the above, will be within 6 (actually obtained: from 5.25 up to 6.25). Further polishing of lithium tetraborate single crystals was performed on resin polishers using two AFM diamond micropowders with a grain size of 2/1 to 1/0 and chromium oxide. This increases the cost of the process, but can significantly reduce the roughness of the treated surface of single crystals. For example, the roughness of the polished surfaces of single crystals after treatment with AFM 1/0 micropowder corresponds to R_a in the range from 3.5 *nm* to 6.5 *nm*. Subsequent use of chromium oxide during polishing can further reduce the roughness. Analysis of the polished surface by atomic force microscopy showed that in the lithium tetraborate single crystal in the plane (100) the microrelief has R_{max}, R_z and R_a, which are 5.26 *nm*, 4.82 *nm* and 1.24 *nm*, respectively, and the ratio R_{max}/R_a is 4.25. The above, just indicates that the more expensive the process of obtaining a high quality surface, the ratio R_{max}/R_a decreases to – 4.

In general, in relation to R_{max}/R_a we have a kind of "roughness arc", when first for a normal untreated rough source surface it is close to 4, then abrasive-diamond treatment of this surface raises this ratio to 6 and then to 8, but further methods of abrasive finishing and polishing reduce the ratio to 6 and then chemical-mechanical polishing to a high-quality surface returns this ratio to values close to 4. This means that if the initial cost of grinding the original surface affects the increase in the ratio, then the subsequent cost of finishing and polishing work reduces the value of the ratio to the original – R_{max}/R_a =4.

Thus, the research showed that there is a possibility under certain conditions to fundamentally change the distribution of micro-irregularities on the treated surface, which will increase the fullness of its profile and form a surface with a kind of "oil pockets".

At one time in [7] it was shown that one of the ways to increase the technical and operational performance of the internal combustion engine is the formation on the surfaces of the cylinders of such an engine special microprofile, which is a flat alternating protrusions with recesses (peculiar "pockets") to accommodate the oil (Fig. 1). This increases the oil capacity and the bearing area of the treated surface. As a result, running-in time is reduced, lubrication costs are reduced, cylinder wear is increased and engine life is increased. It is established that the planar apex of such a surface is 50–66 % at the level of the profile cross section p=1–2 μ*m* from the line of the maximum protrusion, the depth of the lines for oil placement is 2.5–10 μ*m*. Surfaces of this type can be obtained by blunting the protrusions of the microprofile after pre-honing, as well as rolling the final treated surface.

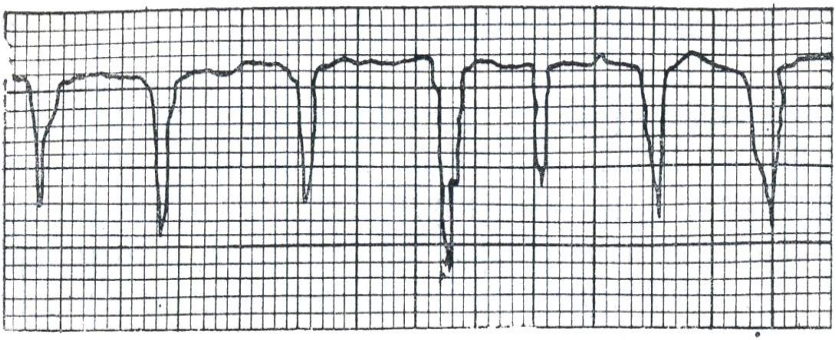

The question arises, is it possible to obtain approximately the same surface immediately in the grinding process without any additional refinement ? That is, is it possible to make a wheel at once to obtain a treated surface with "pockets" ?

Our research has shown that this is possible, but for this we need to use a mixture of abrasives in the working layer. Thus, in [8] we once paid attention to the features of the tool with SHM, when the working layer of the wheel combines two or three grinding powders of different abrasives (diamonds and CBN), namely, additionally introduced into the working layer grinding powder compacts based on cubonite micropowders.

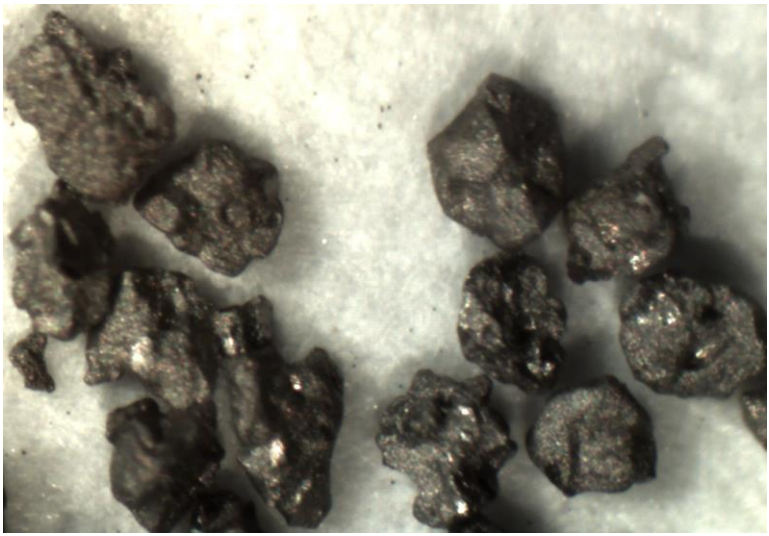

Figure 2 – General view of metallized grinding powders of compacts with grain size KM 400/315 from cubonite micropowders

These compacts have certain abrasive properties [8]. However, it should be noted that, probably due to the somewhat unusual (layered) wear of the grains of compacts, it is possible to form the original heterogeneous, unusual for the tradition. These wheels with SHM, the profile of micro-irregularities of the treated surface with the presence of peculiar "pockets" on the treated surface. However, attention was drawn to the fact that the above pure compacts are to some extent relatively "soft" and it was suggested that such compacts should be made more rigid due to their metallization (Fig. 2).

As the use of a mixture of grinding powders gives a certain effect, at the last stage for comparison the operational indicators of wheels were studied, when they use a mixture of KM compacts of different grain size and standard diamond grains

of corresponding grain sizes. The surface roughness was investigated when using wheels with a mixture in the ratio of 50 to 50 grains from compacts with a grain size of KM 400/315 and the corresponding diamond grains of the AC32 brand. Thus, there is a situation that now only 50% of compacts are in the working layer, and the other 50% are diamonds, which on high-speed steel have a wear mechanism close to compacts, because on them Wear planes are also formed, and this is observed by the nature of micro-irregularities of the treated surface (Fig. 3).

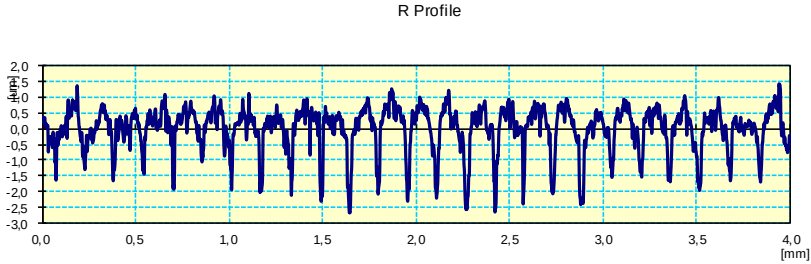

Figure 3 – The profile of microroughnesses of the processed surface in a wheel with a mix of grinding powders of the KM 400/315 compact and AC32 400/315 diamond

4. SUMMARY

Our research has shown that the ratio of roughness R_{max}/R_a is important to assess the distribution of the processing material in the rough layer, and thus to assess the possibility of forming a specific rough layer.

It is established that the simultaneous use of compacts and diamond grains in grain wheels may not improve the situation both in terms of wear resistance of the wheels and the quality of the treated surface, as it is impossible to achieve productive conditions for processing of high-speed steel. At the same time, it was found that with such a mixture in wheels it is possible to achieve a reduction in the roughness of the treated surface and the specific profile of micro-irregularities, when the so-called "oil pockets" are formed. That is, from the above it is clear that there is a real opportunity to implement in one wheels the conditions for obtaining a specific profile of micro-irregularities during grinding, when the so-called "oil pockets" are formed without any additional technological means.

References: 1. *Lavrinenko, V.I. and Novikov, M.V.,* Nadtverdi abrazyvni materiali v mekhanoobrobtsi: entsiklopedichnii dovidnik [Superabrasive Materials in Machining Operations: Encyclopedic Handbook], Novikov, M.V., Ed., Kyiv: Inst. Sverkhtverd. Mater., Nats. Akad. Nauk Ukr., 2013.

2. *Puthanangady T.* Recept Grinding Process Developments in the Optical Fiber Communication Industry // Gohram conferences : Precision Grinding & Finishing in the Global Economy – 2001, Chicago, October, 1 – 3, 2001. **3.** Some Specific Features Inherent in the Relation between the Roughness Parameters of a Treated Surface under Grinding Wheels with a Mixture of SHM Grinding Powders with Superficially Modified Grains / *V.I. Lavrinenko, O.O. Pasichnyi, V.G. Poltoratskyi, V.Yu. Solod, V.L. Dobroskok, E.V. Ostroverkh.* Journal of Superhard Materials, 2021, Vol. 43, No. 6, pp. 444–454. **4.** *Novikov, F.V.,* Vysokoprodyktuvne almazne shlifuvannia [High-performance diamond grinding]. Kharkiv: CHNEU, 2014. 412 p. **5.** *Novikov F.V., and Shkurupiy V.G.* Vlijanie fornu rezyschih zeren pri abrazivnoj obrabotke na parametru sherohovatosti poverchnosti [Influence of the shape of cutting grains during abrasive treatment on the surface roughness parameters]. Fizicheskie i kompjuternue technologii. Trudy XXI Mezdunarodnoi nauchno-prakticheskoi konferencii. [Physical and computer technologies. Proceedings of the XXI International. scientific-practical conference], Kharkiv, 2015. pp. 3–13. **6.** Fizichni zasadu formoutvorennia precizinuch poverkhon pid chas mechinicnoi obrobki nemetalevich materialov [Physical principles of forming precision surfaces during machining of non-metallic materials] *Yu.D. Filatov, VI Sidorko, O.Yu. Filatov, S.V. Kovaliov*. Kyiv: Nauk. dumka, 2017. 247 p. **7.** Chepovetsky I.H. Mehanika kontaknogo vzaimodeistvija pri almaznoi obrabotke [Mechanics of contact interaction in diamond processing]. Kyiv: Nauk. dumka, 1978. 238 p. **8.** *Lavrinenko, V.I., Sytnyk, B.V., Poltorats'ky, V.G., Bochechka, O.O., and Solod, V.Yu.,* Composites based on cBN micron powders structured by carbon binder for the application as functional elements in the working layer of diamond-abrasive tools. Part 1. Composite grits as abrasive elements, J. Superhard Mater., 2014, vol. 36, no. 3, pp. 193–198.

Валерій Лавріненко, Київ, Україна,
Володимир Солод, Кам'янське, Україна

СПІВВІДНОШЕННЯ МІЖ ПАРАМЕТРАМИ ШОРСТКОСТІ І ОСОБЛИВОСТІ ФОРМУВАННЯ ПОВЕРХНІ ІЗ СПЕЦІАЛЬНИМ МІКРОПРОФИЛЕМ

Анотація. *Викладені особливості зв'язку між основними висотними параметрами шорсткості Rmax та R_a, а також між кроковим Sm та висотним параметрами R_a при торцевому шліфуванні кругами з НТМ. Побутує такий досить стійкий міф, що вказані вище параметри як би незалежно існують самі по собі і можливо отримати будь-яке необхідне значення одного параметра і будь-яке бажане значення іншого, або, наприклад, можна подіяти на один параметр, а інші не зміняться. Наслідком такого міфу є те, що дослідники окремо вивчають вплив режимів і умов обробки на конкретні параметри шорсткості, чим вноситься системна похибка, оскільки насправді для однакових умов обробки всі параметри шорсткості пов'язані між собою і впливати тільки на один параметр є неможливим, бо зміняться і інші. Тому метою даної роботи було показати як змінюється співвідношення між основними висотними показниками шорсткості R_{max} та R_a і як це може дозволити досягти умов формування поверхні із спеціальним мікропрофілем при алмазній обробці. Показано, що вказаний зв'язок між вказаними параметрами шорсткості в цілому зводиться до простих відношень. Наприклад, для спеченої і необробленої поверхні твердих сплавів таке відношення близьке до вигляду R_{max}/R_a □ 4. При лезовій обробці сталей різцями з Гексаніту-Р відношення R_{max}/R_a вже є ≈ 6. В цілому, ймовірно більш вірним було би вважати, що для абразивної обробки (в достатньо широкій області) відношення R_{max}/R_a є більш близьким до вигляду R_{max}/R_a ≈ (6–8), причому більші значення є характерними і для чистових методів абразивної обробки. А ось при доведенні кераміки і покриттів це відношення зростає до ≈ 10. В останньому випадку свій внесок у відносне підвищення значення Rmax вносить пористість даних матеріалів, оскільки при доведенні вона*

вже має значення. Наведене вище дозволило нам сформулювати таке положення: чим більш грубою є поверхня, тим вона має менше відношення між R_{max}/R_a, а чим більш довершеною є поверхня, отримана доведенням, поліруванням або іншими фінішними методами, тим це відношення є більшим. Тобто, наприклад, спечена поверхня і поверхня після абразивної обробки звичайними абразивами має відношення в діапазоні $R_{max}/R_a \approx (4–6)$. Обробка шліфувальними кругами з НТМ, коли поверхня має меншу шорсткість, аніж після наведених вище методів, і при тонкому шліфуванні переважно характеризується зростанням відношення до ≈ 8. У випадку доводочних операцій на пористих матеріалах, коли значення Ra є невеликими, це відношення є вже близьким до $R_{max}/R_a \approx 10$. Як раз в цьому випадку дефекти самої обробленої поверхні у вигляді пор або подряпин і є причиною підвищення величини даного відношення. Між тим, низка подальших досліджень засвідчила, що такий висновок є неповним, оскільки відбиває тільки першу частину вказаної тенденції. Виявляється, що якщо нам необхідно отримати ще більш довершену поверхню після шліфування, наприклад, поліруванням з отриманням значення величин шорсткості до 5–10 нм, тобто витрати на процес отримання поверхні зростають, то величина відношення R_{max}/R_a починає знижатися і досягає тієї ситуації, коли вказане вище відношення стає близьким к вигляду $R_{max}/R_a \approx 4$. Тобто у нас відбувається своєрідна «дуга відношення висотних параметрів». Наведені дослідження дозволили виявити умови формування спеціального мікропрофіля оброблюваної поверхні при алмазному шліфуванні. Так, одночасне застосування в кругах зерен компактів і алмазних зерен ситуацію може не поліпшувати як з точки зору зносостійкості кругів так і якості обробленої поверхні, оскільки є неможливим досягти умов продуктивної безприпальної обробки швидкорізальної сталі. Разом з тим, виявлено, що саме при такій суміші в кругах і є можливим досягти зниження шорсткості обробленої поверхні і того специфічного профілю мікронерівностей, коли утворюються так звані ,,масляні кишені". Тобто встановлено, що є реальна можливість реалізувати в одному крузі умови отримання при шліфуванні специфічного специфічного профілю мікронерівностей, коли утворюються так звані ,,масляні кишені" без будь-яких додаткових технологічних засобів.

Ключові слова: *параметри шорсткості; співвідношення між висотними параметрами R_{max}/R_a; спеціальний мікропрофіль.*

UDC 621.91.01 **doi: 10.20998/2078-7405.2022.96.12**

J. Kundrák, I. Deszpoth,
V. Molnár, Miskolc, Hungary

DECISION SUPPORT METHOD FOR THE APPLICABILITY OF HARD TURNING

Abstract. *In this study the applicability of hard turning is analyzed in the case of disc-shaped parts (gear wheels). The relevance of such parts has been increasing in the automotive industry; therefore, the efficiency of large series or mass production has high priority. The novelty of this paper is the collection of factors that has to be considered in preparation for applicability decisions of hard turning in order to ensure efficient machining. This can be the basis of the IT support, i.e. an automation solution for technologists. The introduced process is elaborated on the basis of theoretical considerations and production shop-floor experience.*
Keywords: *hard turning; automation; procedure selection.*

1. INTRODUCTION

The machinability of hardened surfaces has been an issue of high importance for decades in the automotive industry [1, 2]. With the appearance of new machine tools (e.g. hard machining centers) and procedure versions (e.g. hard turning and grinding in one clamping) applied for the efficient machining of hardened surfaces [3, 4], technological improvement has opened new research directions [5, 6]. Therefore, beyond the optimization of the applied technological parameters of a procedure [7, 8], a goal is now the selection of the potentially best procedures and procedure versions for a part [9, 10]. The type of the necessary machine tool on which a part can be machined depends, among other factors, on the specified accuracy and surface quality [11]. In addition to the specified accuracy [12-14] and roughness [15, 16] (e.g. Rz) parameters, functional requirement determining factors must also be considered. Decisions need to be made, for example, on whether periodic or random topography is allowed [17, 18]. The type of clamping and the hardness of the machined material [19] have to be considered, and whether the geometry of the tool and the tool holder allows machining [20]. Another important factor is that the rigidity of the machine tool and the tool have to ensure the specified accuracy [21]. In the topic of machining efficiency a number of issues were studied in our previous works: machinability of various types [22, 23] and geometry [24] of surfaces in the case of disc-shaped parts; ensuring accuracy [25] and surface quality [26] of hard turned and ground parts; optimization of technological data of hard machining [27, 28]; analysis of material removal efficiency [29, 30]; and the necessity of applying coolant and lubricant [31].

Based on the details above, it can be stated that some of thefactors influencing the applicability of hard turning differ from those for soft materials. A possible grouping of the factors influencing the machining (cutting) is the following.

1. Shape and dimensions of the part,
2. Size and continuity of the machinable surfaces,
3. Clamping possibilities on the machine tool,
4. The specified accuracy and roughness parameters,
5. The allowed position and form errors,
6. The hardness of the material and the allowances.

In this study applicability possibilities of hard turning are analyzed by the consideration of the listed factors. The study also aims to analyze how to reach a higher level of productivity and methods for deciding whether a single-point tool or abrasive tool can be used to fulfill the requirements specified in the part's drawing are. Based on the analysis of the listed influencing factors of machinability, a simple but comprehensive series of activities is suggested that can aid decisions on the applicability of the procedure. The novelty of the method is that it considers a number of factors in a complex manner and formally describes the steps of the decision process. The overview analysis is based on theoretical and empirical information and data (e.g. shape accuracy) specified for the part (plant specifications for a given transmission type) to guide the decision process. The method was elaborated for gear wheels often used in transmission systems.

2. FACTORS INFLUENCING THE APPLICABILITY OF HARD TURNING

2.1. Shape and dimensions of the part

The gear wheels built into transmission systems are disc-type parts. The machining technology of their bores is significantly influenced by the rate of the bore's length and diameter (l/d). When standard tools are applied, hard turning is only possible if the bore is short (short bore: $l/d \leq 0.5$; normal bore: $l/d = 0.5–3$). When longer bores are machined, vibration is experienced in the system due to the hard material, the high cutting speed, the chip formation characteristics and the lack of sufficient rigidity. Based on our experience, $l/d \leq 2$ can be recommended as boundary condition. In Table 1, based on the conclusions drawn from the machining of the analyzed gears, examples are demonstrated for the l/d rates of two gears (L_3/d_1 in the table). These falls on one hand to the short and on the other to the lower range of normal bores. This means, they can be turned in hardened state without any risks.

Table 1 – Accuracy, position- and form errors, diameter rates

Bore diameter	Surface	Allowed					L_3/d_1	d_{rc}/d_1
		Position error			Form error			
Ø35G6 Ø83G5	bore	//	0.006	Z1	○	0.012	0.37 1.05	1.45 3.13
	face	↗	0.03	Z1	▱	0.035		
	cone	↗	0.10	Z1	○	0.006		

In Fig. 1 the hard machined surfaces of gear wheels for transmission systems are demonstrated (bore: H, faces: I and II, cone: C). The machining of face and cone surfaces is not always carried out. In order to reach higher productivity and accuracy, machining takes place in one clamping; therefore, two tools are used, one of which is needed for turning the back face through the bore.

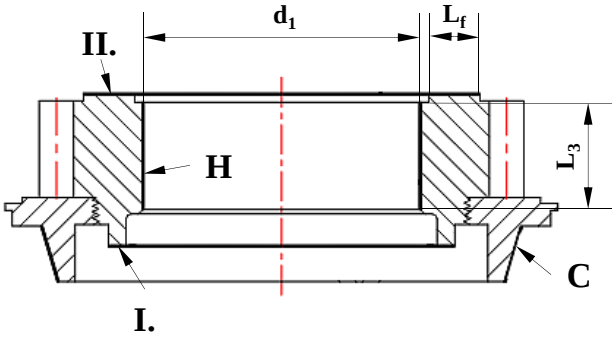

Figure 1 – Machined surfaces of transmission system gears

In the case of bores not only the l/d rate but the impact of the bore diameter has to be analyzed. The tool holder has to fit into the bore (Fig. 2) in such a way that its diameter allows the turning of the back face through the bore (Fig. 3).

For the first criterion the minimum bore diameter that allows the safe fit of the tool holder can be determined by Eq. (1) (the length c is the distance between the tool's center line and the tool tip; these data are provided by the tool manufacturer).

$$d_1 = \frac{d_{sz}}{2} + c + 1 \qquad (1)$$

The second criterion can be defined based on Fig 2. The tool holder has to be fulfill the first criterion and the bore diameter has to allow the radial move of the tool for machining the L_f length. This criterion is determined by Eq. (2).

$$L_f \leq d_1 - d_{sz} \tag{2}$$

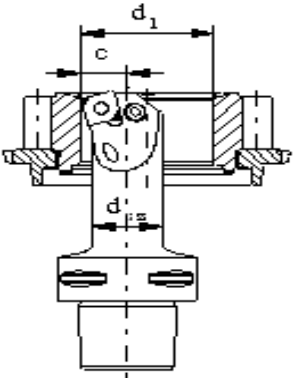

Figure 2 – Dimensions of the bore and the tool holder

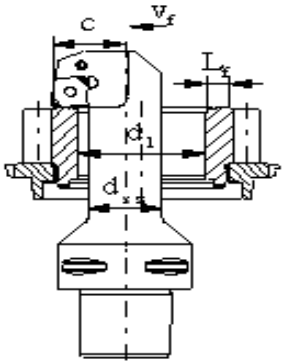

Figure 3 – Necessary bore diameter in face turning

For workpiece dimensions, the ratio of the external and internal diameter (D/d) must be analyzed. In Table 1 the notation of this rate is d_{rc}/d_1. If the ratio is low, i.e. the component is a thin-walled ring-feature part, then the clamping force can be limited, otherwise the deformation, i.e. the roundness caused by the chuck, could be too large.

It is recommended to check the calculated clamping force, although in the case of complex gears applying experiment-based force is suggested instead of calculations. Special chuck jaws are recommended if the diameter rate of the gear is lower than 1.4.

2.2. Size and continuity of machinable surfaces

The applicability of hard turning to disc-shaped gears is not influenced by the length of the machinable surface. Since the machinable surfaces are not very extensive, they do not cause large-scale tool wear on the feed path that would threaten the accuracy or surface roughness.

However, the continuity (interruptions) of the surfaces (e.g. for a lubricating groove) has to be considered. In the case of interrupted surfaces the correction of the cutting data (mainly the cutting speed) may be necessary. It is worth relying on

the recommendations of tool manufacturers, because they recommend different tool materials for the same cutting speed. Based on the interruption, four types of surfaces can be defined: strongly, moderately, slightly interrupted and continuous surfaces. Based on the features and dimensions of the interruptions, the faces of the gears analyzed here are slightly interrupted. The recommendation for the cutting speed in this case is two-thirds of the cutting speed recommended for continuous surfaces, i.e. 200 m/min instead of 300 m/min.

2.3. Clamping possibilities on the machine tool

This is a trivial criterion, but it must not be neglected. A decision about the clamping one is easily made based on the manual of the hard turning center. The existence of proper jigs or clamping jaws (sometimes of special design) is an issue. Jigs and clamping jaws corresponding to the geometrical dimensions, clamping force and the specified accuracy are required.

2.4. Specified accuracy and roughness parameters

The dimension accuracy realizable by hard turning depends mainly on the machine tool. Special precision or high precision lathes built for hard- turning operations are now available. Their static, dynamic and thermic rigidity and their spindle and sled structures can help achieve the accuracy of grinding and a level identical to the accuracy requirements of grinding machines.

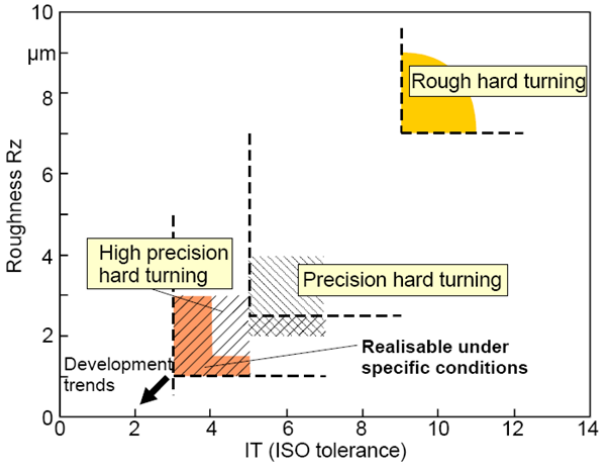

Figure 4 – Hard turning based on accuracy and surface roughness [32]

The machining accuracy of precision turning centers is between IT5 and IT7 (Fig. 4). If the accuracy specification is higher than IT5, an high precision machine tool is necessary. The surfaces that require higher accuracy (between IT 3 and IT5) and Rz<2 roughness, can be machined by precision grinding or honing.

In Table 2 surface roughness values of bores machined on a precision lathe are given as an example, compared to the measured values of the same part machined by grinding. The type of the applied lathe was PVSL Pittler. The lower limit of machining accuracy of this machine tool is IT5 and the Rz surface roughness can be realized between 2 and 6 μm. With this machine tool the required precision values were realizable.

Table 2 – Measured roughness data

Procedure	R_z [μm]	R_{max} [μm]	R_a [μm]
Grinding	2.27–2.31	2.64–2.84	0.27–0.28
Hard turning	1.61–2.67	1.76–2.91	0.27–0.43

Although not shown in the technical drawings, the relative bearing length can be important because of the functionality requirements of the parts. Some measured values are given in Table 3. Selecting the proper parameter values allows a significantly higher relative bearing length in hard turning compared to grinding. The 100% bearing length was obtained at a lower segment depth when the surface was hard turned than with grinding.

Table 3 – Measured relative bearing length

#	Bore diameter	Segment depth [μm]	Relative bearing length, t_p [%]	
			Ground	Hard turned
1	Ø35G7	0.2	0.34	1.65
		0.4	1.50	1.23
		0.6	6.12	24.28
2	Ø83G5	0.2	0.42	1.39
		0.4	2.20	6.49
		0.6	8.52	13.41

2.5. Specified position and shape errors

Based on the state-of-the-art and our measurement database, values can be designated below which the specified position and form error limit the use of hard turning. For position errors, the parallelism of bore slants and the axial run-out to the bore are specified; for form errors the allowed roundness and the face's flatness are specified. Data in the literature for the position and form errors:

- parallelism: 1–3 μm
- axial run-out: no data available
- roundness: 2–3 μm
- flatness: no data available

Our measurement results for the position and shape errors:

- parallelism: 2–3 μm
- axial run-out: 7–9 μm
- roundness: 2–8 μm
- flatness: 5–9 μm

Based on the literature and measurements, concerning position and form errors, hard turning can be applied if:

- parallelism > 0.003 μm
- axial run-out > 0.010 μm
- roundness > 0.003 μm
- flatness > 0.010 μm

Concerning the roundness it is noted that it can be realized if the clamping method and the clamping force correspond to the wall thickness of the gear. The position and form errors were compared for grinding and hard turning (Table 4). It was found that the values of hard turning can match those of grinding.

Table 4 – Measured position and form errors after machining

№	Bore diameter	Surface	After hard turning					After grinding				
			Position error			Form error		Position error			Form error	
1	Ø35G6	bore	//	0.003	Z5	○	0.008	//	0.003	Z5	○	0.007
						⌭	0.013				⌭	0.019
		face	↗	0.007	Z5	▱	0.005	↗	0.023	Z5	▱	0.008
2	Ø83G5	bore	//	0.002	1ZR	○	0.003	//	0.003	1ZR	○	0.003
						⌭	0.008				⌭	0.003
		face	↗	0.007	1ZR	▱	0.006	↗	0.282	1ZR	▱	0.017

2.6. Hardness of the material and the allowances

The PCBN insert manufacturers define the operation range of the inserts in terms of hardness of the machined material between 50 and 65 HRC. This interval has to be considered as the application condition.

Concerning the allowance, the maximum and minimum values have to be determined. In the maximum value the recommendations of the tool manufacturers have to be considered. The gears of transmission systems are case hardened parts. Considering their dimensions and the fact that the finishing is carried out in one pass, an allowance 0.3 mm is recommended.

3. STEPS OF DECISION PROCESS FOR THE APPLICABILITY OF HARD TURNING

As a result of summarizing considerations discussed above, a method was elaborated for deciding whether hard turning or grinding is the more suitable technology to be applied. Based on the criteria system even a third technology can be used if there are too strict accuracy specifications.

Based on the particular situation of production the values of the criteria can be modified without influencing the steps of the process. The method facilitates IT support, meaning that the decision process can be automatized. The steps of the process:

1. Enter the data necessary for the decision.

2. Make a decision about the applicability of hard turning based on the hardness of the workpiece (a too soft or too hard surface is a reason for exclusion).

3. Decide about the applicability of hard turning based on the bore length and diameter rate.

4. Decide about the application of special clamping jaw or exclusion of hard turning based on the rate of root circle diameter and bore diameter.

5. Analyze whether the size of the hard turning center and the chuck jaw allows the workpiece to be clamped.

6. Decide about the applicability of hard turning of the bore (H) based on the accuracy, position and form error, and roughness specifications.

6.1. Select the tool holder, tools and inserts (the dimensions of the tool holder have to correspond to the bore diameter).

6.2. Analyze the allowance of the bore.

- Too small allowance is a reason for exclusion.
- Determination of the number of passes if the allowance is suitable (one or more roughing passes and one smoothing pass).

6.3. Determine the necessary clamping force.

7. Decide about the applicability of hard turning of the right face (I) based on the accuracy, position and form error, and roughness specifications.

7.1. Select the tool holder, tools and inserts

7.2. Analyze the allowance for the right face.

- Too small allowance is a reason for exclusion.
- Determination of the number of passes if the allowance is suitable (one or more passes).

8. Decide about the applicability of hard turning of the left face (II) based on the accuracy, position and form error, and roughness specifications.

8.1. Select the tool holder, tools and inserts.

8.2. Analyze the allowance of the left face.

- Too small allowance is a reason for exclusion.
- Determination of the number of passes if the allowance is suitable (one or more passes).

9. Decide about the applicability of hard turning of the cone surface (C) based on the accuracy, position and form error and roughness specifications.

9.1. Selectof the tool holder, tools and inserts.

9.2. Analyze the allowance of the cone surface

- Too small allowance is a reason for exclusion.
- Determination of the number of passes if the allowance is suitable (one or more passes).

10. If hard turning is not excluded at any of the previous steps, then determine the cutting data

SUMMARY AND CONCLUSIONS

The study is about the applicability of hard turning analyzed through specifications and values for hard turning and grinding and about the selection of technological data (both the factors that have to be considered and the order in which the data should be considered). Based on the introduced method (the series of analysis) and with the help of IT support, the determination of technological data can be realized for hard turning. The method was elaborated for disc-type parts.

The elaboration of the method (process) was based on theoretical and empirical considerations. The main findings are:

- A structured process (algorithm) can be prepared for supporting the decision of applicability of hard turning; therefore, the decision process can be automatized.
- The process can be generalized for hard turning and by applying basic technological calculations, the decision can be made for specific parts.

The method can be extended for other types of typical parts. In the current method the economic and financial factors of the output are not analyzed; the method can be extended by these factors in future research.

References: 1. *O. Koval'chuk, V. Nezhebovsky, O. Permyakov, O. Klochko, S. Ryabchenko.*: Processing of hardened cylindrical gear wheels of the cutting gearbox of the combine ukd 200-500, Cutting & Tools in Technological System, 95, 2021, pp.57–70. **2.** *Grabchenko, A., Fedorovich, V., Pyzhov, I., Ostroverkh, Y.*: Increase of efficiency of diamond grinding superhard of materials, Cutting & Tools in Technological System 93, 2020, pp.24–32. **3.** *Moriwaki, T.*: Multi-functional machine tool, CIRP Annals, 57, 2008, pp.736–749. **4.** *Kundrak, J., Mamalis, A.G., Markopoulos, A.*: Finishing of hardened boreholes: grinding or hard cutting?, Materials and Manufacturing Processes, 19, 2004, pp.979–993. **5.** *Klocke, F., Brinkmeier, E., Weinert, K.:* Capability profile of hard cutting and grinding process, *CIRP Annals, 54*, **2005**, pp.22–54. **6.** *Tönshoff, H.K., Arendt, C., Ben Amor, R*. Cutting of hardened steel, *CIRP Annals, 49*, **2000**, pp. 547–566. **7.** *Hernandez, A.E.B., Beno, T., Repo, J., Wretland, A.*: Integrated optimization model for cutting data selection based on maximal MRR and tool utilization in continuous machining operations, CIRP Journal of Manufacturing Science and Technology, 13., 2016., pp.46–50.
8. *Qiu, J., Ge, R.*: A theoretical model and experimental investigation to predict and evaluate cutting capability of turning center based on material removal rate, 104, 2019, pp. 3287–3302. **9.** *Konig, W., Berktold, A., Koch, K.F.*: Turning versus grinding—A comparison of surface integrity aspects and attainable accuracies, *CIRP Annals, 42*, **1993**, pp. 39–43. **10.** *Bana, V.*: Manufacturing of high precision bores, PhD dissertation, 2006.
11. *Liao, Y., Liao, B.*: Dynamics modeling and modal analysis of machine tool considering joints parameters, Manufacturing Technology 19(2), 2019, pp. 267–272. **12.** *Linins, O., Krizbergs, J., Boiko, I.*: Surface texture metrology gives a better understanding of the surface in its functional state, Key Engineering Materials, 527, 2013, pp. 167–172. **13.** *Yakimov, O., Bovnegra, L., Tonkonogyi, V., Vaysman, V., Strelbitskyi, V., Sinko, I.*: Influence of the geometric characteristics of the discontinuous profile working surfaces of abrasive wheels for precision and temperature when grinding, Cutting & Tools in Technological System 94, 2021, pp. 115–125. **14.** *Prisco, U., Squillace, A., Scherillo, F.,Coticelli, F., Astarita, A.*: Form and dimensional accuracy of surfaces generated by longitudinal turning, Manufacturing Technology, 16(3), 2016, pp. 595–600. **15.** *Neslušan M., Rosipal M., Kolařík K., Ochodek V.*: Application of barkhausen noise for analysis of surface integrity after hard turning, Manufacturing Technology, 12(1), 2012, pp. 60–65. **16.** *Popov, A., Khramenkov, M.***:** Effect of hydraulic oil entering the cutting fluid on the tool life and roughness in turning of stainless steel, Manufacturing Technology, 19(4), 2019, pp. 664–667. **17.** *Kundrak, J., Nagy, A., Markopoulos, A.P., Karkalos, N.E.*: Investigation of surface roughness on face milled parts with round insert in planes parallel to the feed at various cutting speeds, Cutting & Tools in Technological System, 2019, pp. 87–96. **18.** *Zawada-Tomkiewicz, A.*: Analysis of surface roughness parameters achieved by hard turning with the use of PCBN tools, Estonian Journal of Engineering, 17, 2011, pp. 88–99. **19.** *Kundrak, J., Mamalis, A. G., Gyani, K., Bana, V.*: Surface layer microhardness changes with high-speed turning of hardened steels, International Journal of Advanced Manufacturing Technology, 53, 2011, pp. 105–112. **20.** *Zhang, S.J., To, S., Zhang, G.Q., Zhu, Z.W.*: A review of machine-tool vibration and its influence upon surface generation in ultra-precision machining, International Journal of Machine Tools and Manufacture, 91, 2015, pp. 34–42. **21.** *Mamalis, A.G., Kundrak, J., Horvath, M.*: On a novel tool life relation for precision cutting tools, Journal of Manufacturing Science and Engineering, 127, 2005, pp. 328–332. **22.** *Kundrak, J., Molnar, V., Deszpoth, I.*: Comparative analysis of machining procedures, Machines 6, 2018, pp. 1–10. **23.** *Kundrak, J., Molnar, V., Markopoulos, A.P.*: Joint machining: hard turning and grinding, Cutting & Tools in Technological System, 90, 2019, pp. 36–43. **24.** *Kundrak, J., Deszpoth, I., Molnar, V.*: Effects of the bore-hole geometry on the productivity of hard machining, Proceedings of the Thirteenth International Conference on Tools: ICT 2012, Miskolc, 2012, pp. 157–164. **25.** *Kundrak, J., Sztankovics, I., Molnar, V.*: Accuracy and topography analysis of hard machined surfaces, Manufacturing Technology, 21, 2021, pp. 512–519. **26.** *Molnar, V.*: Tribology and topography of hard machined surfaces, Cutting & Tools in Technological System, 94, 2021, pp. 49–59. **27.** *Molnar, V., Deszpoth, I., Kundrak, J., Markopoulos, A.P.*: Efficiency of material removal and machining in cutting, Cutting & Tools in Technological System, 92, 2021, pp. 35–47. **28.** *Kundrak, J.,*

Nagy, A., Markopoulos, A.P., Karkalos, N.E., Skondras-Giousios, D.: Experimental study on surface roughness of face milled parts with round insert at various feed rates, Cutting & Tools in Technological System, 92, 2020, pp. 96–106. **29.** *Molnar, V., Kundrak, J., Deszpoth, I.*: Some economic issues of hard machining, Proceedings of the 3rd International Scientific and Expert Conference with simultaneously organised 17th International Scientific Conference CO-MAT-TECH 2011, Trnava, 2011, pp. 251–254. **30.** *Kundrak, J., Deszpoth, I., Molnar, V.*: Comparative study of material removal in hard machining of bore holes, Tehnicki Vjesnik-Technical Gazette, 21, 2014, pp. 183–189. **31.** *Kundrak, J., Molnar, V.*: Comparison of hard machining procedures on material removal rate, Hungarian Journal of Industry and Chemistry, 39, 2011, pp. 219–224. **32.** *Byrne, G., Dornfeld, D., Denkena, B.*: Advancing cutting technology, CIRP ANNALS, 52(2), 2003.

Янош Кундрак, Іштван Дезпот,
Віктор Мольнар, Мішкольц, Угорщина

МЕТОД ПІДТРИМКИ ПРИЙНЯТТЯ РІШЕННЯ ПРО ЗАСТОСУВАННЯ ЖОРСТКОГО ТОЧІННЯ

Анотація. *У цьому дослідженні проаналізовано застосування жорсткого точіння для дискових деталей (зубчастих коліс). Актуальність таких деталей у автомобільній промисловості зростає; тому ефективність великосерійного чи масового виробництва має першорядне значення. Новизною цієї статті є сукупність факторів, які необхідно враховувати при підготовці рішень щодо застосування жорсткого точіння для забезпечення ефективної обробки. Це, можливо, буде основою ІТ-підтримки, тобто рішенням щодо автоматизації для технологів. Представлений процес розроблено на основі теоретичних міркувань та виробничого досвіду. Оброблюваність загартованих поверхонь протягом десятиліть є проблемою, що має велике значення в автомобільній промисловості. З появою нових верстатів і інструментів (наприклад, твердосплавних різців, оброблювальних центрів) та варіантів процедур (наприклад, жорстке точіння та шліфування з однієї установки), що застосовуються для ефективної обробки загартованих поверхонь, відкрило нові напрямки досліджень. Дане дослідження також спрямоване на аналіз того, як досягти більш високого рівня продуктивності, та методів прийняття рішення про те, чи можна використовувати одноточковий або абразивний інструмент для виконання вимог, зазначених на кресленні деталі. На основі аналізу факторів, що впливають на оброблюваність, пропонується простий, але всеосяжний ряд дій, які можуть допомогти прийняти рішення щодо застосування процедури. Новизна методу у тому, що він комплексно розглядає низку чинників і формально визначає етапи процесу прийняття рішення. Оглядовий аналіз заснований на теоретичній та емпіричній інформації та даних (наприклад, точності форми), зазначених для деталі (технічні характеристики установки для даного типу трансмісії), щоб спрямовувати процес прийняття рішення. Метод був розроблений для зубчастих коліс, що часто використовуються в трансмісійних системах. Метод може бути поширений інші типи типових деталей. У чинній методиці не аналізуються економічні та фінансові фактори виробництва; Метод може бути розширений цими факторами у майбутніх дослідженнях.*

Ключові слова: *токарна обробка; автоматизація; вибір процедури.*

UDC 621.787.4 **doi: 10.20998/2078-7405.2022.96.13**

Ya. Nemyrovskyi, I. Shepelenko,
R. Osin, Kropyvnytsky, Ukraine, E. Posviatenko, Kyiv, Ukraine

IMPROVING THE PROCESSING QUALITY OF CYLINDER LINERS USING COMBINED TECHNOLOGY

Abstract. *Due to the use of surface engineering methods, a combined technology for processing the working surface of internal combustion engines cylinder liners has been developed. The advantages and disadvantages of traditional liners processing technologies are analyzed, which allowed identifying ways to improve them. A new technological process of cylinder liners processing is proposed, which includes operations of deforming broaching and finishing antifriction non-abrasive treatment. The technological equipment and tools for the chosen technological process realization are chosen. Experimental studies of the proposed technical solutions feasibility are carried out. The microrelief of the treated surface, roughness parameters, hardness distribution according to the wall thickness were determined for the studied liners, and the amount of wear was determined for the liners after running-in. Parameters analysis of geometric, mechanical and tribological characteristics of the liners working surface, processed by the existing and proposed technology showed significant advantages of the latter. There is an increase in the productivity of processing part up to 4 times, reducing the cost of the tool up to 3 times, and in general – reducing the cost of restoring the liner. It is proved that the use of the proposed technology allows improving the physical-mechanical characteristics of the working surface: strengthening the surface layer to a depth of 0.3 mm, as well as obtaining a roughness close to the operational.*

Keywords: *deforming broaching; finishing antifriction non-abrasive treatment; cylinder liner; roughness; hardness; durability.*

1. INTRODUCTION

Improving the quality of products in many cases depends on the surface layer properties of the parts working surfaces that are part of the product. Therefore, when choosing a material, processing technology should distinguish between the functions of the core and the surface layer of the part. This design and technological concept of product creation is not only strategic but also universal, as it dominates throughout the life cycle of the product, in particular, in its manufacture, operation and repair, as well as in the restoration of individual components and parts.

To date, many methods have been developed that affect the surface layer properties of the machine parts working surfaces [1-2]. Each of these methods affects the operational properties of working surfaces through a complex of geometric and physical-mechanical characteristics of the surface layer. First of all it is accuracy, roughness, bearing surface area, a microrelief, strengthening, residual stresses, microstructure, texture, adhesive properties of the coating and the base, a resource of plasticity used.

The complex of a surface layer physical-mechanical and geometrical characteristics of friction surfaces received in the course of processing allows increasing wear resistance, fatigue strength, antifriction properties, durability of landings with tension and other properties.

The above determines that the priority of modern mechanical engineering is the engineering of machine parts surfaces, which is to develop new combined technologies that can effectively affect the working surface layer of the part to control its composition, structure and properties.

2. LITERATURE REVIEW

The most effective processes of engineering the machine parts surface, both in the main and in the secondary (repair and restoration) production are combined (hybrid) technologies.

As an example, consider the existing technological process of the cylinder liner working surface processing made of modified gray cast iron SCH20.

According to [3], the condition of the liners surface layer is one of the main factors determining the resource and reliability of the engine. The existing technological process, which includes boring operations with subsequent honing, does not provide the optimal combination of mechanical and geometric characteristics of the working surface. Therefore, engines equipped with such liners are subjected to many hours of running-in on the stand for running-on friction surfaces. This provides the transformation of the initial roughness to equilibrium, the redistribution of residual stresses, etc.

In work [4] the researches of the existing technological process, and also data on influence of deforming broaching on a working surface condition of the processed liner are given and the new technological process of liners processing using cold plastic deformation with the subsequent final honing is offered. The proposed technological process has advantages over the existing one due to the treated surface with improved mechanical characteristics and roughness close to equilibrium that is technological microrelief is almost no different from the microrelief formed during the liners operation process.

However, this technological process has a significant drawback. After the clean honing operation, abrasive microparticles inevitably remain on the working surface of the liner, which leads to accelerated wear of the piston rings. Fig. 1 (a, b) shows fragments of the car piston rings, which can be seen longitudinal traces due to the action of abrasive particles placed on the working surface of the liner.

The aim of this study is to develop a new technological process that combines deforming broaching operation and antifriction coatings application operation by finishing antifriction non-abrasive treatment (FANT), which will allow to provide on a working surface of a liner the complex of geometrical and mechanical

characteristics of the processed surface favorable in relation to wear resistance with simultaneous improvement of antifriction properties.

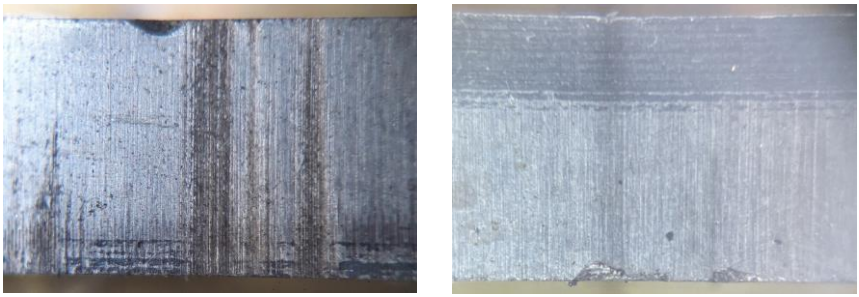

a) b)

Figure 1 – Piston ring fragments with traces of abrasive wear (liner after treatment according to the existing technological process, including honing)

3. RESEARCH METHODOLOGY

The experiments were performed on a batch of 24 liners of boosted diesels made of modified cast iron (type SCH20) when restoring them to the first repair size. In the process of processing it is necessary to remove the allowance of 0.5 mm. 8 liners were processed according to the existing technological process: boring, honing and polishing. The remaining liners were processed by deforming broaching on a vertical broaching machine mod. MA7U-750 in conditions of ISM named after V.M. Bakul NAS Ukraine (Fig. 2).

The tool for broaching is made on the researches basis carried out by authors [5] and consists of a cutting ring on both sides of which groups from hard-alloy deforming elements are placed.

The tool provides the necessary allowance removal for 1 pass that allows reducing hole processing complexity in 4 times. After broaching, the working surface of 8 liners was polished with fine-grained diamond bars ASM20/14 M1. The remaining 8 liners were processed using FANT technology on a vertical honing machine mod. 3M83 in the following modes: pressure of the brass tool P = 6 MPa, rotation speed of the tool V = 0.996 m/s, reciprocating motion speed V_1 = 0.24 m/s.

Repaired engines, in each of which were installed 4 liners, processed according to the existing technological process, and two liners, processed according to the following technological processes: deforming broaching – polishing; deforming broaching – FANT, was subjected to 2-hour run-in. Then the engines came into operation. The study of the liners working surfaces

characteristics, treated using the considered technological processes, was carried out after running-in the engine.

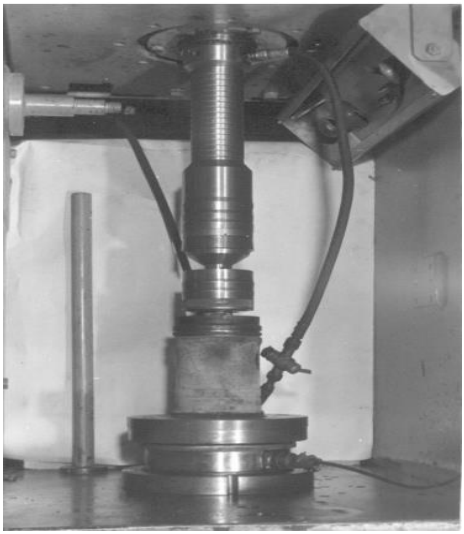

Figure 2 – The process of the ICE liner processing
by deforming – cutting – deforming broach

The microrelief of the treated surface, roughness parameters and hardness distribution according to the wall thickness were determined for the studied liners, and the amount of wear was determined for the liners after running-in. Measurement of the liner working surface wear was performed on a profilograph – profilometer "Talysurf-5". Wear resistance was assessed by linear wear recorded by profilograms taken at a base length of 120 mm. Also on the profilograms taken from the liner surface after processing and running-in, determined the roughness parameters.

The profile of the profilograph was discretized and processed on a PC. In addition to the roughness parameters, histograms were constructed that reflect the empirical law of roughness ordinates distribution. The experimental distribution law was approximated by a number of theoretical distribution laws. The conformity of the experimental distribution law with the theoretical one was assessed by criterion χ^2 [6], with 95% probability.

According to the profilograms taken from the working surfaces of the liners after processing and running-in, the mutual correlation functions of the roughness profiles were additionally calculated.

The Vickers hardness of the liners surface layer, treated in accordance with the considered technological processes, as well as its distribution by wall thickness were measured on the device HPO – 250 at a load of 50 N.

4. RESULTS

Table 1 shows the parameters of geometric, mechanical and tribological characteristics of the ICE liner working surface, treated by the existing process, developed by the authors [4] and according to the proposed process.

Table 1 – Parameters of microrelief roughness and ICE liners working surfaces frictional indicators (above the line – data after processing, below the line – after running-in)

Type of processing	Ra, μm	Rmax, μm	Rz, μm	Rp, μm	t_t, %	t_p=10%, %	S_m, μm	HV, GPa	Wear after two hours of running-in, μm
Deforming broaching	1,08	12	7,8	2,35	59	52	146	2,92	-
Boring + double honing	1,45 / 0,20	13,8 / 2,4	10,7 / 1,66	2,45 / 0,46	43 / 49	24 / 38	90 / 125	2,35 / 2,35	7,2
Deforming broaching + honing	0,85 / 0,18	7,5 / 1,8	5,99 / 1,05	1,51 / 0,22	66 / 63	60 / 58	155 / 153	2,8 / 2,7	5,5
Deforming broaching + FANT	0,81 / 0,16	7,21 / 1,6	5,2 / 1,02	0,6 / 0,28	68 / 65	62 / 59	164 / 162	2,86 / 2,85	4,2

Analysis of the data in Table 1 shows that the operation of deforming broaching significantly improves the surface layer microrelief, which in this case (Fig. 3) has support sites alternating with cavities and playing the role of lubrication tanks during operation.

It should be noted that the operation of deforming broaching significantly increases the parameter S_m in comparison with boring, which, according to the data presented in works [7, 8], increases the fatigue strength of the treated surface. Moreover, the use of finishing operations after broaching also leads to an increase in this parameter, especially when using FANT.

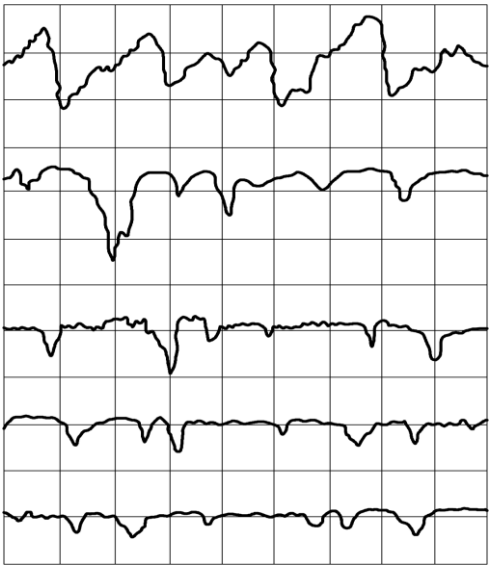

Figure 3 – Microroughnesses profilograms of the ICE liner working cavity after processing: a) boring; b) boring + honing; c) deforming broaching; d) deforming broaching + polishing; e) deforming broaching + FANT

After running-in, the height parameters of roughness decreased slightly, and the supporting lenght of the profile and the step along the midline did not change. The microrelief of the surface treated by the existing technological process differs from the microrelief obtained after treatment, in accordance with the technological processes based on broaching. Particularly noticeable differences in the values of the profile supporting length.

In the process of running-in, the values of the roughness height parameters also decrease, but in contrast to the microrelief obtained after broaching, the average step of the profile microroughnesses along the midline and the profile supporting length increased markedly. Therefore, the change in the roughness parameters obtained by the existing technological process during operation is more significant than when using technological processes based on broaching. This indicates the difference in the restructuring of the roughness technological parameters obtained after the compared technological processes during their operation.

Comparison of two technological processes based on broaching showed that the technological roughness and microrelief of the treated surface are very close. Although when using FANT the parameters of technological roughness R_p and S_m

are slightly better, this is explained by the process of rubbing the antifriction material on the liner working surface.

Roughness reconstruction was evaluated according to the method described in work [9], comparing the laws of roughness ordinates distribution after processing and operation. The distribution of the surface roughness ordinates treated by technological processes based on broaching corresponds to Weibull law (Fig. 4 a, b).

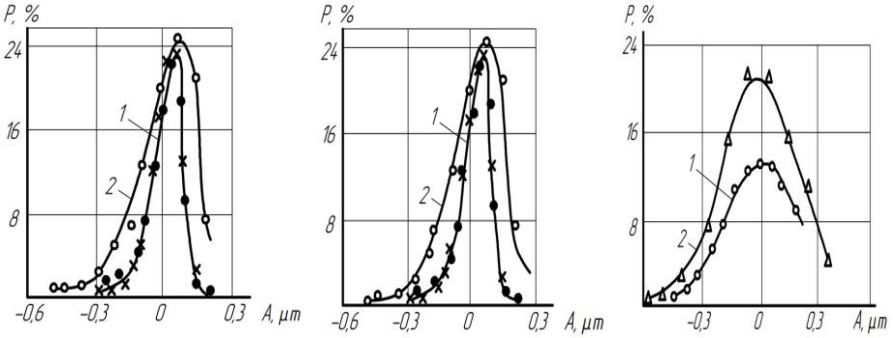

Figure 4 – Laws of roughness ordinates distribution:
1 – after processing; 2 – after operation.
Treating by technological process on the basis of broaching:
a) broaching and honing; b) broaching and FANT; c) the existing technological process

It should be noted that after operation the law of roughness ordinates distribution for the considered technological processes practically does not change (Fig. 4 a, b, curves 2). This indicates a slight restructuring of the rough layer during operation, which is confirmed by the analysis of mutual correlation functions of the roughness profiles recorded before and after operation. The value of the coefficient of their mutual correlation is greater than zero that is in the process of the engine running-out on the liner working surface reproduces the roughness, which is close to technological. The given data testify to insignificant transformations of the liner surface layer treated by technological process on the basis of broaching.

However, two technological processes are considered, which include the broaching operation with subsequent finishing operations: honing and FANT are somewhat different. Thus, after the clean honing operation, abrasive microparticles remain on the treated surface, which impairs the wear resistance of the surface, interaction with the piston ring surface and leaving traces on it in the form of longitudinal lines (Fig. 1). These shortcomings are reflected in the amount of wear.

The minimum wear of the liner surface is observed when processing using FANT and after two hours of running-in is 4.2 μm. At the same time, the wear of the liner surface when processing it after broaching by honing is slightly higher and is 5.6 μm.

Another picture is observed in the analysis of data obtained on the liners, processed by the existing process, which includes the operations of boring and honing. In this case, the roughness ordinates distribution, determined by the method [9], obeys the law of normal distribution (Fig. 4, c). During operation, the type of distribution law changed became logarithmically normal and approached Weibull distribution law. This means that after the restructuring that took place during operation, the difference in the nature of the profiles ordinates distribution treated by technological processes based on boring and broaching has decreased significantly. Some difference in the roughness ordinates distribution of the running-in surfaces is due to the influence of the treated surface initial state, namely – technological inheritance. Analysis of profiles mutual correlation functions confidence intervals before and after operation shows that the value of the cross-correlation coefficient is 0 that is during engine operation process on the liner working surface occurs a rough layer restructuring and a new microrelief is formed, completely different from the technological one.

Thus, the given material testifies that the most effective of the considered technological processes is the process consisting of operations of broaching and FANT. It provides minimal transformation of the rough layer during operation process, improved typological characteristics and the absence of abrasive particles on the treated surface and minimal wear of the liner working surface during operation.

Comparison of physical-mechanical characteristics of the surface layer treated by two different technological processes (boring, honing and broaching, FANT) showed a large difference between them (Fig. 5). The operation of deforming broaching significantly (up to 25%) strengthens the surface layer of the liner material. Depth of hardening thus reaches about 0.3 mm that guarantees existence of the strengthened material in friction pair even at long operation. Thus, the combination of cold plastic deformation and FANT allowed developing a successful version of the technological process for the diesel liner inner surface treating made from gray modified cast iron.

As shown by the results of technical-economic calculations, the use of the developed technological process can increase the productivity of the hole processing up to 4 times, reduce tool costs by 3 times, which reduces the cost of restoring the liner by about 4 times. Moreover, the use of the proposed technological process provides a liner working surface with improved physical-mechanical and tribological characteristics and roughness close to equilibrium.

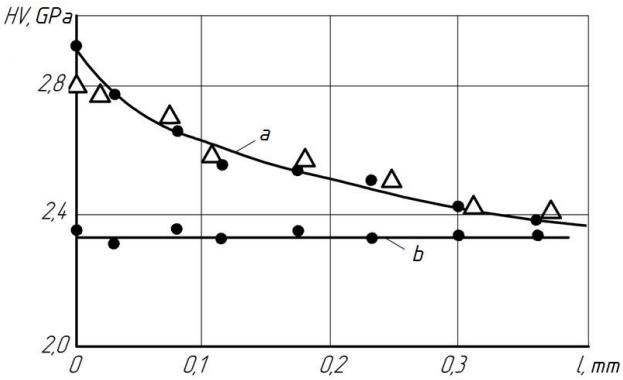

Figure 5 – Hardness distribution according to the wall thickness of the diesel liner during processing: a – according to the new technological process (• – after broaching; Δ – after broaching and FANT); b – according to the existing technological process (boring and honing)

5. CONCLUSIONS

1. The expediency of combining the cold plastic deformation operation and FANT, which allows offering the technology for processing the cylinder liners of internal combustion engines.

2. A new technological process of ICE liners processing has been developed, which includes deformation broaching operations and FANT, which provides receiving a working surface of the part with improved physical-mechanical and tribological characteristics and roughness close to equilibrium.

3. The effectiveness of the proposed technology is confirmed by improving the operational characteristics of the cylinder liners working surface.

References: 1. *Tikhonenko V.V., Shkilko A.M.* Reinforcing technologies for the formation of wear-resistant surface layers. Physical engineering of the surface, 2012, no. 4, pp. 237-243. **2.** *Suslov A.G.* Kachestvo poverhnostnogo sloja detalej mashin [The quality of machine parts surface layer]. Moscow, High school, 2000. 320 p. **3.** *Korneev V.M., Kravchenko I.N., Novikov V.S.* Tekhnologiya remonta mashin [The technology of repair of cars]. Moscow, RGAU-MSKHA, 2019, 266 p. **4.** *Nemyrovskyi Ya.B.* Naukovi osnovi zabezpechennya tochnosti pri deformuyuchomu protyaguvanni. Diss. doct. techn. nauk [Scientific bases for ensuring accuracy at deforming broaching. Dokt. tech. sci. diss.] Kyiv, 2018. 451 p. **5.** *Rosenberg A.M.* Mehanika plasticheskogo deformirovanija v processah rezanija i deformirujushhego protjagivanija [Mechanics of plastic deformation in the processes of cutting and deforming broaching]. Kiev, High school, 1998. 320 p. **6.** *Wentzel E.S.* Teoriya veroyatnostej i eyo inzhenernye prilozheniya [Probability theory and its engineering applications]. Moscow, High school, 2006. 575 p. **7.** *Schneider Yu.G.* Ekspluatacionnye svojstva detalej s regulyarnym mikrorel'efom [Operational properties of details with a regular microrelief]. *Leningrad*, Mechanical engineering, 1982. 248 p. **8.** *Ryzhov E.V., Klimenko S.A., Gutsalenko O.G.* Tekhnologicheskoe obespechenie kachestva detalej s pokrytiyami [Technological quality assurance of

coated parts]. Kyiv, Scientific thought, 1994. 181 p. **9.** *Shepelenko I.V.* Naukovi osnovi tekhnologiї nanesennya antifrikcijnih pokrittiv z vikoristannyam plastichnogo deformuvannya. Diss. doct. techn. Nauk [Scientific bases of technology of drawing antifriction coating with use of plastic deformation. Dokt. tech. sci. diss.] Kyiv, 2021. 465 p.

Яків Немировський, Ігор Шепеленко,
Руслан Осін, Кропивницький, Україна, Едуард Посвятенко, Київ, Україна

ПІДВИЩЕННЯ ЯКОСТІ ОБРОБКИ ГІЛЬЗ ЦИЛІНДРІВ ЗАСТОСУВАННЯМ КОМБІНОВАНОЇ ТЕХНОЛОГІЇ

Анотація. *За рахунок використання методів інженерії поверхні розроблено комбінована технологія обробки робочої поверхні гільз циліндрів двигунів внутрішнього згорання. Проаналізовані переваги та недоліки традиційних технологій обробки гільз. Показано, що після використання фінішної операції хонінгування на робочій поверхні гільзи залишаються абразивні мікрочастки, що призводить до прискореного зносу поршневих кілець. Запропоновано новий технологічний процес обробки гільз циліндрів, що вміщує операції комбінованого протягування та нанесення покриттів фінішною антифрикційною безабразивною обробкою. Вибрано технологічне оснащення та інструмент для реалізації технологічного процесу. Проведені експериментальні дослідження доцільності запропонованих технічних рішень. Вивчення характеристик робочих поверхонь гільз, оброблених з використанням розглянутих технологічних процесів, здійснювалося після обкатки двигуна. Для досліджуваних гільз визначено мікрорельєф обробленої поверхні, параметри шорсткості, розподіл твердості за товщиною стінки, а для гільз після обкатки – величину зносу. Аналіз параметрів геометричних, механічних та трибологічних характеристик робочої поверхні гільз, оброблених за існуючою та пропонованою технологією, показав суттєві переваги останньої. Встановлено, що використання комбінованого протягування дозволяє сформувати мікрорельєф поверхневого шару, який являє собою опорні площадки із впадинами, які грають роль змащувальних резервуарів при експлуатації. Нанесення покриття фінішною антифрикційною безабразивною обробкою, суттєво не змінюючи мікрорельєф, підвищує антифрикційні властивості поверхні. Доведено, що застосування розробленої технології обробки гільз циліндрів забезпечує отримання шорсткості, близькою до експлуатаційної, зміцнення поверхневого шару на глибину до 0,3 мм, поліпшені трибологічні характеристики, відсутність частинок абразиву на обробленій поверхні і мінімальний знос робочої поверхні гільзи при її експлуатації.*

Ключові слова: *деформуюче протягування; фінішна антифрикційна безабразивна обробка; гільза циліндрів; шорсткість; твердість; зносостійкість.*

UDC 621.9.048 **doi: 10.20998/2078-7405.2022.96.14**

A. Mitsyk, V. Fedorovich, A. Grabchenko, Kharkiv, Ukraine

MAIN TECHNOLOGICAL FACTORS DETERMINING THE EFFICIENCY AND QUALITY OF THE VIBRATION PROCESS

Abstract. *The factors that determine the efficiency and quality of vibration treatment are indicated. Characteristic cases of interaction of abrasive granules with the processed surface are noted. The influence of the hardness of the processed part material and the shape of its surface, as well as the influence of chemically active solutions on the efficiency and quality of vibration processing, is substantiated. The characteristics of abrasive granules and their volume ratio with the processed parts are given. It is indicated that the underestimation of the possibilities of vibration processing technologies is explained by their insufficient studies. It has been established that vibration processing, depending on the characteristics and composition of the processing medium, is a mechanical or mechanochemical removal of the smallest particles of metal or its oxides and plastic deformation of microroughness due to mutual collisions of the medium granules with the processed surface, caused by vibrations of the reservoir in which the processing medium and, the processed parts are placed. It is noted that, according to the classification, vibration treatment refers to mechanical processing methods and, in particular, to the group of mechanical-chemical processing methods or to combined methods when chemically active solutions are introduced into the working medium, It is also noted that vibration treatment refers to dynamic, and for technological purposes – to dimensionless processing methods, according to the type of tool used - to the group of processing methods with a free abrasive. It has been established that the efficiency of vibration processing depends on the oscillation modes of the vibrating machine, the mass of the processed parts and abrasive granules, the hardness of the parts material and the shape of their treated surfaces, the characteristics of the abrasive medium, the volume ratio of the parts and abrasive granules, as well as on the composition of the chemically active solution. The characteristic cases of interaction of abrasive granules with the processed surface are given. The situations of the highest processing productivity for performing the operations of vibration grinding, vibration polishing, washing and descaling have been established. It is noted how the hardness of the processed part and the shape of their surface affects the performance and quality of vibration processing operations. The characteristics of the working medium, which affects the efficiency and quality of vibration treatment, are given, including the influence of grain size and hardness of the material of abrasive granules. The volume ratios of abrasive and processed parts are considered. The types of actions on the vibration treatment processes are given.*

Keywords: *vibration treatment; processed parts; vibration machine reservoir; abrasive granules; the hardness of the granule material; abrasive grain size, chemically active solution.*

Introduction

Vibration treatment, depending on the characteristics and composition of the processing medium, is a mechanical or mechanochemical removal of the smallest particles of metal or its oxides and plastic deformation of microroughness due to mutual collisions of the granules of the medium with the processed surface, caused by oscillations of the reservoir in which the working medium and the processed parts are placed.

In accordance with the existing classification, vibration treatment refers to mechanical processing methods, and when chemically active solutions are introduced into the working medium, to combined methods, in particular, to the group of mechanical processing methods. Vibration treatment refers to dynamic processing methods, and according to the type of tool used, vibration processing belongs to the group of processing methods with a free abrasive [1].

Despite the widespread application of vibration treatment, its implementation until recently was limited to such simple operations as cleaning parts, removing burrs, and rounding sharp edges. The underestimation of the possibilities of this technological process is explained by its insufficient knowledge.

Factors affecting the efficiency and quality of vibration treatment

The last studies carried out have included solving particular problems to identify the influence of one or a small number of factors on the processing efficiency. Comprehensive studies have shown that the effectiveness of vibration treatment depends on many factors, the main of which are:

1. Processing mode and mass of processed parts and abrasive granules.
2. The hardness of the material and the shape of the processed surfaces.
3. Characteristics of the abrasive material.
4. Volumetric ratio of processed parts and abrasive granules in the vibrating machine reservoir.
5. The composition of the chemically active solution that intensifies the processing.

Microchips are removed from the part processed surface in oscillating reservoirs, during the relative movement of parts and granules. Therefore, it is natural that the mode indicators of processing (frequency and amplitude of oscillations of the reservoir, the trajectory of its movement) have a great influence on the nature of the interaction of the mass elements loaded into the reservoir [2].

Typical cases of interaction of abrasive granules with the part processed surface

Let us consider three most characteristic cases of the interaction of abrasive granules with the processed surface.

1. Abrasive granules and parts move in the same direction with the oscillating movement of the reservoir parallel to the surface to be processed.

In this case, the relative slip speed of the abrasive granule and the processed part, that is, the speed of processing $V_{\text{proc.}}$ will be equal to $V_{\text{proc.}} = V_{\text{p}} \pm V_{\text{gr}}$, where V_{p} is the speed of the processed part, V_{gr} is the speed of the abrasive granule.

2. Abrasive granules and parts move, as in the first case, but their relative movement is perpendicular to the processed surface. In this case, the abrasive granule collides with the processed surface at a speed of $V_{\text{proc.}}$, that is, $V_{\text{proc.}} = V_{\text{p}} + V_{\text{gr}}$.

3. The abrasive granule and the part move along a curved path, in particular, along a circle. In this case, the abrasive granule meets the processed surface at an angle or tangentially.

As can be seen from the above formulas, the relative sliding speed, which is one of the main factors for increasing the efficiency of processing, depends on the absolute values of the speeds of movement of abrasive granules and processed parts [3].

In its turn, these speeds depend on the frequency and amplitude of oscillations, the trajectory of the reservoir, as well as on the ratio of the masses of the processed parts and abrasive granules. The greater the difference in these masses, the greater the speed of mutual slippage will be. With a small difference in the masses of parts and abrasive granules, and, accordingly, a slight difference from inertia, the slip speed between them will be low, which, all other conditions being equal, will lead to a decrease in efficiency of treatment. Therefore, the efficiency of vibration treatment of parts with low mass and dimensions can be ensured by increasing the speed of the reservoir motion [4, 5].

From the analysis of the considered schemes of interaction of granules with the processed surface, the following conclusions can be drawn:

1. In the first case, the minimum amount of metal is removed, since the pressure of the granule to the part is very small and is created only by the static pressure of the medium. Obviously, such an interaction, associated with the use of the energy of the vibrational and centrifugal actions of the working medium, will be the best for performing vibration grinding and vibration polishing operations [6].

2. In the second case, the granule collides with the processed surface, as a result of which imprints of abrasive grains, chips or tearing of metal appear on it. This nature of the interaction of abrasive granules with the processed surface will be the most productive for cleaning parts with using the shock wave effect, as a result, removing scale and a defective metal layer in rough cleaning operations with a large metal removal [7].

3. In the third case, when the abrasive granule and the processed part move along a curved path, an intermediate nature of the interaction takes place.

The hardness of the processed part material.

The hardness of the processed part material affects the productivity and quality of machined surfaces. The higher it is, the shallower the abrasive grains

will be introduced into the part. This reduces the removal of metal from the processed surface while reducing its microroughness [8, 9].

The shape of the processed part surface.

The shape of the surface to be processed also affects the efficiency of the process. Collisions of abrasive granules with complex elements that form grooves and recesses in parts of various types do not always occur at optimal angles. This causes a sharp decrease in productivity. Moreover, there are cases when the shape of the processed surface is such that it is impossible for abrasive granules to collide with it [10].

Characteristics of abrasive granules that affect the efficiency and quality of vibration treatment.

The most important characteristics of abrasive granules that affect the efficiency of vibration treatment include the mass, size, shape and hardness of the granules [11].

During the interaction of the medium elements in the reservoir, when a direct blow is applied by a granule to the processed surface, its force is proportional to the mass of this granule. Therefore, an increase in the latter leads to an increase in the amount of metal removed. A significant increase in the mass of the abrasive granule can cause a deterioration of the quality of processing, as well as a decrease in the slip speed. A detailed study of this issue made it possible to draw a general conclusion: abrasive granules with an extremely large mass should be used for rough cleaning operation, and for finishing operations, with a relatively small mass.

The dimensions of the granules are related to their weight. Therefore, in the general case, the recommendations for their choice are similar to the previous ones. However, often the sizes of abrasive granules are chosen so as to ensure their access to closed or semi-closed surfaces to be processed. In addition, there are cases when the processing of individual surfaces is undesirable. Then the sizes of the granules are chosen so that they do not collide with such surfaces.

The forms of abrasive granules do not have a noticeable effect on the efficiency of vibration treatment. But with difficult access of abrasive granules to the processed surfaces, it becomes necessary to select a rational form of granules in order to ensure processing [12].

Grain size of the abrasive material.

The grain size of the abrasive material is largely reflected in both the quality and productivity of processing. When using a coarse-grained abrasive, the number of grains in contact with the processed surface is significantly reduced. In this case,

other things being equal (in particular, at the same pressure), the penetration of grains into the metal occurs to a greater depth and larger metal chips are removed.

With a small grain size, the number of contacts with the surface increases sharply, but the penetration of grains occurs at a shallow depth. This contributes to the removal of small chips and a decrease in the height of micro-roughness [13].

The hardness of the abrasive granules material.

The hardness of abrasive granules is one of the main characteristics that have a significant impact on the efficiency of the vibration process. During vibration processing, the volume of the abrasive filler loaded into the reservoir, as a rule, exceeds the volume of the processed parts. In this regard, the granules in the process of treatment come into contact with each other more often than with parts. This causes increased wear of the abrasive due to its abrasion and chipping of the grains.

The appearance of wear products in the abrasive mass clogs the pores between the grains of the granules and leads to the "loading" of the abrasive, and as a result, to a decrease in its cutting properties. The flaking large abrasive grains, falling between the granule and the processed surface, leave deep imprints on the latter [14].

Volume ratio of abrasive and processed parts.

The volume ratio of abrasive and processed parts in the reservoir is largely reflected in the productivity of vibration treatment. If the number of parts in the vibrating machine reservoir is large, then the abrasive granules will be in contact with the processed surfaces of only individual parts. In this case the treatment process is implemented slowly. If the number of processed parts is small compared to the loaded mass of the abrasive, then the possibilities of the vibrating machine will not be fully used [2].

Chemically active solutions.

Chemically active solutions have different effects on the vibration treatment process. In some cases, chemical solutions, reacting with the surface layer of the metal, change its properties and thereby change the intensity of processing. Under other conditions, the components of the solution, entering into chemical reactions with the metal, form films on the processed surfaces, which are easily removed by abrasive granules. Sometimes the solutions may include additives that help restore the cutting properties of the abrasive, remove processing waste, etc. [15].

Chemically active solutions should not be complex in composition, safe for maintenance personnel and medium ally friendly when descending into industrial effluents without sludge and neutralization. The dosage of the applied solution has

a great influence on the quality of processing and the productivity of the treatment. Both its insufficient and excessive amount has a negative effect on the treatment process. The use of chemically active solutions in the cutting process produces a cooling, lubricating, dispersing and washing effect.

Chemically active solutions with an acidic medium are designed for cleaning steel parts, destroying and removing scale, and intensifying grinding. Chemically active solutions with an alkaline medium are designed for rounding sharp edges and polishing. Entering into a chemical reaction with the surface of the part, they facilitate micro-cutting and plastic deformation. Solutions with a neutral medium, having a cleaning and washing ability, are intended for washing and removing wear products.

In all cases, the use of chemically active solutions of the required compositions leads to an increase in productivity and an increase in the quality of vibration processing.

Conclusions.

The development and perfection of existing technological processes of vibration treatment requires comprehensive research, taking into account the variety of factors affecting its efficiency and quality. The lack of such data is the main reason for the insufficient implementation of the vibration treatment process in the metalworking branches of mechanical engineering and instrument making.

References: 1. *Babichev A.P.* Osnovy vibracionnoj tehnologii / A.P. Babichev, I.A. Babichev. Rostov-n/D: Izdatel'skij centr DGTU, 2008. 694 p. **2.** *Kartashov I.N.* Obrabotka detalej svobodnymi abrazivami v vibrirujushhih rezervuarah / I.N. Kartashov, M.E. Shainskij, V.A. Vlasov. Kyiv: Vishha shkola, 1975. 188 p. **3.** *Mamalis, A.G., Grabchenko, A.I., Mitsyk, A.V., Fedorovich, V.A., Kundrák, J.* Mathematical simulation of motion of working medium at finishing – grinding treatment in the oscillating reservoir. The International Journal of Advanced Manufacturing Technology 70, pp. 263 – 276 (2014). https://doi.org/10.1007/s00170-013-5257-6 **4.** *Politov I.V., Kuznecov N.A.* Vibracionnaja obrabotka detalej mashin i priborov. Leningrad: Lenizdat, 1965. 125 p. **5.** *Mitsyk A.V., Fedorovich V.O.* Osoblivosti tehnologij vidalennja zadirok, skruglennja i poliruvannja gostrih kromok pri vibracijnij ozdobljuval'no-zachishhuval'nij obrobci detalej. Vazhke mashinobuduvannja. Problemi ta perspektivi rozvitku: tezi dopovidej XIX mizhnar. nauk.-tehn. konf. (m. Kramators'k, 1 – 4 chervnja 2021 r.). Kramators'k, DDMA, 2021. pp. 105 – 106. **6.** *Kundrák J., Mitsyk A.V., Fedorovich V.A., Markopoulos A.P., Grabchenko A.I.* Simulation of the Circulating Motion of the Working Medium and Metal Removal during Multi-Energy Processing under the Action of Vibration and Centrifugal Forces. Machines Vol. 9 (6) 118, pp. 1 – 22, (2021). https://doi.org/10.3390/machines9060118 **7.** *Mitsyk A.V., Fedorovich V.A., Grabchenko A.I.* The effect of a shock wave in an oscillating working medium during vibration finishing-grinding processing. Cutting & Tools in Technological System. Kharkiv, NTU «KhPI», 2020. № 93. pp. 62 – 67. http://doi.org/10.20998/2078-7405.2020.93.06 **8.** Instrument dlja obrobki detalej vil'nimi abrazivami: monografija / M.O. Kalmykov, T.O. Shumakova, V.B. Strutins'kij, L.M. Lubens'ka; Kyiv – Luhans'k: «Noulidzh», 2010. 214 p. **9.** *Lubens'ka L.M., Strutins'kij V.B., Jasunik S.M., Kalmykov M.O.,* Ozdobljuval'no-abrazivni metodi obrobki: pidruchnik. Luhans'k – Kyiv: Vid-vo «Noulidzh», 2011. 268 p. **10.** *Venckevich Gzhegozh* Vlijanie nekotoryh parametrov abrazivnogo napolnitelja na jeffektivnost' processa shlifovanija v vibrirujushhih rezervuarah: dis. … kand. tehn. nauk: 05.02.08 / OPI. Odessa, 1986. 175 p. **11.** Obrobka u vil'nih abrazivah: monografija /

Branspiz O.V., Kalmykov M.O., Jasunik S.M. Luhans'k: «Noulidzh», 2010. 318 p. **12.** Primenenie vibracionnyh tehnologij na operacijah otdelochno-zachistnoj obrabotki detalej (ochistka, mojka, udalenie obloja i zacsencev, obrabotka kromok): monografija / Babichev A.P., Motrenko P.D., Gillespi L.K. i dr.; pod red. A.P. Babicheva. Rostov-na-Donu: Izd-vo DGTU, 2010. 289 p. **13.** Otdelochno-uprochnjajushhaja obrabotka detalej mnogokontaktnym vibroudarnym instrumentom / A.P. Babichev, P.D. Motrenko, I.A. Babichev i dr.; pod red. A.P. Babicheva. Rostov n/D: Izdatel'skij centr DGTU, 2003. 213 p. **14.** Primenenie vibracionnyh tehnologij dlja povyshenija kachestva poverhnosti i ekspluatacionnyh svojstv detalej / A.P. Babichev, P.D. Motrenko, V.A. Lebedev i dr.; pod red. A.P. Babicheva. Rostov n/D: Izdatel'skij centr DGTU, 2006. 213 p. **15.** *Bereshhenko A.A.* Vibrohimicheskaja obrabotka uglerodistyh i legirovannyh stalej: dis. … kand. him. nauk: 05.17.03 / Institut obshhej i neorganicheskoj himii AN USSR. Kyiv, 1980. 132 p.

Андрій Міцик, Володимир Федорович, Анатолій Грабченко, Харків, Україна

ОСНОВНІ ТЕХНОЛОГІЧНІ ФАКТОРИ, ЩО ВИЗНАЧАЮТЬ ЕФЕКТИВНІСТЬ І ЯКІСТЬ ПРОЦЕСУ ВІБРАЦІЙНОЇ ОБРОБКИ

Анотація. *Вказані фактори, що визначають ефективність та якість вібраційної обробки. Відзначено характерні випадки взаємодії абразивних гранул з оброблюваною поверхнею. Обґрунтовано вплив твердості матеріалу оброблюваної деталі та форми її поверхні, а також вплив хімічно-активних розчинів на ефективність та якість вібраційної обробки. Дана характеристика абразивних гранул та їх об'ємне співвідношення з оброблюваними деталями. Вказано, що недооцінка можливостей технологій віброобробки пояснюється їхньою недостатньою вивченістю. Встановлено, що віброобробка в залежності від характеристики та складу оброблювального середовища являє собою механічний або механохімічний зйом дрібних частинок металу або його окислів і пластичного деформування мікронерівностей внаслідок взаємних зіткнень гранул середовища з оброблюваною поверхнею, викликаних коливаннями резервуара, в якому розміщені оброблювальні деталі. Зазначено, що згідно з класифікацією віброобробка належати до методів механічної обробки, а при введенні до складу робочого середовища хімічно- активних розчинів до комбінованих методів, зокрема до групи механохімічних методів обробки. Також зазначено, що віброобробка відноситься до динамічних, а за технологічним призначенням – до безрозмірних методів обробки, за видом інструменту, що застосовується – до групи методів обробки вільним абразивом. Встановлено, що ефективність віброобробки залежить від режимів коливань віброверстата, маси оброблюваних деталей та гранул абразиву, твердості матеріалу деталей та форми їх оброблюваних поверхонь, характеристики абразивного середовища, об'ємного співвідношення деталей та гранул абразиву, а також складу хімічно-активного розчину. Наведено характерні випадки взаємодії абразивних гранул з оброблюваною поверхнею. Встановлено ситуації найбільшої продуктивності обробки для виконання операцій віброшліфування, віброполірування, миття та очищення від окалини. Відзначено, як твердість оброблюваної деталі та форма її поверхні впливає на продуктивність та якість операцій віброобробки. Дано характеристику робочого середовища, що впливає на ефективність та якість віброобробки, у тому числі оцінено вплив зернистості та твердості матеріалу абразивних гранул. Розглянуто об'ємні співвідношення абразиву та оброблюваних деталей. Наведені види впливу на процеси віброобробки.*

Ключові слова: *віброобробка; оброблювані деталі; резервуар; абразивні гранули; твердість матеріалу гранули; зернистість абразиву; хімічно-активний розчин.*

UDC 621.86.065 **doi: 10.20998/2078-7405.2022.96.15**

V. Kurgan, I. Sydorenko, V. Vaysman, A.
Pavlyshko, V. Litvinov, V. Vovk, Odesa, Ukraine

THE EFFECT OF ELASTIC RECOIL OF CLOSED-TYPE LIFTING ROPES AFTER THEIR MANUFACTURE AND DRAWING

Abstract. *A study was made of stresses and factors of internal forces in the elements of ropes of a closed structure during their manufacture. It is established that when twisting a rope of closed construction, its shaped wires suffer from bending deformation, twisting and stretching. In this case, the shaped wires are subjected to a complex load with the concomitant rotation of the axes of the stress tensor. The stresses in the elastic cross-sectional area of the rope wire are considered and its limit is determined for shaped cross-sections and for asymmetric shaped cross-sections. Formulas for approximate determination of tangential and normal stresses in the elements of a closed rope of non-circular profile are obtained: (wedge-shaped, zeta-shaped and x-shaped).*
Keywords: *ropes of closed construction; stress; internal force factors; cross section; shaped wires; elastic region; normal stress; elastic-plastic deformation.*

Experience in the manufacture and operation of ropes of closed design shows that immediately after twisting the closed rope, which is an elastic-plastic system, at the first load acquires significant elongations, and its stress-strain state changes significantly. As a result, a number of serious structural defects (bundles, "waves", wire breaks, etc.) often appear during the first cycles of rope operation, which is the reason for the failure of a new rope [1, 2].

The influence of the presence of gap between the wires in the outer layers and its value on the compatibility of operation of the layers in the radial direction and the preservation of the structural integrity of the rope during operation is revealed [3]. Analysis of the stress-strain state of closed rope elements under axial tension and torsion [4]. The closed rope consists of an outer layer of Z-profile wires, a subsurface layer of alternating round and H-profile wires [5, 6, 7]. Evaluation of extended structural elements using non-contact mobile systems using body waves and directional waves (piezoelectric, electromagnetic-acoustic transducers) [8]. The axial forces and torques in the cross sections of the layers are found to be redistributed when a rope turns under an external torque, which leads to a decrease in the safety factor of the rope, a violation of the compatibility of the axial and radial displacements of the layers, and a violation of the structural integrity of the rope in the form of breaks in the outer layer wires [9, 10]. The influence of wire cracks on the amplitude distribution of the generated field is specified for two steel rope kinds assuming surface and inner defects [11]. The behavior of short and very short fatigue cracks emanating from so-called "smooth" specimens with stress concentration is described [12].

To assess the reliability of the rope and prevent the occurrence of these defects, as well as to assess its strength and durability, it is necessary to know the stress-strain state of its constituent elements of wires, both during its manufacture and after the first axial load. It is established that when twisting a rope of closed construction shaped wires suffer together with bending and torsional deformation, and then during extraction during operation - tensile deformation. In this case, the shaped wires are subjected to a complex load with the concomitant rotation of the axes of the stress tensor. It should be noted that the bending of shaped wires of some profiles is oblique [3, 4]. For example, when twisting z-shaped and 8-shaped wires, the plane of the bending moment, which contains the normal of the helix, does not coincide with the main axis of the wire cross section y_0 or z_0 (Fig. 1).

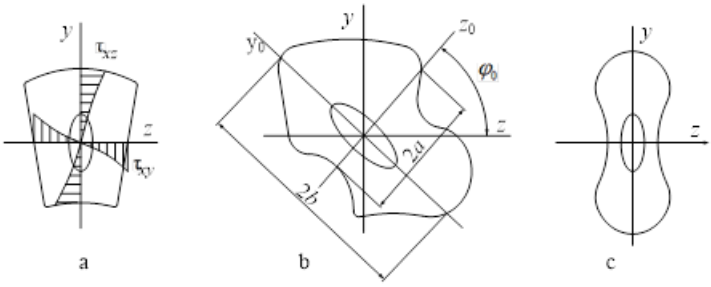

Figure 1 – Sections of shaped wires of closed ropes: wedge-shaped symmetrical (a); z-shaped asymmetric (b); 8-shaped symmetrical (c)

These wires experience oblique bending, and wires of round, x-shaped and wedge-shaped profiles undergo flat bending. Thus, the material of the wires is subjected to a complex load, the analysis of which the existing theories of plasticity do not solve. There are known developments of some methods for solving this problem, but these methods can be obtained only local solutions that meet the rigid arameters [1, 2, 5].

Thus, the study of technological stresses and internal power factors in the shaped wires of closed ropes in general form is an urgent scientific and applied task.

Given the complexity of the task of analysis of technological stresses and internal force factors in the shaped wires of closed ropes, the study is proposed to approximate its solution under the general assumption that the wire material is ideal – elastic-plastic, and the entire cross section of wires covered by elastic-plastic deformation.

Consider the stress in the elastic cross-sectional area of the rope wire and determine its limit. Normal bending stress is determined by:

– for shaped cross-sections symmetrical with respect to the bending plane *xy* (wedge-shaped, 8-shaped) wire ropes (see Fig. 1, a and c) by expression

$$\sigma_{x,y}^{be} = E\chi y, \tag{1}$$

where $\sigma_{x,y}^{be}$ – normal bending stress; $\chi = \sin^2\alpha / R$ - curvature of the centerline of the wire; R – wire twisting radius; E – Jung's module.

– (z-shaped) wire ropes (see Fig. 1, b) by expression for asymmetric shaped cross-sections

$$\sigma_{x,y}^{be} = E\chi\left(z_0 \sin\psi + y_0 \cos\psi\right), \tag{2}$$

where z_0 and y_0 – the main central axes of the wire.

In Figure 1, b φ_0 is the polar angle, which is calculated from the main central axis z_0.

Analyzing the plots of tangential stresses during torsion of non-round rods, for which exact solutions are obtained, it can be noted that they have slight nonlinearity (Fig. 1, a). This nonlinearity is smaller the greater the sloping delineation of the wire profile, and for elliptical and round cross-sections of wires the nature of the change in tangential stresses across the section is linear.

This fact gives the right to make a few additional assumptions. First, for smoothly delineated profiles of sections of shaped wires of a closed rope, the displacements γ_{xy} and γ_{xz} with a sufficiently probable approximation can be calculated from the linear functions of the *z* and *y* coordinates (Fig. 2).

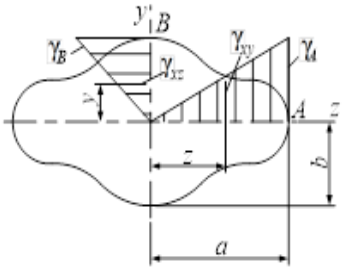

Figure 2 – Smoothly outlined cross-sectional profile of the shaped wire

Coordinate functions for this case

$$\begin{cases} \gamma_{xy} = \dfrac{\gamma_A}{a} z, & 0 \le z \le a; \\ \gamma_{xz} = \dfrac{\gamma_B}{b} y, & 0 \le y \le b; \end{cases} \tag{3}$$

$$\frac{\gamma_A}{\gamma_B} = -\frac{b}{a}, \tag{4}$$

where a and b – segments on the main axes of the cross section of the wire.

Secondly, the torque in the cross section of the wire with a smoothly delineated profile is determined by the expression

$$M_x = \int_F \left(\tau_{xy} z - \tau_{xz} y\right) \cdot dF = G \int_F \left(\gamma_{xy} z - \gamma_{xz} y\right) \cdot dF \,, \tag{5}$$

where τ_{xy} and τ_{xz} – projections of full stress on the corresponding planes; G – shear strength modulus.

Substitute formula (3) into expression (5) and, given equality (4), we obtain

$$\begin{cases} \tau_{xy} = \dfrac{b^2 M_x}{a^2 I_z + b^2 I_y} z \\ \tau_{xz} = -\dfrac{a^2 M_x}{a^2 I_z + b^2 I_y} y \end{cases}. \tag{6}$$

Total tangential stress:

$$\tau_{tors} = \sqrt{\tau_{xy}^2 + \tau_{xz}^2} = \frac{M_x}{a^2 I_x + b^2 I_y} \sqrt{b^4 z^2 + a^4 y^2} \,, \tag{7}$$

The twisting angle of the shaped wires is determined by the formula

$$\varphi = \frac{M_x l}{G I_к}, \tag{8}$$

where I_{tors} – the moment of inertia at pure torsion with a sufficient degree of accuracy can be determined by the formula of Saint-Venan [6].

$$I_{tors} = \frac{F^4}{4\pi^2 I_p} \,, \tag{9}$$

where F and I_p – plane and polar moment of inertia of the wire cross section, respectively.

From formula (8) we obtain:

$$M_x = G \cdot I_{tors} \cdot \frac{\varphi}{l} \,, \tag{10}$$

Thirdly, the moment of elastic recoil of each layer of wires of the closed rope, taking into account expression (1) is determined [1]:

$$M_{tors}^{techn} = n \cdot [(1 + \cos^2 \alpha) \sin \alpha M_z + \cos^3 \alpha M_x] \,,$$

where n – the number of wires in each layer; α – the twist angle of the wires; M_z – the moment of bending relative to the z-axis of the cross section of each wire; M_x – torque in the cross section of each wire.

Based on the accepted assumptions and mathematical studies of stresses arising in the process of making ropes, simplified formulas for determining the bending and torques in the cross sections of closed rope wires, taking into account the coefficients A_1, B_1, N_1, N_2, N_3. Formulas for their determination in the polar coordinate system starting at the center of gravity of the wire cross section were obtained in [3].

With an approximate solution of the problem obtained:

– for shaped cross-sections of wires symmetrical about the plane of bending *xy* (x-shaped):

$$M_z = \sigma_{fl} \cdot E \cdot \chi \cdot A_1;$$

$$C_1 = \frac{GI_{tors}}{a^2 I_z + b^2 I_y}; \tag{11}$$

$$M_x = \sigma_{fl} \cdot \Theta C_1 \left(a^2 A_1 + b^2 B_1\right),$$

where σ_{fl} – conditional estimated yield strength; C_1 – coefficient that determines the dependence of the modulus of elasticity of the second kind on the axial moments of inertia for symmetrical shaped cross sections of wires; Θ – twisting of the axial line of the wire;

– for asymmetrical shaped cross-sections of wires (z-shaped):

$$\begin{cases} M_{z0} = \sigma_{fl} E\chi\left(N_2 \cdot \sin\psi + N_3 \cos\psi\right) \\ M_{y0} = \sigma_{fl} E\chi\left(N_2 \cdot \cos\psi + N_1 \sin\psi\right) \end{cases},$$

$$C_2 = \frac{GI_{tors}}{a^2 I_{z0} + b^2 I_{y0}},$$

$$M_x = \sigma_{fl} \cdot \Theta C_2 \left(b^2 N_1 + a^2 N_3\right),$$

where ψ – the angle that determines the position of the main central axes of inertia of the section relative to the axis perpendicular to the plane of bending of the wire; C_1 – the coefficient that determines the dependence of the modulus of elasticity of the second kind on the axial moments of inertia for asymmetric shaped cross-sections of wires; I_{z0}, I_{y0}, I_z, I_y – the main central moments of inertia of the cross section of the wire.

$$\begin{cases} A_1 = \dfrac{2}{3\sqrt{b_2}} \displaystyle\int_{\varphi_{i-1}}^{\varphi_i} \left(\frac{\cos^2\varphi \rho_i^3(\varphi)}{\sqrt{1-l^2\sin^2\varphi}} \right) \mathrm{d}\varphi; \\ B_1 = \dfrac{2}{3\sqrt{b_2}} \displaystyle\int_{\varphi_{i-1}}^{\varphi_i} \left(\frac{\sin^2\varphi \rho_i^3(\varphi)}{\sqrt{1-l^2\sin^2\varphi}} \right) \mathrm{d}\varphi; \end{cases}; \tag{12}$$

$$\begin{cases} N_1 = \dfrac{1}{3} \displaystyle\int_{\varphi_{i-1}}^{\varphi_i} \left(\frac{\cos^2\varphi}{\Delta(\varphi)} \cdot \rho_i^3(\varphi) \right) \cdot \mathrm{d}\varphi; \\ N_2 = \dfrac{1}{6} \displaystyle\int_{\varphi_{i-1}}^{\varphi_i} \left(\frac{\sin^2\varphi}{\Delta(\varphi)} \cdot \rho_i^3(\varphi) \right) \cdot \mathrm{d}\varphi; \\ N_3 = \dfrac{1}{3} \displaystyle\int_{\varphi_{i-1}}^{\varphi_i} \left(\frac{\sin^2\varphi}{\Delta(\varphi)} \cdot \rho_i^3(\varphi) \right) \cdot \mathrm{d}\varphi, \end{cases} \tag{13}$$

where

$$\begin{cases} b_2 = E^2\chi^2 + 3C^2a^4\Theta^2; \\ l^2 = \dfrac{d_2}{b_2} - 1; \\ d_2 = 3C^2b^4\Theta^2; \end{cases} \tag{14}$$

The obtained results can be compared with the coefficients A_0, B_0 and C_0, which characterize the degree of plastic deformation under uniaxial loading (stretching) and have the same intensity as under complex loading.

$$\begin{cases} \Delta(\varphi) = \sqrt{A_0\cos^2\varphi + 0{,}5B_0\sin 2\varphi + C_0\sin^2\varphi}; \\ A_0 = (E\chi\sin\psi)^2 + 3C_2^2b^4\Theta^2; B_0 = E^2\chi^2\sin 2\psi; \\ C_0 = (E\chi\cos\psi)^2 + 3C_2^2a^4\Theta^2; \end{cases} \tag{15}$$

where φ and $\rho_i(\varphi)$ – current polar angle and radius-vector of points of the contour line of section; $\Delta(\varphi)$ – increase in the current polar angle; A_0, C_0 – characterize the degree of plastic deformation under uniaxial loading (stretching).

Conclusions.

1. Further study of the elastic recoil after pulling the closed rope using expressions (3) and (4) shows that the stress-strain state of the components of the closed ropes changes, while the redistribution of stresses in the cross sections of wires, and the moment of elastic recoil of the rope as a whole decreases. This significantly improves its operating conditions and increases service life.

2. The main criterion that determines the change in the moment of elastic recoil is the symmetry or asymmetry of the shaped cross section of the wire. In order to evaluate the effect of stretching on the magnitude of the moment of elastic recoil of the rope, a comparative analysis of the obtained experimental results was carried out, as a result of which a significant difference was observed in the distribution of forces over the layers of an unstretched and pre-stretched rope with a subsequent nominal load.

3. Calculations of technological internal force factors in the cross sections of wires and moments of elastic recoil on the layers of the rope make it possible not only to assess the degree of technological imbalance of the rope, but also rationally choose the direction of twisting in the layers. As a result, reduce the moment of elastic recoil and ensure the reliability and durability of the rope structure during its operation.

References: 1. *Kozlov V.T.* An experimental study of the moments of elastic recoil rope closed. Wire ropes: Scientific and Technical, 1999, Issue. 6, pp. 45-49. **2.** *Kozlov V.T., Kalinichenko P.M.* Svivochnyh study stress and internal force factors in ropes closed construction. Wire ropes: Scientific and Technical, 1999, Issue. 5, pp. 71-75. **3.** *Danenko, V.F., Gurevich, L.M.* Optimization of the Gaps in Spiral Closed Ropes to Ensure Their Structural Integrity. *Russ. Metall.* **2021,** 643–647 (2021). https://doi.org/10.1134/S0036029521050062. **4.** *Harutyunyan, N.H., Abrahamian, B.L.* Torsion of elastic bodies. Moscow 2003. **5.** *Gurevich, L., Danenko, V., Bogdanov, A. et al.* Analysis of the stress-strain state of steel closed ropes under tension and torsion. *Int J Adv Manuf Technol* **118,** 15–22 (2022). https://doi.org/10.1007/s00170-021-07128-w. **6.** *Saint-Venant 5.* Memoir of the torsion of prisms. – Moscow: Fizmatgiz, 2001. **7.** *Feyrer K.* (2015) Wire Ropes, Elements and Definitions. In: Wire Ropes. Springer, Berlin, Heidelberg. https://doi.org/10.1007/978-3-642-54996-0_1. **8.** *Kurz, J.H., Laguerre, L., Niese, F. et al.* NDT for need based maintenance of bridge cables, ropes and pre-stressed elements. *J Civil Struct Health Monit* **3,** 285–295 (2013). https://doi.org/10.1007/s13349-013-0052-5. **9.** *Kurgan V., Sydorenko I., Prokopovich I., Yeputatov Y., Levynskyi O.* (2021) Synthesis of Elastic Characteristics Based on Nonlinear Elastic Coupling. In: Tonkonogyi V. et al. (eds) Advanced Manufacturing Processes II. InterPartner 2020. Lecture Notes in Mechanical Engineering. Springer, Cham. https://doi.org/10.1007/978-3-030-68014-5_17. **10.** *Danenko, V.F., Gurevich, L.M.* Simulation of the State of Stress in Locked-Coil Ropes during Tension and Torsion. *Russ. Metall.* **2021,** 1196–1202 (2021). https://doi.org/10.1134/S0036029521100128. **11.** *Pištora J., Lesňák M., Valíček J., Harničárová M., Vrabko V.* (2019) Magnetic Field Distribution Around Magnetized Steel Ropes and Its Modulation by Rope Defects. In: Öchsner A., Altenbach H. (eds) Engineering Design Applications. Advanced Structured Materials, vol 92. Springer, Cham. https://doi.org/10.1007/978-3-319-79005-3_15. **12.** *Weiss M.P., Ashkenazi R., Elata D.* (2006) A

Unified Fatigue and Fracture Model Applied to Steel Wire Ropes. In: Gdoutos E.E. (eds) Fracture of Nano and Engineering Materials and Structures. Springer, Dordrecht. https://doi.org/10.1007/1-4020-4972-2_116.

Віктор Курган, Ігор Сидоренко, Владислав Вайсман,
Андрій Павлишко, Володимир Літвінов,
Вікторія Вовк, Одеса, Україна

ЕФЕКТ ПРУЖНОЇ ВІДДАЧІ ВАНТАЖОПІДІЙМАЛЬНИХ КАНАТІВ ЗАКРИТОГО ТИПУ ПІСЛЯ ЇХ ВИГОТОВЛЕННЯ ТА ВИТЯЖКИ

Анотація. *Відмінність закритих та напівзакритих канатів від інших їх видів полягає у застосуванні при їх звиванні дроту не тільки круглого, а і не круглого (клиноподібного, z-подібного, 8-подібного та x-подібного) перерізу, що дозволяє відтворити так званий ефект "замка" у вигляді щільного прилягання звитих дротин не круглого перерізу однієї до одної. Ця відмінність обумовлює формування між двома або трьома зовнішніми шарами каната замкнутих порожнин по усій його довжині, наявність яких забезпечує надійний захист каната від проникнення в його середину вологи, агресивних розчинів і виходу мастила з каната назовні. Завдяки такій захищеності канати даної конструкції знаходять широке застосування у підйомнотранспортному обладнанні, що використовується в будуванні технічних споруд, суднобудуванні, ливарному і хімічному виробництвах, в гірничодобувному обладнанні, в конструкціях висотних споруд, радіо і телевеж, а також мостів. В роботі проведено дослідження напружень та внутрішніх силових чинників в елементах канатів закритої конструкції при їх виготовленні. Встановлено, що при звиванні каната закритої конструкції, його фасонні дроти потерпають від деформації вигину, кручення і розтягування. При цьому фасонні дротини зазнають складного навантажування з супутнім поворотом осей тензора напружень. Розглянуто напруження в пружній області поперечного перерізу дроту каната і визначено його межу для фасонних поперечних перерізів і для несиметричних фасонних перерізів. Отримано формули для приблизного визначення дотичних та нормальних напружень в елементах закритого канату не круглого профілю: (клиноподібних, z-подібних та x-подібних). Отримані результати дають можливість оцінити ступінь технологічної неврівноваженості каната, раціонально вибрати направлення звивання по шарах, зменшити момент пружної віддачі і забезпечити надійність та довговічність структури каната в процесі його роботи.*

Ключові слова: *канати закритої конструкції; напруження; внутрішні силові чинники; поперечний переріз; фасонні дроти; пружна область; нормальне напруження; пружно-пластична деформація.*

CONTENT

Á. Bányai. Optimisation of purchasing strategy of tools and components based on exchange curve theory 3

Ya. Garachenko. Evaluation of performance efficiency of packing a group of products in the workplace of additive machine using a genetic algorithm 14

M.Z. Akkad, T. Bányai. Analysis and comparison of THE waste management development in hungary and Slovakia 22

Á. Francuz, T. Bányai. Optimisation of milkrun routes in manufacturing systems in the automotive industry 32

V. Fedorovich, I. Pyzhov, Y. Ostroverkh. Methodology of definition of optimal diamond wheel characteristics at stages of production and operation 42

I.T. Christodoulou, V.E. Alexopoulou, N.E. Karkalos, E.L. Papazoglou, A.P. Markopoulos. On the surface roughness of 3d printed parts with fdm by a low-budget commercial printer 52

V. Molnár. Wear resistance of hard turned surfaces 65

I. Sztankovics, J. Kundrák. Theoretical value and experimental study of arithmetic mean deviation in rotational turning 73

V. Fedorovich, I. Pyzhov,Y. Ostroverkh, L. Pupan, Ya. Garachenko. Methodology for developing an expert system for the grinding of superhard materials 82

B. Varga; B. Mikó. The effect of the point sampling to the result of coordinate measuring of free-form surface 89

V. Lavrinenko, V. Solod. The ralationship betwheen the parameters of roughness and features of surface formation with a special microprofile 99

J. Kundrák, I. Deszpoth, V. Molnár. Decision support method for the applicability of hard turning..... 110

Ya. Nemyrovskyi, I. Shepelenko, R. Osin, E. Posviatenko. Improving the processing quality of cylinder liners using combined technology..... 121

A. Mitsyk, V. Fedorovich, A. Grabchenko. Main technological factors determining the efficiency and quality of the vibration process 131

V. Kurgan, I. Sydorenko, V. Vaysman, A. Pavlyshko, V. Litvinov, V. Vovk. The effect of elastic recoil of closed-type lifting ropes after their manufacture and drawing 138

Наукове видання

РІЗАННЯ ТА ІНСТРУМЕНТИ
в технологічних системах

Міжнародний науково-технічний збірник

Випуск № 96

Укладач *д.т.н., проф. О.М. Шелковий*
Оригинал-макет *А.М. Борзенко*
Відп. за випуск *к.т.н., проф. Є.В. Островерх*

В авторській редакції

Матеріали відтворено з авторських оригіналів

Підп. до друку 12.02.2022.Формат 60x84 1/16. ПапірСоруРарег.
Друк - ризографія. Гарнитура Таймс. Умов.друк.арк. 10,93. Облік.вид.арк. 11,0. Наклад 30 прим.
1-й завод 1-100. Зам. № 1149. Ціна договірна.

Видавничий центр НТУ «ХПІ»
Свідоцтво про державну реєстрацію ДК № 116 від 10.07.2000 р.
61002, Харків, вул. Кирпичова, 2